

**B U L L E T I N**

DE LA SOCIÉTÉ DES SCIENCES  
ET DES LETTRES DE ŁÓDŹ

---

**SÉRIE:**  
**RECHERCHES SUR LES DÉFORMATIONS**

---

Volume LXIV, no. 3



# B U L L E T I N

## DE LA SOCIÉTÉ DES SCIENCES ET DES LETTRES DE ŁÓDŹ

---

### SÉRIE: RECHERCHES SUR LES DÉFORMATIONS

---

Volume LXIV, no. 3

Rédacteur en chef et de la Série: JULIAN ŁAWRYNOWICZ

Comité de Rédaction de la Série

P. DOLBEAULT (Paris), O. MARTIO (Helsinki), W. A. RODRIGUES, Jr. (Campinas, SP),  
B. SENDOV (Sofia), D. SHOIKHET (Karmiel), C. SURRY (Font Romeu), O. SUZUKI (Tokyo),  
E. VESENTINI (Torino), L. WOJTCZAK (Łódź), Ilona ZASADA (Łódź), Yu. ZELINSKIĬ (Kyiv)

Secrétaire de la Série:  
JERZY RUTKOWSKI



ŁÓDŹ 2014

LÓDZKIE TOWARZYSTWO NAUKOWE  
PL-90-505 Łódź, ul. M. Curie-Skłodowskiej 11  
tel. (42) 66-55-459, fax (42) 66 55 464  
sprzedaż wydawnictw: tel. (42) 66 55 448, <http://sklep.ltn.lodz.pl>  
e-mail: [biuro@ltn.lodz.pl](mailto:biuro@ltn.lodz.pl); <http://www.ltn.lodz.pl/>

REDAKCJA NACZELNA WYDAWNICTW  
LÓDZKIEGO TOWARZYSTWA NAUKOWEGO  
Krystyna Czyżewska, Wanda M. Krajewska (redaktor naczelny),  
Edward Karasiński, Henryk Piekarski, Jan Szymczak

**Wydano z pomocą finansową Ministerstwa Nauki  
i Szkolnictwa Wyższego**

© Copyright by Łódzkie Towarzystwo Naukowe, 2014

PL ISSN 0459-6854

Wydanie 1.  
Nakład 200 egz.  
Skład komputerowy: Zofia Fijarczyk  
Druk i oprawa: 2K Łódź sp. z o.o.  
Łódź, ul. Płocka 35/45  
[www.2k.com.pl](http://www.2k.com.pl), [2k@2k.com.pl](mailto:2k@2k.com.pl)

The journal appears in the bases *Copernicus* and *EBSCOhost*

## INSTRUCTION AUX AUTEURS

1. La présente Série du Bulletin de la Société des Sciences et des Lettres de Łódź comprend des communications du domaine des mathématiques, de la physique ainsi que de leurs applications liées aux déformations au sens large.
2. Toute communications est présentée à la séance d'une Commission de la Société par un des membres (avec deux opinions de spécialistes designés par la Rédaction). Elle doit lui être adressée directement par l'auteur.
3. L'article doit être écrit en anglais, français, allemand ou russe et débuté par un résumé en anglais ou en langue de la communication présentée. Dans tous les travaux écrits par des auteurs étrangers le titre et le résumé en polonais seront préparés par la rédaction. Il faut fournir le texte original qui ne peut contenir plus de 15 pages (plus 2 copies).
4. Comme des articles seront reproduits par un procédé photographique, les auteurs sont priés de les préparer avec soin. Le texte tapé sur un ordinateur de la classe IBM PC avec l'utilisation d'un imprimante de laser, est absolument indispensable. Il doit être tapé préféablement en *AMS-TEX* ou, exceptionnellement, en *Plain-TEX* ou *LATEX*. Après l'acceptation de texte les auteurs sont priés d'envoyer les disquettes (PC). Quelle que soient les dimensions des feuilles de papier utilisées, le texte ne doit pas dépasser un cadre de frappe de 12.3×18.7 cm (0.9 cm pour la page courante y compris). Les deux marges doivent être le la même largeur.
5. Le nom de l'auteur (avec de prénom complet), écrit en italique sera placé à la 1ère page, 5.6 cm au dessous du bord supérieur du cadre de frappe; le titre de l'acticle, en majuscules d'orateur 14 points, 7.1 cm au dessous de même bord.
6. Le texte doit être tapé avec les caractères Times 10 points typographiques et l'interligne de 14 points hors de formules longues. Les résumés, les renvois, la bibliographie et l'adresse de l'auteurs doivent être tapés avec le petites caractères 8 points typographiques et l'interligne de 12 points. Ne laissez pas de "blancs" inutiles pour respecter la densité du texte. En commençant le texte ou une formule par l'alinéa il faut taper 6 mm ou 2 cm de la marge gauche, respectivement.
7. Les texte des théorèmes, propositions, lemmes et corollaries doivent être écrits en italique.
8. Les articles cités seront rangés dans l'ordre alphabétique et précédés de leurs numéros placés entre crochets. Après les références, l'auteur indiquera son adress complète.
9. Envoi par la poste: protégez le manuscrit à l'aide de cartons.
10. Les auteurs recevront une copie de fascicule correspondant à titre gratuit.

Adresse de la Rédaction de la Série:  
Département de la Physique d'état solide  
de l'Université de Łódź  
Pomorska 149/153, PL-90-236 Łódź, Pologne

*Name and surname of the authors*

## **TITLE – INSTRUCTION FOR AUTHORS SUBMITTING THE PAPERS FOR BULLETIN**

### **Summary**

Abstract should be written in clear and concise way, and should present all the main points of the paper. In particular, new results obtained, new approaches or methods applied, scientific significance of the paper and conclusions should be emphasized.

### **1. General information**

The paper for BULLETIN DE LA SOCIÉTÉ DES SCIENCES ET DES LETTRES DE ŁÓDŹ should be written in LaTeX, preferably in LaTeX 2e, using the style (the file **bull.cls**).

### **2. How to prepare a manuscript**

To prepare the LaTeX 2e source file of your paper, copy the template file **instr.tex** with **Fig1.eps**, give the title of the paper, the authors with their affiliations/addresses, and go on with the body of the paper using all other means and commands of the standard class/style ‘bull.cls’.

#### **2.1. Example of a figure**

Figures (including graphs and images) should be carefully prepared and submitted in electronic form (as separate files) in Encapsulated PostScript (EPS) format.



Fig. 1: The figure caption is located below the figure itself; it is automatically centered and should be typeset in small letters.

#### **2.2. Example of a table**

Tab. 1: The table caption is located above the table itself; it is automatically centered and should be typeset in small letters.

Description 1	Description 2	Description 3	Description 4
Row 1, Col 1	Row 1, Col 2	Row 1, Col 3	Row 1, Col 4
Row 2, Col 1	Row 2, Col 2	Row 2, Col 3	Row 2, Col 4

### 2.3. “Ghostwriting” and “guest authorship” are strictly forbidden

The printed version of an article is primary (comparing with the electronic version). Each contribution submitted is sent for evaluation to two independent referees before publishing.

### 3. How to submit a manuscript

Manuscripts have to be submitted in electronic form, preferably via e-mail as attachment files sent to the address **zofja@uni.lodz.pl**. If a whole manuscript exceeds 2 MB composed of more than one file, all parts of the manuscript, i.e. the text (including equations, tables, acknowledgements and references) and figures, should be ZIP-compressed to one file prior to transfer. If authors are unable to send their manuscript electronically, it should be provided on a disk (DOS format floppy or CD-ROM), containing the text and all electronic figures, and may be sent by regular mail to the address: **Department of Solid State Physics, University of Lodz, Bulletin de la Société des Sciences et des Lettres de Łódź, Pomorska 149/153, 90-236 Łódź, Poland.**

### References

[1]

Affiliation/Address

## TABLE DES MATIÈRES

1. <b>R. K. Kovacheva</b> , Distribution of points of interpolation of multipoint Padé approximants; the nonequilibrium case .....	11–20
2. <b>P. Miškinis</b> and <b>V. Valuntaitė</b> , Dependence of crystal semiconductor solar cell electromotive force on illuminance as a dynamical system .....	21–29
3. <b>G. Ivanova</b> and <b>E. Wagner-Bojakowska</b> , On some subfamilies of Darboux quasi-continuous functions .....	31–43
4. <b>N. Skoulidis</b> and <b>H. M. Polatoglou</b> , Dependence of the curvature of Si/Ge cantilevers on the size, composition, and temperature .....	45–54
5. <b>S. Szumiński</b> , Semi-magic squares and Kirchhoff’s voltage law	55–68
6. <b>M. Zubert</b> , <b>M. Janicki</b> , <b>T. Raszkowski</b> , <b>A. Samson</b> , <b>P. S. Nowak</b> , and <b>K. Pomorski</b> , The heat transport in nanoelectronic devices and PDEs translation into hardware description languages .....	69–80
7. <b>M. Nowak-Kępczyk</b> , An algebra governing reduction of quaternary structures to ternary structures II. A study of the multiplication table for the resulting algebra generators .....	81–90
8. <b>A. Partyka</b> , Teichmüller distance in the class of weakly quasiregular functions .....	91–100
9. <b>K. Podlaski</b> and <b>G. Wiatrowski</b> , Different approaches to particle swarm optimization for discrete systems .....	101–114
10. <b>K. Podlaski</b> and <b>G. Wiatrowski</b> , Effect of neighbours distribution on hybrid genetic approach to particle swarm optimization applied to traveling salesman problem .....	115–125



Professor Zygmunt Charzyński (centre) among the participants of the IV International Conference on Analytic Functions in Łódź (1.-7.09.1966).



## B U L L E T I N

DE LA SOCIÉTÉ DES SCIENCES ET DES LETTRES DE ŁÓDŹ

2014

Vol. LXIV

Recherches sur les déformations

no. 3

pp. 11–20

*In memory of*  
*Professor Zygmunt Charzyński (1914–2001)*

*Ralitza K. Kovacheva*

**DISTRIBUTION OF POINTS OF INTERPOLATION  
OF MULTIPOINT PADÉ APPROXIMANTS;  
THE NONEQUILIBRIUM CASE**

**Summary**

Given a regular compact set  $E$ , a unit measure  $\mu$  supported by  $\partial E$  and a triangular point set  $\beta := \{\beta_{n,k}\}$ ,  $\beta \subset \partial E$ , we provide a necessary and sufficient condition for the points  $\beta$  to be distributed according to the measure  $\mu$ . The results are provided in terms of multipoint Padé approximants with fixed degree of the denominators.

*Keywords and phrases:* multipoint Padé approximant, meromorphic continuation, maximal convergence

**1. Introduction**

We first introduce notations and concepts needed for the further considerations.

Given a compact set  $E \subset \mathbb{C}$ , we say that  $E$  is *regular*, if the unbounded component of the complement  $E^c := \overline{\mathbb{C}} \setminus E$  is solvable with respect to Dirichlet problem. We will assume throughout the paper that  $E$  possesses a connected complement  $E^c$ . Set  $\text{Cap}(E)$  for the Green's capacity and let  $G_E(z, \infty)$  be the Green's function of  $E$  with pole at infinity. As known, the capacity  $\text{Cap}(E)$  is positive, if  $E$  is regular [5, 13, 15]. Given a number  $\rho > 1$ , we set

$$E_\rho := \{z, G_E(z, \infty) < \ln \rho\}, \partial E_\rho := \Gamma_\rho.$$

Set  $\mathcal{B}(E)$  for the class of the unit Borel measures supported by  $E$  ( $\text{supp}(\dots) \subset E$ .) We say that the sequence of Borel measures  $\{\mu_n\}$  converges in the weak topology to a measure  $\mu$  if

$$\int g(t)d\mu_n \rightarrow \int g(t)d\mu$$

for every function  $g$  continuous on  $\mathbb{C}$  with compact support. We associate with the measure  $\mu \in \mathcal{B}(E)$  the logarithmic potential  $U^\mu(z)$ , that is

$$U^\mu(z) := \int \log \frac{1}{|z-t|} d\mu.$$

We also need the concept of a *balayage measure*, that is: Given a set  $S$ ,  $S \supset E$ , the measure  $\tilde{\mu}^{\partial S}$  is the balayage measure of  $\mu$  onto  $\partial S$ , if  $\text{supp } \tilde{\mu} \subset \partial S$ ,  $\|\mu\| = \|\tilde{\mu}\|$  and

$$U^{\tilde{\mu}}(z) \begin{cases} \leq U^\mu(z), & z \in \mathbb{C} \\ = U^\mu(z), & z \in S^c. \end{cases}$$

Finally, given a polynomial  $p$  of degree nonexceeding  $n$  ( $p \in \Pi_n$ ), we denote by  $\mu_p$  the counting measure of  $p$ , that is

$$\mu_p(F) := \frac{\text{number of zeros of } p \text{ on } F}{\text{deg } p},$$

where  $F$  is a point set in  $\mathbb{C}$ .

Let  $\mu \in \mathcal{B}(E)$ . We say that  $\mu$  is the *equilibrium measure* of  $E$  and denote it by  $\mu_E$ , if

$$\inf_{\mu \in \mathcal{B}(E)} \int \int \log \frac{1}{|z-t|} d\mu(t)d\mu(z) = \int \int \log \frac{1}{|z-t|} d\mu_E(t)d\mu_E(z).$$

Recall that  $\mu_E \in \mathcal{B}(E)$  is unique.

Given a domain  $B \subset \mathbb{C}$ , a function  $g$  and a number  $m \in \mathbb{N}$ , we say that  $g$  is  $m$ -meromorphic in  $B$  ( $g \in \mathcal{M}_m(B)$ ) if in each subdomain  $g$  has no more than  $m$  of poles (poles are counted with regard to their multiplicities). Let now the function  $f$  be holomorphic on the compactum  $E$  ( $f \in \mathcal{A}(E)$ .) In other words, is holomorphic in some open neighborhood of  $E$ . Let  $m \in \mathbb{N} \cup \{0\}$  be fixed. We introduce *the radius of  $m$ -meromorphy with respect to  $E$* , that is

$$\rho_m(f) := \sup_{\rho} \{\rho, f \in \mathcal{M}_m(E_\rho)\}.$$

By convention,  $\rho_0(f)$  stands for the *radius of holomorphy*. By the accepted definition,  $\rho_0(f) = 1$  iff  $f$  possesses a nonpolar singularity on  $E$ .

Let  $\beta$  be an infinite triangular point table,

$$\beta := \{\{\beta_{n,k}\}_{k=1}^n\}_{n=1,2,\dots}, \beta_{n,k} \in E$$

with no concentration points outside  $E$ . We write  $\beta \in E$ . Set

$$\omega_n(z) := \prod_{k=1}^n (z - \beta_{n,k}).$$

Let  $f \in \mathcal{A}(E)$  and  $(n, m)$  be a fixed pair of nonnegative integers. The rational function

$$\pi_{n,m}^\beta = \pi_{n,m}^{\beta,f} := p/q,$$

where the polynomials  $p \in \Pi_n$  and  $q \in \Pi_m$  are chosen in the way that

$$\frac{fq - p}{\omega_{n+m+1}} \in \mathcal{A}(E)$$

is called a  $\beta$ -multipoint Padé approximant of  $f$  of order  $(n, m)$ . This construction was introduced by E. B. Saff in [14]. As well known, the function  $\pi_{n,m}^\beta$  always exists and is unique [14]. In the partial case, when  $\beta \equiv 0$ , the multipoint Padé approximant  $\pi_{n,m}^\beta$  coincides with the classical Padé approximant  $\pi_{n,m}$  of order  $(n, m)$  [9].

Set

$$(1.1) \quad \pi_{n,m}^\beta := \frac{P_{n,m}^\beta}{Q_{n,m}^\beta},$$

where the polynomials  $P_{n,m}^\beta$  and  $Q_{n,m}^\beta$  do not have common divisors. The zeros of  $Q_{n,m}^\beta$  are called *free zeros* of  $\pi_{n,m}^\beta$ ;  $\deg Q_{n,m}^\beta \leq m$ .

We say that the points  $\beta_{n,k}, \beta_{n,k} \in E$  are *uniformly distributed relatively to the equilibrium measure of  $E$* , if

$$\tilde{\mu}_{\omega_n}^{\partial E} \longrightarrow \mu_E, \quad n \rightarrow \infty$$

being a positive constant. Different constructions are given in [1, 11, 16]. Note that if  $\beta \subset \partial E$ , then

$$|\omega_n(z)|^{1/n} \rightarrow \text{Cap}(E)e^{G_E(z, \infty)}$$

uniformly inside  $E^c$  (on compact subsets of  $E^c$ .)

Following J. L. Walsh [16], we introduce the term of a *maximal convergence* of polynomials. Given a regular compact set  $E$ , equipped with the max norm  $\|\cdot\|_E$  and  $f \in \mathcal{A}(E)$  with  $\rho_0(f) < \infty$ , we say that the sequence  $\{p_n\}, p_n \in \Pi_n, n = 1, 2, \dots$  converges *maximally to  $f$  on  $E$*  if

$$\limsup_{n \rightarrow \infty} \|f - p_n\|_E^{1/n} \leq 1/\rho_0(f).$$

As established in [16], there holds for every  $\rho \in (1, \rho_0(f))$

$$\limsup_{n \rightarrow \infty} \|f - p_n\|_{E_\rho}^{1/n} \leq \rho/\rho_0(f).$$

The next theorem is due to J. L. Walsh ([16], Chp. 7.3, Theorem 3.)

**Theorem A, [16].** *Let  $E$  be a regular compact set and the point table  $\beta \in E$  be given. Given a function  $f \in \mathcal{A}(E)$ , denote for every  $n \in \mathbb{N}$  by  $p_n(f)$  the polynomial in the class  $\Pi_n$  which interpolates  $f$  at the zeros of  $\omega_{n+1}$ . Then for each function  $f$  holomorphic on  $E$ , but nonentire, the polynomials  $p_n(f)$  converge to  $f$  on  $E$  as  $n \rightarrow \infty$  iff the points  $\beta$  are uniformly distributed with respect to the equilibrium measure of  $E$ .*

In analogy with the maximal convergence of polynomials, we introduce a *maximal convergence of sequences of rational functions with fixed number of the free poles*. Before, we introduce the term of a *normalization of a polynomial  $q(z)$  respectively a given open set  $\Omega$* : that is,

$$q(z) = \prod (z - \alpha'_k) \prod (1 - z/\alpha''_k) := \tilde{q}(z)q^*(z),$$

where  $\alpha'_k, \alpha''_k$  are the zeros lying inside, resp. outside  $\Omega$ .

Furthermore, we recall the notion of  $m_1$ - Hausdorff measure and  $m_1$ -almost uniform convergence inside  $D$  (cf. [7]). Let  $e$  be a subset of  $\mathbb{C}$ , we set

$$m_1(e) := \inf \left\{ \sum_{\nu} |V_{\nu}| \right\}$$

where the infimum is taken over all coverings  $\{V_{\nu}\}$  of  $e$  by disks  $U_{\nu}$  and  $|V_{\nu}|$  is the radius of the disk  $V_{\nu}$ .

Let  $D$  be a domain in  $\mathbb{C}$  and  $\varphi$  a function defined in  $D$  with values in  $\overline{\mathbb{C}}$ . A sequence of functions  $\{\varphi_n\}$ , meromorphic in  $D$ , is said to converge to a function  $\varphi$   *$m_1$ -almost uniformly inside  $D$*  if for any compact subset  $K \subset D$  and every  $\varepsilon > 0$  there exists a set  $K_{\varepsilon} \subset K$  such that  $m_1(K \setminus K_{\varepsilon}) < \varepsilon$  and the sequence  $\{\varphi_n\}$  converges uniformly to  $\varphi$  on  $K_{\varepsilon}$ .

We are now capable of extending the concept of a *maximal convergence of sequences of rational functions with bounded number of free poles*.

Let now  $f \in \mathcal{A}(E)$  with  $\rho_m(f) < \infty$ . Let the sequence  $\{r_{n,m}\}$  be given,  $m$ -fixed,  $n \rightarrow \infty$ . By presumption, the denominators are normalized with respect to the the set  $E_{\rho_m(f)}$ . The sequence

$$r_{n,m} = p_{n,m}/q_{n,m} \in \mathcal{R}_{n,m}, \quad m\text{-fixed}, \quad n \rightarrow \infty$$

converges maximally to  $f$ , if for every compact set  $K \in E_{\rho_m(f)}$  and every  $\varepsilon > 0$  there exists a set  $K_{\varepsilon} \subset K$  such that  $m_1(K \setminus K_{\varepsilon}) < \varepsilon$  and

$$\limsup_{n \rightarrow \infty} \|(f - r_{n,m})\|_{K_{\varepsilon}}^{1/n} \leq \|e^{G_E(z, \infty)}\|_{K/\rho_m(f)}.$$

From the properties of the convergence of functions in  $m_1$ -measure, it follows [7] that if  $f$  has exactly  $m$  poles in  $E_{\rho_m(f)}$ , then so do all functions  $r_{n,m}$  for  $n$  large enough, and on each compact subset  $K$  which does not contain poles of  $f$  the inequality

$$\limsup \|f - r_{n,m}\|_K^{1/n} \leq \|e^{G_E(z, \infty)}\|_{K/\rho_m(f)}$$

holds. Furthermore, as it was proved in [6], both last inequalities are equalities.

In [10], N. Ikononov considered the maximal convergence of multipoint Padé approximants with fixed number of the free poles. Before presenting his result, we introduce the functions

$$f_t(z) := \frac{1}{t - z}.$$

Ikononov proved

**Theorem B.** *Let  $E$  be a regular compact set with connected complement and the point table  $\beta \in E$ . Let  $m \in \mathbb{N}$  be fixed. Let the polynomial  $Q(z) \in \Pi_m$  of degree exactly  $m$  have all its zeros in  $E^c$  and the number  $R$  be such that  $Q(z) \neq 0$  for  $z \in E \cup E_R^c$ . If for every number  $t \in \Gamma_R$*

$$\limsup \|f - \pi_{n,m}^{\beta, f_t}\|_E \leq 1/\rho_0, \quad n \rightarrow \infty, \quad m - \text{fixed}$$

then the points  $\beta$  are uniformly distributed with respect to the equilibrium measure of  $E$ .

Combining Theorem B with the direct result by Gonchar [7], we arrive at an analogue of Theorem A, namely

**Corollary 1.** *Given a regular compact set  $E$  with connected complement and a triangular point table  $\beta \in \partial E$  with no concentration points outside  $E$ , let  $m \in \mathbb{N}$  be fixed.*

*Then for each function  $f \in \mathcal{A}(E)$  with  $\rho_m(f) < \infty$  the multipoint Padé approximants  $\pi_{n,m}^{\beta,f}$  converge to  $f$  maximally on  $E$  iff the points  $\beta$  are uniformly distributed with respect to the equilibrium measure of  $E$ .*

## 2. Statement of the new results

We now pose the question about the general case when the points  $\beta$  do not have exactly the equilibrium distribution on  $\partial E$ .

Let the compact set  $E$  be regular, with connected complement  $E^c$  and  $\mu$  be a unit Borel measure supported by  $E$  ( $\text{supp}\mu \subset E$ .) As above, we denote by  $U^\mu$  the logarithmic potential associated with the measure  $\mu$ ; recall that

$$U^\mu(z) := \int_{\text{supp}\mu} \log \frac{1}{|t-z|} d\mu(t).$$

Introduce the numbers

$$\varrho_1 := \inf_{z \in E} e^{-U^\mu(z)}, \quad \varrho_1 \geq 0$$

and

$$\varrho_2 := \max_{z \in E} e^{-U^\mu(z)}.$$

As known ([15], Theorem III.1),

$$e^{-U^\mu(z)} \geq \varrho_1, \quad z \in E^c.$$

Set for  $r > \varrho_1$

$$E_\mu(r) := \{z, e^{-U^\mu(z)} < r\}.$$

Because of the semicontinuity of the function  $\chi(z) := e^{-U^\mu(z)}$ , the set  $E_\mu(r)$  is open; apparently,  $E_\mu(r_1) \subset E_\mu(r_2)$  if  $r_1 \leq r_2$ . Furthermore,  $E_\mu(r) \supset E$  if  $r > \varrho_2$ .

Let  $f \in \mathcal{A}(E)$  and  $m \in \mathbb{N}$  be fixed. We introduce in analogy with the previous case the terms of radius  $R_{m,\mu} = R_{m,\mu}(f)$  and of domain of  $m$ -meromorphy

$$D_{m,\mu} = D_{m,\mu}(f) := E_\mu(R_{m,\mu})$$

according to the measure  $\mu$ ,  $m \in \mathbb{N}$ ; that is:

$$R_{m,\mu} := \sup\{r, f \in \mathcal{A}(E_\mu(r))\}, \quad D_m := E_\mu(R_{m,\mu}).$$

Furthermore, we introduce the term of a *maximal convergence related to  $\mu$* . We say that the sequences of rational functions  $\{r_{n,m}\}$ ,  $r_{n,m} = p_{n,m}/q_{n,m}$  with a fixed

number of the poles =  $m$  converges maximally to the function  $f$ ,  $R_{m,\mu} < \infty$ , if for any  $\varepsilon > 0$  and every compact set  $K \subset D_{m,\mu}$  there exists a set  $K_\varepsilon \subset K$  such that  $m_1(K \setminus K_\varepsilon) < \varepsilon$  and

$$\limsup_{n \rightarrow \infty} \|f - r_{n,m}\|_{K_\varepsilon}^{1/n} \leq \frac{\|e^{-U^\mu}\|_K}{R_{m,\mu}(f)}$$

The next result is due to Hernandez and Calle Ysern

**Theorem C, [2].** *Let  $E$  be a compact set in the complex plane with connected complement and let  $\mu \in \mathcal{B}(E)$ . Assume that*

$$\beta, \beta := \{\beta_{n,k}\}_{k=1, n=1}^{n, \infty} \subset E$$

*is a triangular point set on  $E$  and  $m \in \mathbb{N}$  is fixed. Let  $\mu_n$  be the counting measures associated with the polynomials*

$$\omega_n, \omega_n(z) := \prod_{k=1}^n (z - \beta_{n,k}).$$

*Suppose that  $\mu_n \rightarrow \mu$  as  $n \rightarrow \infty$ . Let  $f \in \mathcal{A}(E)$  and  $R_{m,\mu}(f) < \infty$ . Then the sequence  $\pi_{n,m}^{\beta,f}$  converges maximally to  $f$ , i.e., for every  $\varepsilon > 0$  there exists a compact set  $K_\varepsilon$  such that*

$$m_1(K \setminus K_\varepsilon) < \varepsilon$$

*and*

$$\limsup_{n \rightarrow \infty} \|f - \pi_{n,m}^{\beta,f}\|_{K_\varepsilon}^{1/n} \leq \frac{\|e^{-U^\mu}\|_K}{R_{m,\mu}}.$$

As it follows from the results in [7], for the particular case, when the function  $f$  has exactly  $m$  poles in the domain  $D_{m,\mu}$ , on each compact set  $K \subset E_\mu(R_{m,\mu})$  which does not contain poles of  $f$  there holds

$$\limsup_{n \rightarrow \infty} \|f - \pi_{n,m}^\beta\|_K^{1/n} \leq \frac{\|e^{-U^\mu}\|_K}{R_{m,\mu}} \quad (1)$$

Let now  $t_0 \notin E$  be fixed; set

$$f_{t_0}(z) := \frac{1}{t_0 - z}.$$

From the definition, we see that  $f_{t_0} \in \mathcal{A}(E_\mu(r))$  for every  $r < e^{-U^\mu(t_0)}$ ; hence,  $R_{m,\mu}(f_{t_0}) = e^{-U^\mu(t_0)}$ . In the present paper, we prove

**Theorem 1.** *Let  $E$  be a regular compact set with connected complement, suppose that  $\mu \in \mathcal{B}(\partial E)$  and let the point table  $\beta \in \partial E$  be given. Let  $\varrho_1$  and  $\varrho_2$  be as above. Given a polynomial  $Q$  of degree exactly  $m$ , assume that all zeros of  $Q(z)$  are situated in an open set  $E_\mu(r) \setminus E$ ,  $\varrho_1 < r$ . Let  $t_0 \in E^c$  be such that  $e^{-U^\mu(t_0)} > \max(\varrho_2, r)$ . Suppose that the sequence of multipoint Padé approximants  $\pi_{n,m}^{\beta,f_{t_0}}$ ,  $n \rightarrow \infty$  converges maximally to  $f_{t_0}$ . Then the points  $\beta$  are uniformly distributed with respect to the measure  $\mu$ .*

Combining this result and Theorem C, we come to

**Corollary 2.** *Let  $E$  be a regular compactum in  $\mathbb{C}$  with connected and regular complement, let  $\mu$  be a unit Borel measure supported by  $\partial E$  and  $t_0 \notin E_\mu(\varrho_2)$ . Let*

$$\beta \in \partial E := \{\beta_{n,k}\}_{k=1,n=1}^{n,\infty}$$

*be a triangular point set and  $m \in \mathbb{N}$  be fixed. Then for every function  $f \in \mathcal{A}(E)$  with  $R_{m,\mu} < \infty$  the associated sequence  $\{\pi_{n,m}^{f;\mu}\}$  converges maximally to  $f$  iff  $\mu_{\omega_n} \rightarrow \mu$  as  $n \rightarrow \infty$ .*

Before providing the proof, we mention some results in the same area. In [8], R. Grothmann investigated the distribution of interpolation points in approximation by polynomials. He showed that if the function  $f \in \mathcal{A}(E)$  is not entire and if a sequence of interpolating polynomials converge maximally to  $f$ , then the points of interpolation are uniformly distributed with respect to the equilibrium measure of  $E$ , at least for a subsequence.

In [3], the distribution of interpolating points of sequences of multipoint Padé approximants  $\pi_{n,m_n}$  was considered, under the assumptions that  $m_n = o(n/\ln n)$  as  $n \rightarrow \infty$  and the sequence  $\{\pi_{n,m_n}\}$  converges maximally to  $f$  inside the largest domain of meromorphic continuation of  $f$ . It was shown that if the function  $f$  is not meromorphic in  $\mathbb{C}$ , then the interpolation points have the equilibrium distribution for an appropriate sequence of integers.

### 3. Proofs

The proof will be preceded by basic facts.

Recall [13] that  $U_\mu$  is a function superharmonic in  $\mathbb{C}$ , subharmonic in  $\overline{\mathbb{C}} \setminus \text{supp}(\mu)$ , harmonic in  $\mathbb{C} \setminus \text{supp}(\mu)$  and

$$U_\mu(z) = \ln \frac{1}{|z|} + o(1), z \rightarrow \infty.$$

Let  $\mu_n \rightarrow \mu$ ,  $\mu_n \in \mathcal{B}(E)$  and  $z_n \rightarrow z_0 \in \mathbb{C}$ . Then *the descent principle* ([13], Theorem 1.6.8.) says that

$$\liminf U^{\mu_n}(z_n) \geq U^\mu(z_0), n \rightarrow \infty$$

and

$$U^{\mu_n}(z_n) \rightarrow U^\mu(z_0), n \rightarrow \infty$$

uniformly inside  $E^c$ .

Suppose that  $\{\mu_n\}$  is an infinite sequence of Borel measures in  $\mathcal{B}(E)$ . Then according to Helly's selection theorem there is an infinite subsequence  $\Lambda$  and a measure  $\mu \in \mathcal{B}(E)$  such that  $\mu_n \rightarrow \mu$  as  $n \in \Lambda$ .

Carleson Lemma [4]: *Given the measures  $\mu_1, \mu_2$  supported by  $\partial E$ , suppose that  $U^{\mu_1}(z) = U^{\mu_2}(z)$  for every  $z \in E^c$ . Then  $\mu_1 = \mu_2$ .*

In what follows, we will use the notation

$$\pi_{n-m+1,m}^{\beta, f_{t_0}} := \pi_{n,m} = P_{n,m}/Q_{n,m}.$$

This is justified, because  $m$  is fixed. Note that under these notations,

$$\deg P_{n,m} \leq n - m - 1, \quad \deg Q_{n,m} = m$$

for  $n$  large enough. Set  $t := t_0$ .

Since the function  $f_t$  has exactly  $m$  poles in  $E_\mu(e^{-U^\mu(t)}) \setminus E$ , the associated  $\beta$ -multipoint Padé approximants  $\pi_{n,m}$  have necessarily also  $m$  free poles and they accumulate around the zeros of the polynomial  $Q$  (see [7]).

Fix a number  $\delta > 0$ , such that  $\max(r + \delta, \varrho_2 + \delta) < e^{-U^\mu(t)}$ . Set  $\rho := \max(r + \delta, \varrho_2 + \delta)$ . Select a closed smooth curve  $\gamma \in E_\mu(e^{-U^\mu(t_0)}) \setminus E_\rho$  such that  $\gamma$  winds around every point in  $E_\mu(\rho)$  exactly once. This is possible because of the choice of the number  $\rho$ . Under this construction,  $D_m(f_t)$  contains the interior of the curve  $\gamma$ .

Using the definition of multipoint Padé approximant, we get

$$\frac{1}{t-z} - \pi_{n,m}(z) = \frac{\omega_n(z) Q_{n,m}(t) Q(t)}{\omega_n(t) Q_{n,m}(z) Q(z)} \frac{1}{t-z}, z \in E,$$

from which it follows that

$$\frac{1}{t-z} - \pi_{n,m}(z) = \frac{\omega_n(z) Q_{n,m}(t) Q(t)}{\omega_n(t) Q_{n,m}(z) Q(z)} \frac{1}{t-z}, z \in \gamma. \quad (2)$$

By (1), for every  $z \in \gamma$ ,

$$\limsup |f_t(z) - \pi_{n,m}(z)|^{1/n} = \limsup \|f_t - \pi_{n,m}\|_{\{z\}}^{1/n} \leq \frac{e^{-U^\mu(z)}}{e^{-U^\mu(t)}}. \quad (3)$$

By (2)

$$\left| \frac{\omega_{n+m+1}(z) Q_{n,m}(t) Q(t)}{\omega_{n+m+1}(t) Q_{n,m}(z) Q(z)} \frac{1}{t-z} \right|^{1/n} \leq \frac{e^{-U^\mu(z)}}{e^{-U^\mu(t)}}.$$

Hence, for every  $z \in \gamma$

$$\frac{e^{-U^\mu(z)}}{e^{-U^\mu(t)}} \geq \frac{e^{U^{(n)}(t)}}{e^{U^{(n)}(z)}} C,$$

where  $U^{(n)}$  is the logarithmic potential associated with the polynomial  $\omega_n$  and  $C$  is a positive constant, independent on  $n$

$$\left( \text{say } C \geq \frac{\min_{z \in \gamma} |Q(z)|}{|Q(t)|} \right).$$

In other words,

$$U^\mu(t) - U^\mu(z) \geq U^{(n)}(t) - U^{(n)}(z) + o(1)$$

By Helly's selection theorem, there is a sequence  $\Lambda$  such that  $\mu_n \rightarrow \omega$ . Since the point  $t$  and the curve  $\gamma$  are lying in  $E^c$  and the triangular point set  $\omega$  does not have concentration points outside  $E$ , it follows from the descent principle that

$$U^{(n)}(t) \rightarrow U^\omega(t), n \in \Lambda.$$

Hence,

$$U^\mu(t) - U^\mu(z) \geq U^\omega(t) - U^\omega(z)$$

Recall that this inequality is valid for every  $z \in \gamma$ . From here,

$$U^\mu(t) - U^\omega(t) \geq U^\mu(z) - U^\omega(z).$$

From this inequality we deduce that

$$(U^\mu(t) - U^\omega(t)) \geq \max_{z \in \gamma} (U^\mu(z) - U^\omega(z))$$

On the other hand, the function  $U^\mu(t) - U^\omega(t)$  is harmonic in  $\mathbb{C} \setminus E$  and thus obeys the maximum principle for harmonic functions. Thus,

$$\max_{z \in \gamma} (U^\mu(z) - U^\omega(z)) \geq U^\mu(t) - U^\omega(t),$$

since by construction the exterior of the cycle  $\gamma$  contains the point  $t$ . Thus, the last inequality is valid only if  $U^\mu(t) - U^\omega(t) \equiv \text{Constant}$  in the exterior of  $\gamma$ . On the other hand,  $(U^\mu(t) - U^\omega(t))(\infty) = 0$ . Therefore,  $U^\mu(t) \equiv U^\omega(t)$  outside  $\gamma$ , and, by the maximum principle again, everywhere in  $E^c$ .

The theorem is proved.

## References

- [1] Th. Bagby, *On interpolation by rational functions*, Duke Math. J. **36** (1969), 95–104.
- [2] M. Bello Hernández and B. De La Calli Ysern, *Meromorphic continuation of functions and arbitrary distribution of interpolation points*, J. of Mathematical Analysis and Applications **403** (2013), 107–119.
- [3] H. P. Blatt and R. K. Kovacheva, *Growth behavior and zero distribution of rational approximants*, J. of Approximation Theory, accepted, to appear 2014.
- [4] I. Carleson, *Mergelyan's theorem on uniform polynomial approximation*, Math. Scand. **15** (1964), 167–175.
- [5] G. M. Golusin, *Geometric theory of function of a complex variable*, in Russian, Nauka, Moscow 1966.
- [6] A. A. Gončar, *On a theorem of Saff*, Mat. Sbornik **94** (136) (1974), 152–157; English translation in Math. USSR Sbornik **23**, no. 1 (1974), 149–154.
- [7] A. A. Gončar, *On the convergence of generalized Padé approximants of meromorphic functions*, Mat. Sbornik **98**, no. 140 (1975), 564–577; English translation in Math. USSR Sbornik **27**, no. 4 (1975), 503–514.
- [8] R. Grothmann, *Distribution of interpolation points*, Arkiv för matematik **34** (1996).
- [9] O. Perron, *Die Lehre von den Kettenbrüchen*, Teubner, Leipzig 1929.
- [10] N. Ikononov, *Multipoint multipoint Padé approximants and uniform distribution of points of interpolation*, Comptes rendus de l'Académie bulgare des Sciences, **66**, no. 8 (2013).
- [11] R. K. Kovacheva, *Generalized Padé approximants of Kakehashi's type and meromorphic continuation of functions*, Deformation of mathematical structures, Kluwer Academic Publishers, 1989, 151–159.
- [12] Vl. Andrievskij, H. P. Blatt and R. K. Kovacheva, *On the distribution of zeros and poles of rational approximants on intervals*, Abstract Analysis and Applications **2012** (2012); article ID 961209, 2012. doi:10.1155/2012/961209.

- [13] E. B. Saff and V. Totik, *Logarithmic potentials with external fields*, Springer, Grundlehren der mathematischen Wissenschaften, 1997.
- [14] E. B. Saff, *An extension of Montessus de Ballore's theorem on the convergence of interpolating rational functions*, J. of Approximation Theory **6** (1972), 63–68.
- [15] M. Tsuji, *Potential Theory in Modern Function Theory*, Maruzen, Tokyo 1959.
- [16] J. L. Walsh, *Interpolation and Approximation by Rational Functions in the complex domain*, Amer. Math. Soc. Second edition, 1960, Translation into Russian, Izd. IL, Moscow 1961.

Institute of Mathematics and Informatics  
Bulgarian Academy of Sciences  
Acad. Bonchev str, 1113 Sofia  
Bulgaria  
e-mail:rkovach@math.bas.bg

Presented by Leon Mikołajczyk at the Session of the Mathematical-Physical Commission of the Łódź Society of Sciences and Arts on December 18, 2014

### **ROZMIESZCZENIE PUNKTÓW INTERPOLACJI WIELOPUNKTOWYCH APROKSYMANT PADÉ; PRZYPADEK NIERÓWNOŚCI**

#### **S t r e s z c z e n i e**

Przy danym regularnym zbiorze zwartym  $E$ , miarze jednostkowej  $\mu$  spełniającej warunek  $\text{supp}\mu = \partial E$  i trójkątowym zbiorze punktów  $\beta = \{\beta_{n,k}\}$ ,  $\beta \in \partial E$ , znajdujemy warunek konieczny i dostateczny na to, by punkty  $\beta$  były rozłożone według miary  $\mu$ . Wynik ten jest podany w terminach wielopunktowych aproksymant Padé o stałym stopniu mianowników.

*Słowa kluczowe:* miara Borela, wielopunktowa aproksymanta Padé, przedłużenie meromorficzne, maksymalna zbieżność

## B U L L E T I N

DE LA SOCIÉTÉ DES SCIENCES ET DES LETTRES DE ŁÓDŹ

2014

Vol. LXIV

Recherches sur les déformations

no. 3

pp. 21–29

*In memory of  
Professor Zygmunt Charzyński (1914–2001)*

*Paulius Miškinis and Vaida Valuntaitė***DEPENDENCE OF CRYSTAL SEMICONDUCTOR  
SOLAR CELL ELECTROMOTIVE FORCE  
ON ILLUMINANCE AS A DYNAMICAL SYSTEM****Summary**

This paper deals with the examination of polycrystal silicon solar cells of various areas in active parts. The impact of illuminance on changes of the solar cell electromotive force (EMF) is analyzed. A mathematical model for a solar cell electromotive force dependence on illuminance is presented. For this purpose, a selection of experimental data trend function was carried out, and the Pearson correlation coefficients were established. The most optimal results were obtained in case of an exponential function with the strongest correlation observed ( $R^2 = 0.983$ ). The analysis has shown that in case of  $100 \text{ W/m}^2$  illuminance the EMF saturation is obtained (the EMF changes insignificantly and fluctuates at around 2 V), what in turn indicates that upon reaching such an illuminance, a solar cell has the greatest work efficiency. A first-order differential equation satisfied by the trend function has been compiled. The analysis revealed that when interpreting illuminance as a variable of time, an interpretation of the dynamic system of the proposed mathematical model can be presented.

*Keywords and phrases:* solar cell, electromotive force, illuminance, dynamic system

**1. Introduction**

As oil supplies are decreasing and the global warming is threatening, photovoltaic devices are becoming more and more popular as a renewable and environmentally friendly energy alternative [1]. Solar cells are electronic devices which turn sunlight into electricity [2]. A significant advantage of solar cells, as compared with ordinary fuel, is their ability to turn the free radiation obtained from the sun into electricity

with almost no pollution emissions. Solar cells can be classified into three main categories: monocrystalline silicon, polycrystalline silicon, and amorphous silicon. The efficiency of monocrystalline silicon solar cells is the highest (25 %), as compared with polycrystalline silicon (20 %) and amorphous silicon (10 %) solar cells, but they are most expensive. Crystalline silicon solar cells are used most often (around 90 %), and their coefficient of performance reaches 16–17 %. The manufacturing and usage of multijunction thin-film solar cells, however, is gradually increasing (the coefficient of their performance reaches 55 %) [3].

When looking for solutions to decrease the increasing energy prices and to reduce the environmental impact caused by energy, an increasingly bigger role is played by renewable energy sources, one of which is solar energy [4]. The option of solar energy usage is a solution for many people who have no access to an electricity network due to distance, small number of inhabitants, poverty or geographical situation. During the recent years, solar energy usage has increased because of improved technologies, reduced spending on production, and the governmental policy encouraging the renewable energy development [5]. Solar energy is being widely used worldwide as a source of energy for individual houses, commercial buildings, in industry, as well as for the lighting of streets, gardens and parks, and for water pumps.

Although the Lithuanian geographical latitude is not very favourable for solar energy usage, as compared with that of the countries located closer to the equator, the solar energy falling onto the earth surface here diffuses on a much more larger surface than in the geographical latitudes where the Sun is in zenith at midday. The annual amount of solar energy falling onto the surface of 1 m<sup>2</sup> area in place Lithuania exceeds 1000 kWh/m [6]. In the Lithuanian climate conditions, the cost of installation of 1 kW solar energy production reaches EUR 2.9–4.1 thousand per year. A photo-voltage system system with a 1 kW installed capacity produces 880–940 kWh of electricity, and the cost of its production is 0.41–0.43 EUR/kWh [7]. Photoelectricity is currently rather expensive, but with the rapid development of technologies the prices are forecast to become equal in 2018–2020 Lithuania has an obligation to the European Union to increase the share of renewable energy sources (RES) in electricity production to at least 20 % (which also include 10 MW of solar power plants) until 2020. Currently, the energy obtained from RES makes around 15 % of the final energy consumption in Lithuania [8].

**The aim of the study** was to examine changes of a solar cell's electromotive force, the reasons determining changes under various conditions for illuminance, and to draw a mathematical model for a solar cell electromotive force's dependency on illuminance.

## 2. Collection of experimental data

The research was carried out on a rooftop of a five-storey house during the period 18 March – 13 May 2012. A fixed exposition stand was mounted on the rooftop, and

other equipment necessary for the research was installed in an apartment located on the fifth floor of the house. Two solar cells (SCs) were installed on the rooftop, whereas a computer and a data converter were installed in the apartment. The created automated SC parameter measurement equipment included SCs integrated into lamps, a data collector, a portable computer, and software.

An analogue signal was converted into a digital one by a ADC-16 converter. The data collector was connected to the computer, enabling to register and collect data on the solar cell electromotive force. The PicoLog and Microsoft Excel programmes were used for data collection and analysis. SCs parameters were measured continuously, by recording the average 10-minute values in the computer database.

Two polycrystalline silicon solar cells with different areas of active parts were used for the experiment (area of the first SC  $5.58 \text{ cm}^2$  and of the second SC  $10.08 \text{ cm}^2$ );  $30 \text{ k}\Omega$  external resistances were connected to the polycrystalline solar cells to measure a drop of voltage in the resistances, *i.e.* the power of the electromotive force. Internal resistances of the solar cells ( $10 \Omega$ ) were significantly lower than external resistances.

The illuminance data, obtained from a company involved in the examination of solar modules, were used for the analysis of results. The illuminance was measured by a *Sunny SensorBox* meteorological station mounted on a horizontal surface of the SC module. During our experiment, polycrystalline silicon solar cells integrated into lamps were also exhibited in the horizontal position.

### 3. The dependence of solar cell electromotive force on illuminance

The SC monitoring data analysis revealed the existence of EMF periodic changes in the course of the day. Figure 1 presents data of the total period of the experiment, grouped by hours. The research results show that the EMF of the SC is observed from 5–6 h a.m. when the sun goes up, and it is no longer recorded after sunset (9–10 p.m.). The highest values of EMF are recorded at 2–3 p.m. when the sun is in the zenith.

Where there is a sufficiently large amount of experimental data collected, the abundance of the data almost surely reflects the shape of the approximation curve. Our case is exactly like that. Figure 2 presents experimental data obtained when researching EMF dependence on illuminance:  $\varepsilon = \varepsilon(E)$ .

Noteworthy, there are two important features of Figure 2:

- firstly, the data start at the beginning of the coordinates. This confirms the physical nature of the dependence: no illuminance – no EMF;
- secondly, an almost horizontal positioning of the data is clearly seen, which testifies to the saturation mode in the  $\varepsilon = \varepsilon(E)$  dependence: when illuminance  $E$  reaches the value  $E = 100 \text{ W/m}^2$ , the EMF of saturation no longer increases and equals about 2 V.

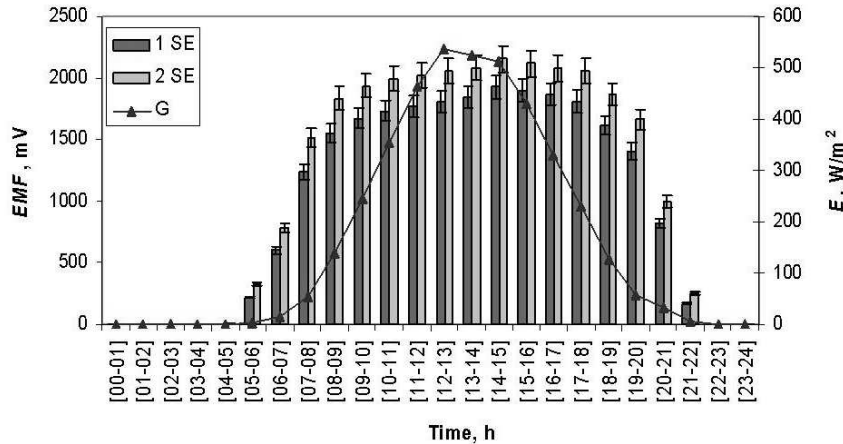


Fig. 1: Change of SC electromotive force and sun radiation intensity during a day (8 March – 13 May, 2012)

Generally, the selection of the approximation curve is a rather complicated issue requiring a special grounding. In our case, we will show the experimental data presented in Figure 2 as being of continuous dependence  $\varepsilon(E)$  of EMF on illuminance  $E$  (trend). We will consider this function not only as continuous, but as differentiated as well:  $\varepsilon(E) \in C^1[a, b]$  [9, 10]. To determine the trend function, we will make the presumption that the experimental data present the function of a fading exponent with respect to the saturation value:

$$(1) \quad \varepsilon = a(1 - e^{-bE}).$$

In this dependence,  $a$  and  $b$  are unknown parameters the values of which have to be determined. By using the Mathematica 8.0 programme package we obtain that  $a = 2085 \text{ mV}$  and  $b = 4.90 \cdot 10^{-2} \text{ m}^2/\text{W}$ . Figure 2 presents experimental data and the trend approximating it 1, with the parameters  $a$  and  $b$ .

The physical meaning of parameters  $a$  and  $b$  is seen in Figure 2. Parameter  $a$  means the maximum asymptotic EMF value  $\varepsilon_m$ , and parameter  $b$  is related to the illuminance  $E$  measurement units enabling to move to non-dimensional variables. The value  $E_0 \equiv 1/b = 20.4 \text{ W/m}^2$  is the value of illuminance at which EMF is reduced  $e$  times against the maximum value  $\varepsilon_m$  (Figure 3).

The selection of the trend function is related to a physical law under study. When the physical law is known, the trend function is most often related to the law or its modification. There are cases, however, when it is difficult, or even impossible, to establish the trend function in advance. In such cases, several approximations with various mathematical functions have to be carried out, and the Pearson correlation coefficient should be used [11]. In this case, the correlation coefficient is the criterion which helps to select the best approximation curve.

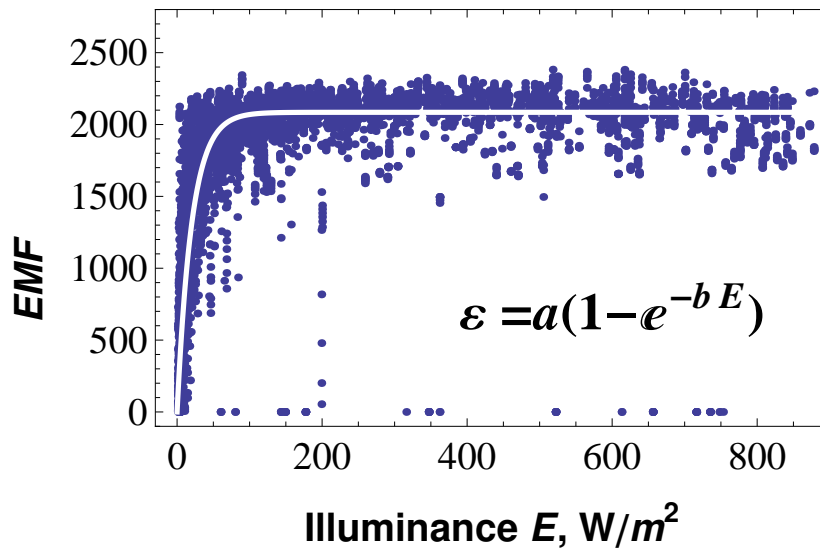


Fig. 2: Experimental data of EMF dependence on illuminance and the trend approximating it ( $a = 2085 \text{ mV}$ ,  $b = 4.90 \cdot 10^{-2} \text{ m}^2/\text{W}$ )

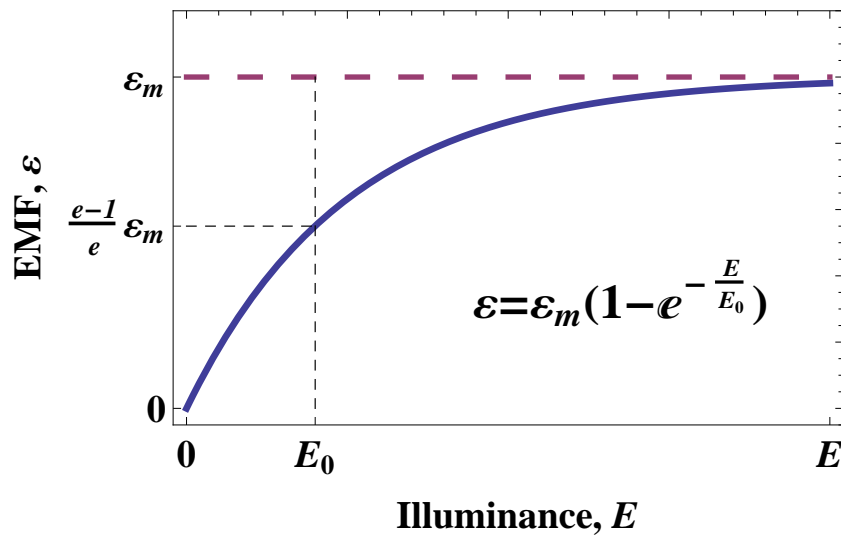


Fig. 3: Qualitative interpretation of the trend dependence ( $\varepsilon_m = 2085 \text{ mV}$ ;  $E_0 = 20.4 \text{ W/m}^2$ )

In addition to the experimental function 1, approximations with the power function and the logarithm function were performed. The results of these approximations are presented in Table 1.

Table 1: Various approximation functions, their parameters and correlation coefficients

Function	Parameters		$R^2$
	$a$	$b$	
$ax^b$	953	0.1248	0.569
$a \ln x + b$	276.9	225.7	0.727
$a(1 - e^{-bx})$	2085	$4.90 \cdot 10^{-2}$	0.983

As we can see, when considering the value of the correlation coefficient, the approximation carried out with an exponential function is the best.

#### 4. The mathematical model as a dynamical system

According to the general definition, a dynamical system is a set of the  $n$ -dimensional smooth manifold  $\mathcal{M}^n$  and a one-parameter group of diffeomorphisms  $g^t$  (see *e.g.* [12]):

$$(2) \quad DS = \{\mathcal{M}^n, g^t\},$$

Is it possible to consider solution 1 as an evolutionary function of a dynamical system?

The first step: we have to consider the illuminance  $E$  as a time variable. The next step: we have to find the differential equation and initial conditions with solution 1.

Finding a trend 1 is not yet a mathematical model. To find a differential equation the solution of which is the function 1, we will use of the method of undetermined coefficients [13]. We will establish the function 1 derivative:

$$(3) \quad \varepsilon' = abe^{-bE}.$$

Since there are two unknown coefficients in the function 1, a system of two equations, 1 and 3, is fully sufficient to establish the unknown differential equation of the mathematical model.

We will write down system of equations 1, 3:

$$(4) \quad \begin{cases} \varepsilon = a(1 - e^{-bE}), \\ \varepsilon' = abe^{-bE}, \end{cases}$$

there  $\varepsilon'$  means a derivative with respect to the illuminance  $E$ .

We will solve the system 4 with respect to functions  $\varepsilon$  and  $\varepsilon'$ , by eliminating an independent variable – illuminance  $E$ . It follows from the first equation that

$$(5) \quad ae^{-bE} = a - \varepsilon.$$

Upon entering the expression into the second equation of the system, we obtain a differential equation:

$$(6) \quad \varepsilon' = b(a - \varepsilon).$$

Considering the feature of the experimental data and the trend 1

$$(7) \quad \varepsilon(0) = 0,$$

we will get an answer to the modelling question: the differential equation 6 together with the initial conditions 7, make a Cauchy problem of the dependence under study.

Now let us make sure that the function 1 satisfies the differential equation 6 and the initial condition 7. Generally, a relevant programme package is suggested to be used for reaching this aim, but in our case the procedure is not complicated and can be performed manually: by entering function 1 into equation 6 and conditions 7, we obtain an identity.

## 5. Conclusions

The modelling of the solar cell EMF and illuminance has shown that in case of illuminance of  $100 \text{ W/m}^2$ , EMF reaches a value of around 2 V and then changes insignificantly with an increase of illuminance; consequently, this means that in case of the above illuminance the SC operates at its highest efficiency. The research results show that the illuminance reaches the value of  $100 \text{ W/m}^2$  at 8–9 a.m., and the value decreases to  $< 100 \text{ W/m}^2$  at 7–8 p.m., *i.e.* SCs work most efficiently during the above hours.

The established differential equation 6, together with the initial condition 7, can be interpreted as a continuous dynamic system in which the role of time is played by illuminance  $E$ . This dynamic system is linear. Its phase portrait, with a change of the parameter  $b$ , includes straight lines of various trends, going through the beginning of the coordinates.

It should be stressed that in cases allowing a change of the other parameters of SC, which were fixed in our case, the determined dependency of SC EMF on illuminance  $\varepsilon = f(E)$  1 can be more complicated. The corresponding differential equation can be a nonlinear one. As a consequence, the phase portrait of such a system will be different. However, there remains the main idea that the dependence of the crystal semiconductor SC electromotive force on illuminance can be interpreted as a dynamic system.

The general understanding that a dynamic system is a set of the  $n$ -dimensional smooth manifold  $\mathcal{M}^n$  and a one-parameter group of diffeomorphisms 2, can be generalized. It is enough to require one-side differentiability instead of smoothness, whereas the group of diffeomorphisms can be restricted to its semigroup  $g^{t+}$ . The DS generalized in this way enables the usage of singular integro-differential operators instead of a classical evolution operator [14].

We see that the interpretation of the SC illuminance  $E$  as the “time” variable is productive since it allows applying powerful DS methods for the SC mathematical modelling. The other possible sphere of mathematical modelling is related to the analysis of the fluctuation of experimental values with respect to the trend.

### Acknowledgements

Paulius Miškinis would like to express his cordial thanks to Prof. Julian Ławrynowicz as a many-year organizer of the Będlewo Conferences. He is indebted to Prof. J. Ławrynowicz for stimulating discussions, for his interest to and support of his work, for the possibility to meet interesting people.

### References

- [1] T. Ma and Y. Nakamori, *Modeling technological change in energy systems – from optimization to agent-based modeling*, Energy **34**, no. 7 (2009), 873–879.
- [2] T. Markvart, *Solar electricity for the third millennium*, Photovolt. Bull., Elsevier Advanced Technology **1** (2001), 7–11.
- [3] V. Adomavičius, *Atsinaujinančiųjų energijos išteklių naudojimo galimybės daugiabučiuose namuose*, Lietuvos taikomųjų mokslų akademijos mokslo darbai: tarptautinis inovacinis taikomųjų mokslų darbų žurnalas, Official Journal of Lithuanian Applied Sciences Academy, Klaipėdos Universitetas (2010), 107–122 (in Lithuanian).
- [4] N. L. Panwar, S. C. Kaushik and S. Kothari, *Role of renewable energy sources in environmental protection*, Renew. Sustain. Energ. Rev. **15** (2011), 1513–1524.
- [5] G. R. Timilsina, L. Kurdgelashvili and P. A. Narber, *Solar energy: Markets, economics and policies*, Renew. Sustain. Energ. Rev. **16** (2012), 449–465.
- [6] M. Šūri, T. A. Hiild and E. G. Dlp, *PVGIS: a web-based solar radiation database for calculation of PV potential in Europe*, Int. J. of Sustain. Energ. **24**, no. 2 (2005), 55–67.
- [7] V. Mačiulis, *Lietuvos Saulė - galimybės energetikos sektoriui*, Energijos erdvė **5**, no. 7 (2010) (in Lithuanian).
- [8] National Energy Strategy (Nacionalinė energetikos (energetinės nepriklausomybės) strategija), Projektas. Patvirtinta Lietuvos Respublikos Seimo 2010 m. spalio 6 d., Vilnius (in Lithuanian).
- [9] R. Slingerland and L. Kump, *Mathematical Modelling of Earth's Dynamical Systems*, Princeton University Press, Princeton-New Jersey 2011.
- [10] A. A. Samarskij and A. P. Mihajlov, *Matematicheskoe Modelirovanie. Idei, metody, primery*, 2-nd ed., Moscow 2001 (in Russian).
- [11] W. P. Fox, F. R. Goirdano and M. D. Weir, *First Course in Mathematical Modeling*, Tomson Learning, Third Edition, 2003.
- [12] V. I. Arnold, *Ordinary Differential Equations*, Various editions from MIT Press and from Springer Verlag, chapter 1 "Fundamental concepts". Springer Science & Business Media, 1992.
- [13] W. A. Adkins and M. G. Davidson, *Ordinary Differential Equations*, Springer, New York 2012.
- [14] P. Miškinis, *Nonlinear and Nonlocal Integrable Models*, Technika, Vilnius 2003 (in Lithuanian).

Vilnius Gediminas Technical University  
Saulėtekio Ave. 11, LT-10223 Vilnius  
Lithuania  
e-mails: paulius.miskinis@vgtu.lt  
vaida.valuntaite@vgtu.lt

Presented by Jakub Rembieliński at the Session of the Mathematical-Physical Commission of the Łódź Society of Sciences and Arts on November 20, 2014

## ZALEŻNOŚĆ SIŁY ELEKTROMOTORYCZNEJ KOMÓRKI SŁONECZNEJ KRYSZTAŁU PÓLPRZEWODNIKA NA OŚWIETLENIE JAKO UKŁAD DYNAMICZNY

### S t r e s z c z e n i e

Autorzy zajmują się badaniem polikrystalicznych krzemowych komórek słonecznych z różnych obszarów ich aktywnych części. Analizowany jest wpływ natężenia oświetlenia na zmiany siły elektromotorycznej komórki słonecznej. Przedstawiono model matematyczny zależności siły elektromotorycznej komórki słonecznej na oświetlenie. W tym celu wybrano eksperymentalną funkcję trendu danych i wyznaczono współczynniki korelacji Pearsona. Najbardziej optymalne wyniki uzyskano dla funkcji wykładniczej z najsilniejszą obserwowaną korelacją ( $R^2 = 0.983$ ). Analiza wykazała, że dla natężenia oświetlenia  $100 \text{ W/m}^2$  otrzymuje się nasycenie siły elektromotorycznej (siła ta zmienia się nieistotnie i fluktuuje wokół 2 V), co z kolei oznacza, że przy osiągnięciu takiego natężenia oświetlenia ogniwo słoneczne ma największą wydajność pracy. Uzyskano równanie różniczkowe pierwszego rzędu, które spełnia funkcja trendu. Analiza wykazała, że przy interpretacji natężenia jako zmiennej zależnej od czasu dochodzimy do interpretacji dynamicznej przedstawionego modelu matematycznego.

*Słowa kluczowe:* komórka słoneczna, siła elektromotoryczna, oświetlenie, układ dynamiczny



## B U L L E T I N

DE LA SOCIÉTÉ DES SCIENCES ET DES LETTRES DE ŁÓDŹ

2014

Vol. LXIV

Recherches sur les déformations

no. 3

pp. 31–43

*In memory of*  
*Professor Zygmunt Charzyński (1914–2001)*

*Gertruda Ivanova and Elżbieta Wagner-Bojakowska*

### ON SOME SUBFAMILIES OF DARBOUX QUASI-CONTINUOUS FUNCTIONS

#### Summary

The proof that the family of strong Świątkowski functions with nowhere dense set of discontinuity points is dense in the family  $\mathcal{DQ}$  of the Darboux quasi-continuous functions is given. Also a generalization of the strong Świątkowski property is considered and the conditions under which the family of functions having the  $\mathcal{A}$ -Darboux property with nowhere dense set of discontinuity points is contained and dense in the family  $\mathcal{DQ}$  are given.

*Keywords and phrases:* Darboux property, strong Świątkowski property, quasi-continuity

In this note we introduce some families of functions  $f : \mathbb{R} \rightarrow \mathbb{R}$  modifying Darboux property analogously as it was done by A. Maliszewski in [10]. Here the continuity is replaced with  $\mathcal{A}$ -continuity, i.e. continuity with respect to a family  $\mathcal{A}$  of subsets in the domain. We prove that if  $\mathcal{A}$  has the (\*)-property then the family of functions having the  $\mathcal{A}$ -Darboux property with nowhere dense set of discontinuity points is contained and dense in the family  $\mathcal{DQ}$  of the Darboux quasi-continuous functions. Moreover, we prove that the family of the strong Świątkowski functions with nowhere dense sets of discontinuity points is dense in the family  $\mathcal{DQ}$  of the Darboux quasi-continuous functions.

In 1977 T. Mańk and T. Świątkowski in [11] defined a modification of the Darboux property. They considered a family of functions with so called Świątkowski property.

To simplify our notation, we shall write:

$$\langle a, b \rangle = (\min\{a, b\}, \max\{a, b\}).$$

**Definition 1.** [11] *A function  $f : \mathbb{R} \rightarrow \mathbb{R}$  has the Świątkowski property if for each interval  $(a, b) \subset \mathbb{R}$  there exists a point  $x_0 \in (a, b)$  such that  $f(x_0) \in \langle f(a), f(b) \rangle$  and  $f$  is continuous at  $x_0$ .*

In 1995 A. Maliszewski investigated a class of functions which possess a stronger property.

**Definition 2.** [10] *A function  $f : \mathbb{R} \rightarrow \mathbb{R}$  has the strong Świątkowski property (briefly  $f \in \mathcal{D}_s$ ) if for each interval  $(a, b) \subset \mathbb{R}$  and for each  $\lambda \in \langle f(a), f(b) \rangle$  there exists a point  $x_0 \in (a, b)$  such that  $f(x_0) = \lambda$  and  $f$  is continuous at  $x_0$ .*

Z. Grande in 2009 considered a modification of the strong Świątkowski property replacing the continuity with approximate continuity.

**Definition 3.** [3] *A function  $f : \mathbb{R} \rightarrow \mathbb{R}$  has the ap-Darboux property (briefly  $f \in \mathcal{D}_{ap}$ ) if for each interval  $(a, b) \subset \mathbb{R}$  and for each  $\lambda \in \langle f(a), f(b) \rangle$  there exists a point  $x_0 \in (a, b)$  such that  $f(x_0) = \lambda$  and  $f$  is approximately continuous at  $x_0$ .*

Let  $\mathcal{I}$  be the  $\sigma$ -ideal of sets of the first category. In [4] and [5] we introduced a family of functions  $f : \mathbb{R} \rightarrow \mathbb{R}$  modifying the Darboux property analogously as it was done by Z. Grande and replacing approximate continuity with  $\mathcal{I}$ -approximate continuity, i.e. continuity with respect to the  $\mathcal{I}$ -density topology in the domain (see [2, 13, 14, 17, 18]).

**Definition 4.** [5] *A function  $f : \mathbb{R} \rightarrow \mathbb{R}$  has the  $\mathcal{I}$ -ap-Darboux property (briefly  $f \in \mathcal{D}_{\mathcal{I}-ap}$ ) if for each interval  $(a, b) \subset \mathbb{R}$  and for each  $\lambda \in \langle f(a), f(b) \rangle$  there exists a point  $x_0 \in (a, b)$  such that  $f(x_0) = \lambda$  and  $f$  is  $\mathcal{I}$ -approximately continuous at  $x_0$ .*

Let  $\mathcal{A} \subset \mathcal{P}(\mathbb{R})$ , where  $\mathcal{P}(\mathbb{R})$  is the power set of  $\mathbb{R}$ . To simplify our considerations we need the following definition.

**Definition 5.** *A function  $f : \mathbb{R} \rightarrow \mathbb{R}$  is  $\mathcal{A}$ -continuous at a point  $x \in \mathbb{R}$  if for each open set  $V \subset \mathbb{R}$  with  $f(x) \in V$  there exists a set  $A \in \mathcal{A}$  such that  $x \in A$  and  $f(A) \subset V$ . We will say that  $f : \mathbb{R} \rightarrow \mathbb{R}$  is  $\mathcal{A}$ -continuous if  $f$  is  $\mathcal{A}$ -continuous at each point  $x \in \mathbb{R}$ .*

If  $\mathcal{A}$  is the Euclidean topology  $\tau_e$ , then the notion of the  $\mathcal{A}$ -continuity coincides with the notion of the continuity in the classical sense; if  $\mathcal{A}$  is the density topology  $\tau_d$ , then we have approximate continuity; and if  $\mathcal{A}$  is the  $\mathcal{I}$ -density topology  $\tau_{\mathcal{I}}$ , then we obtain  $\mathcal{I}$ -approximate continuity. If  $\mathcal{A}$  is an arbitrary topology  $\tau$  on  $\mathbb{R}$ , then  $\mathcal{A}$ -continuity is a continuity between  $(\mathbb{R}, \tau)$  and  $(\mathbb{R}, \tau_e)$ .

Of course,  $\mathcal{A}$  need not to be a topology. Let us denote by  $\overline{A}$  ( $Int(A)$ ) the closure (interior) of the set  $A$  in the Euclidean topology. A set  $A \subset \mathbb{R}$  is said to be semi-open

if there is an open set  $U$  such that  $U \subset A \subset \overline{U}$  (see [9]). It is not difficult to see that  $A$  is semi-open iff  $A \subset \overline{\text{Int}(A)}$ . The family of all semi-open sets will be denoted by  $\mathcal{S}$ . A function  $f : \mathbb{R} \rightarrow \mathbb{R}$  is semi-continuous if for each set  $V$  open in the Euclidean topology the set  $f^{-1}(V)$  is semi-open (see [9]).

**Definition 6.** *A function  $f : \mathbb{R} \rightarrow \mathbb{R}$  is quasi-continuous at a point  $x$  if for every neighbourhood  $U$  of  $x$  and for every neighbourhood  $V$  of  $f(x)$  there exists a non-empty open set  $G \subset U$  such that  $f(G) \subset V$ . A function  $f : \mathbb{R} \rightarrow \mathbb{R}$  is quasi-continuous (briefly  $f \in \mathcal{Q}$ ) if it is quasi-continuous at each point.*

A. Neubrunnová proved in [12] that  $f$  is semi-continuous if and only if it is quasi-continuous.

It is easy to see that  $\mathcal{S}$  is not a topology and if  $\mathcal{A}$  is the family of semi-open sets  $\mathcal{S}$ , then  $\mathcal{A}$ -continuity coincides with quasi-continuity.

Let  $D(f)$  denote the set of discontinuity points of  $f$ .

**Definition 7.** (compare [15]) *A function  $f : \mathbb{R} \rightarrow \mathbb{R}$  is internally Darboux quasi-continuous if it is Darboux quasi-continuous and the set  $D(f)$  of discontinuity points of  $f$  is nowhere dense.*

The family of all internally Darboux quasi-continuous functions we will denote by  $\mathcal{DQ}_i$ .

**Definition 8.** [6] *A function  $f : \mathbb{R} \rightarrow \mathbb{R}$  has the  $\mathcal{A}$ -Darboux property (briefly  $f \in \mathcal{D}_{\mathcal{A}}$ ) if for each interval  $(a, b) \subset \mathbb{R}$  and each  $\lambda \in (f(a), f(b))$  there exists a point  $x \in (a, b)$  such that  $f(x) = \lambda$  and  $f$  is  $\mathcal{A}$ -continuous at  $x$ .*

It is easy to see that if  $\mathcal{A}$  is the Euclidean topology  $\tau_e$ , then  $\mathcal{D}_{\mathcal{A}} = \mathcal{D}_{\tau_e} = \mathcal{D}_s$ , if  $\mathcal{A}$  is the density topology  $\tau_d$ , then  $\mathcal{D}_{\mathcal{A}} = \mathcal{D}_{\tau_d} = \mathcal{D}_{ap}$  and if  $\mathcal{A}$  is the  $\mathcal{I}$ -density topology, then  $\mathcal{D}_{\mathcal{A}} = \mathcal{D}_{\tau_{\mathcal{I}}} = \mathcal{D}_{\mathcal{I}-ap}$ .

The family of all functions having the  $\mathcal{A}$ -Darboux property with nowhere dense set of discontinuity points we will denote by  $\mathcal{D}_{\mathcal{A}i}$ .

The set  $A$  is of the first category at the point  $x$  (see [7]) if there exists an open neighbourhood  $G$  of  $x$  such that  $A \cap G$  is of the first category. We will denote by  $D(A)$  the set of all points  $x$  such that  $A$  is not of the first category at  $x$ .

Let  $\mathcal{B}a$  be a family of all sets having the Baire property.

**Definition 9.** *The family  $\mathcal{A}$  have the  $(*)$ -property, if*

1.  $\tau_e \subset \mathcal{A} \subset \mathcal{B}a$ ;
2.  $A \subset D(A)$  for each  $A \in \mathcal{A}$ .

Clearly, there is a wide class of topologies having the  $(*)$ -property: Euclidean topology,  $\mathcal{I}$ -density topology, topologies constructed in [8] by E. Łazarow,

R. A. Johnson, W. Wilczyński or topology constructed by Wiertelak in [16]. Also the family of semi-open sets has this property, but it does not have the density topology.

**Definition 10.** *We will say that  $f : \mathbb{R} \rightarrow \mathbb{R}$  has the q-property if for each  $(a, b) \subset \mathbb{R}$  and for each non-empty open interval  $(C, D) \subset f((a, b))$  there exists a non-empty open interval  $(c, d) \subset (a, b)$  such that  $f((c, d)) \subset (C, D)$ .*

In [6] we proved that the Darboux function  $f : \mathbb{R} \rightarrow \mathbb{R}$  has the q-property iff  $f$  is quasi-continuous (Lemma 1) and if the family  $\mathcal{A}$  has the (\*)-property and  $f \in \mathcal{D}_{\mathcal{A}}$ , then  $f$  has the q-property. Consequently, if  $\mathcal{A}$  has the (\*)-property, then  $\mathcal{D}_s \subset \mathcal{D}_{\mathcal{A}} \subset \mathcal{DQ}$  ([6], Theorem 1).

Let  $\mathcal{U}$  be a family of all functions such that for each  $a < b$  and for each set  $A \subset [a, b]$  with  $\text{card}(A) < \text{card}(\mathbb{R})$ , the set  $f([a, b] \setminus A)$  is dense in  $\langle f(a), f(b) \rangle$ . Let  $\mathcal{QU} = \mathcal{Q} \cap \mathcal{U}$ . As  $\mathcal{D} \subset \mathcal{U}$  (for more details see [1]), we have  $\mathcal{DQ} \subset \mathcal{QU}$ .

Let us introduce a metric  $\rho$  in the space  $\mathcal{UQ}$  in a following way:

$$\rho(f, g) = \min \{1, \sup \{|f(t) - g(t)| : t \in \mathbb{R}\}\}.$$

We proved also that if  $\mathcal{A}$  has the (\*)-property, then  $\mathcal{D}_{\mathcal{A}}$  is dense in  $(\mathcal{DQ}, \rho)$  and the closure of  $\mathcal{D}_{\mathcal{A}}$  equals  $\mathcal{QU}$  ([6], Corollary 1).

Let us show the stronger result, it means, that not only  $\mathcal{D}_{\mathcal{A}}$  but also  $\mathcal{D}_{\mathcal{A}i}$  is dense in  $(\mathcal{DQ}, \rho)$ . For this purpose we need the following lemma:

**Theorem 1.** *For each function  $f \in \mathcal{DQ}$  and for each number  $\epsilon > 0$  there exists a function  $h \in \mathcal{DQ}_i$  such that  $\rho(f, h) < \epsilon$ .*

*Proof.* Let  $f \in \mathcal{DQ}$  and  $\epsilon > 0$ . Fix  $n_0 \in \mathbb{N}$  such that  $1/n_0 < \epsilon$ . Put

$$E_0 = \{x \in \mathbb{R} : \text{osc}(f, x) \geq \frac{1}{n_0}\}.$$

As  $f$  is quasi-continuous, the set of continuity points of  $f$  is dense in  $(\mathbb{R}, \tau_{\epsilon})$  and of type  $G_{\delta}$ , so it is residual. Of course,  $E_0 \subset D(f)$  and  $E_0$  is closed (as oscillation is upper semi-continuous function). So  $E_0$  is closed and nowhere dense set.

If there exists a number  $a$  such that  $(-\infty, a)$  is a component interval of  $\mathbb{R} \setminus E_0$ , then put  $E_1 = \{a - i + 1 : i \in \mathbb{N}\}$ . In the opposite case  $E_1 = \emptyset$ . If there exists a number  $b$  such that  $(b, \infty)$  is a component interval of  $\mathbb{R} \setminus E_0$ , then put  $E_2 = \{b + i - 1 : i \in \mathbb{N}\}$ . In the opposite case  $E_2 = \emptyset$ .

Put  $E = E_0 \cup E_1 \cup E_2$ . It is not difficult to see that  $E$  is closed and nowhere dense.

Put

$$\mathbb{R} \setminus E = \bigcup_{n=1}^{\infty} (a_n, b_n),$$

where  $\{(a_n, b_n)\}_{n \in \mathbb{N}}$  is the sequence of all component intervals of  $\mathbb{R} \setminus E$ .

Let us modify the function  $f$ . Fix  $n \in \mathbb{N}$  and let  $I_0 \subset (a_n, b_n)$  be a nondegenerate closed interval concentric with  $(a_n, b_n)$ .

As  $(a_n, b_n) \subset \mathbb{R} \setminus E_0$ , for each  $x \in (a_n, b_n)$  there exists a number  $\delta_x > 0$  such that  $\text{osc}(f, (x - \delta_x, x + \delta_x)) < 1/n_0$ . We can assume that  $\delta_x < \min I_0 - a_n$ . Let us choose from the cover  $\{(x - \delta_x, x + \delta_x) : x \in I_0\}$  of the interval  $I_0$  the minimal finite subcover, i.e. cover which does not contain unnecessary intervals. Denote the intervals from this subcover by  $(c_k^n, d_k^n)$ , where  $k = 0, 1, 2, \dots, k_0$ ,  $d_k^n < c_{k+2}^n$  for each  $k = 0, 1, 2, \dots, k_0 - 2$  and  $c_1^n > \min I_0$ ,  $d_{k_0-1}^n < \max I_0$ .

Put

$$J_0 = \overline{\bigcup_{k=0}^{k_0} (c_k^n, d_k^n)}.$$

Hence  $J_0 \subset (a_n, b_n)$ . Let us consider the interval

$$I_{-1} = \left[ \frac{1}{2} (a_n + \min J_0), \min J_0 \right].$$

Obviously,  $I_{-1} \subset (a_n, b_n)$ .

For each  $x \in I_{-1}$  select a number  $\delta_x < \min\{\min I_{-1} - a_n, c_1^n - c_0^n\}$  such that  $\text{osc}(f, (x - \delta_x, x + \delta_x)) < 1/n_0$ . From the family  $\{(x - \delta_x, x + \delta_x) : x \in I_{-1}\}$  choose the minimal finite cover. Denote the intervals from this cover by  $(c_k^n, d_k^n)$ , where  $k = -1, -2, \dots, -k_{-1}$ ,  $d_k^n < c_{k+2}^n$  for each  $k = -1, -2, \dots, -k_{-1}$  and  $c_{-k_{-1}+1}^n > \min I_{-1}$ ,  $d_{-2}^n < \max I_{-1}$ . Together with such chosen family it is a finite minimum cover of the interval  $[\min I_{-1}, \max I_0]$ . Let

$$J_{-1} = \overline{\bigcup_{k=1}^{k_{-1}} (c_{-k}^n, d_{-k}^n)}.$$

Analogously we construct the interval

$$I_1 = \left[ \max J_0, \frac{1}{2} (\max J_0 + b_n) \right]$$

and repeat the same procedure: for each  $x \in I_1$  we select a number  $\delta_x < \min\{b_n - \max I_1, d_{k_0}^n - d_{k_0-1}^n\}$ . From the family  $\{(x - \delta_x, x + \delta_x) : x \in I_1\}$  we choose the minimal finite cover. Denote the intervals from this cover by  $(c_{k_0+1}^n, d_{k_0+1}^n), \dots, (c_{k_0+k_1}^n, d_{k_0+k_1}^n)$ , where  $d_{k_0+k}^n < c_{k_0+k+2}^n$  for each  $k = -1, 0, \dots, k_1 - 2$ , and put

$$J_1 = \overline{\bigcup_{k=1}^{k_1} (c_{k_0+k}^n, d_{k_0+k}^n)}.$$

Let  $i \in \mathbb{N} \setminus \{1\}$ . Assume that we have constructed intervals  $I_j$  and  $J_j$  for  $j \in \{-i+1, -i+2, \dots, i-1\}$  and chosen minimal and finite cover  $\{(c_k^n, d_k^n) : k = -i_-, \dots, i_+\}$  of the interval  $[\min I_{-i+1}, \max I_{i-1}]$ , where

$$i_- = \sum_{j=1}^{i-1} k_{-j} \quad \text{and} \quad i_+ = \sum_{j=0}^{i-1} k_j.$$

Put

$$I_{-i} = \left[ \frac{1}{2} (a_n + \min J_{-i+1}), \min J_{-i+1} \right]$$

and

$$I_i = \left[ \max J_{i-1}, \frac{1}{2} (\max J_{i-1} + b_n) \right].$$

For each  $x \in I_{-i}$  select a number

$$\delta_x < \min\{\min I_{-i} - a_n, c_{-i-1}^n - c_{-i}^n\}$$

such that  $\text{osc}(f, (x - \delta_x, x + \delta_x)) < 1/n_0$ .

From the family  $\{(x - \delta_x, x + \delta_x) : x \in I_{-i}\}$  choose the minimal finite cover. Denote the intervals from this cover by  $(c_k^n, d_k^n)$ , where

$$k = -i_- - 1, -i_- - 2, \dots, -i_- - k_{-i}, \quad d_k^n < c_{k+2}^n$$

for each

$$k = -i_- - 1, -i_- - 2, \dots, -i_- - k_{-i}$$

and

$$c_{-i_- - k_{-i} + 1}^n > \min I_{-i}, \quad d_{-i_- - 2}^n < \max I_{-i}.$$

Together with the preselected cover the family chosen in such a way is a finite minimum cover of the interval  $[\min I_{-i}, \max I_{-i}]$ . Put

$$J_{-i} = \overline{\bigcup_{k=1}^{k_{-i}} (c_{-i_- - k}^n, d_{-i_- - k}^n)}.$$

Analogously for each  $x \in I_i$  find a number

$$\delta_x < \min\{b_n - \max I_i, d_{i_+}^n - d_{i_+ - 1}^n\}$$

such that  $\text{osc}(f, (x - \delta_x, x + \delta_x)) < 1/n_0$ .

From the family  $\{(x - \delta_x, x + \delta_x) : x \in I_i\}$  choose the minimal finite cover. Denote the intervals from this cover by  $(c_k^n, d_k^n)$ , where

$$k = i_+ + 1, i_+ + 2, \dots, i_+ + k_i, \quad d_k^n < c_{k+2}^n$$

for each

$$k = i_+ - 1, i_+, \dots, i_+ + k_i - 2$$

and

$$c_{i_+ + 1}^n > \min I_i, \quad d_{i_+ + k_i - 1}^n < \max I_i.$$

Together with the preselected cover such chosen family is a finite minimum cover of the interval  $[\min I_i, \max I_i]$ . Put

$$J_i = \overline{\bigcup_{k=1}^{k_i} (c_{i_+ + k}^n, d_{i_+ + k}^n)}.$$

Next, we proceed inductively and result is the sequence (infinite in both directions) of open intervals  $(c_k^n, d_k^n)_{k \in \mathbb{Z}}$  such that:

- (i)  $\bigcup_{k \in \mathbb{Z}} (c_k^n, d_k^n) = (a_n, b_n)$ ,
- (ii)  $\forall k \in \mathbb{Z} c_k^n < c_{k+1}^n < d_k^n < c_{k+2}^n < d_{k+1}^n < c_{k+3}^n < d_{k+2}^n < \dots$ ,
- (iii)  $d_k^n - c_k^n \xrightarrow{k \rightarrow \infty} 0$  and  $d_k^n - c_k^n \xrightarrow{k \rightarrow -\infty} 0$ .

Let us define the function  $h_n$  on the interval  $(a_n, b_n)$ . Let  $k$  be an arbitrary integer. Choose the points  $y_k^n \in (c_{k+1}^n, d_k^n)$  for  $k \in \mathbb{Z}$ . In each interval  $(y_{k-1}^n, y_k^n)$  contained in  $(c_k^n, d_k^n)$  find two points  $t_k^n$  and  $z_k^n$  (for example  $y_{k-1}^n < t_k^n < z_k^n < y_k^n$ ). It is easy to see that

$$(a_n, b_n) = \bigcup_{k \in \mathbb{Z}} [y_{k-1}^n, y_k^n].$$

For each  $n \in \mathbb{N}$  define a function  $h_n$  on the interval  $(a_n, b_n)$  in the following way:

$$h_n(x) = \begin{cases} f(x) & \text{for } x = y_k^n, k \in \mathbb{Z}, \\ \sup\{f(t) : t \in [y_{k-1}^n, y_k^n]\} & \text{for } x = t_k^n, k \in \mathbb{Z}, \\ \inf\{f(t) : t \in [y_{k-1}^n, y_k^n]\} & \text{for } x = z_k^n, k \in \mathbb{Z}, \\ \text{linear} & \text{on the intervals } [y_{k-1}^n, t_k^n], [t_k^n, z_k^n], \\ & [z_k^n, y_k^n], k \in \mathbb{Z}. \end{cases}$$

Therefore  $h_n$  is defined on the interval  $(a_n, b_n)$ , i.e. on the component interval of  $\mathbb{R} \setminus E$ .

As

$$[y_{k-1}^n, y_k^n] \subset (c_k^n, d_k^n)$$

for  $k \in \mathbb{Z}$ ,  $n \in \mathbb{N}$  and

$$\text{osc}(f, (c_k^n, d_k^n)) < \frac{1}{n_0},$$

hence from the construction of the function  $h_n$  it follows that

$$\sup\{|f(x) - h_n(x)| : x \in [y_{k-1}^n, y_k^n]\} \leq \frac{1}{n_0} < \epsilon.$$

So  $\rho(f|_{(a_n, b_n)}, h_n) \leq \frac{1}{n_0} < \epsilon$ .

Put

$$h(x) = \begin{cases} h_n(x) & \text{for } x \in (a_n, b_n), n \in \mathbb{N}, \\ f(x) & \text{for } x \in E. \end{cases}$$

It is easy to see that at each point of  $\mathbb{R} \setminus E$  the function  $h$  is continuous. Therefore the set of discontinuity points of  $h$  is nowhere dense.

Let us prove that  $h$  has the Darboux property.

Let  $[x', x'']$  be an arbitrary interval. We will show that the set  $h([x', x''])$  is connected.

1. If  $[x', x''] \cap E = \emptyset$ , then  $[x', x'']$  is contained in a component of the set  $\mathbb{R} \setminus E$ , where  $h$  is continuous, so  $h([x', x''])$  is connected.

2. If  $[x', x''] \cap E \neq \emptyset$ , then

$$(1) \quad \begin{aligned} [x', x''] &= [\min([x', x''] \cap E), \max([x', x''] \cap E)] \\ &\cup [x', \min([x', x''] \cap E)] \cup [\max([x', x''] \cap E), x'']. \end{aligned}$$

It may happen that some intervals in formula (1) are single-point. Then this point belongs to another summand of (1), therefore we consider the case, when all summands of (1) are nondegenerate intervals.

Consider an interval  $[x', \min([x', x''] \cap E)]$ . It is a part of a component interval  $(a_n, b_n)$  with an attached right end, i.e.  $[x', \min([x', x''] \cap E)] = [x', b_n]$ . Hence there exists a number  $k \in \mathbb{N}$  such that  $y_k^n \in [x', b_n]$ . From the construction of  $h$  we have for each  $i \in \mathbb{N}$ ,  $j \in \mathbb{Z}$

$$(2) \quad f([y_j^i, y_{j+1}^i]) \subset h([y_j^i, y_{j+1}^i]) \subset \overline{f([y_j^i, y_{j+1}^i])}.$$

Observe that

$$[x', b_n] = [x', y_k^n] \cup [y_k^n, b_n] = [x', y_k^n] \cup \bigcup_{j=k}^{\infty} [y_j^n, y_{j+1}^n] \cup \{b_n\}.$$

Hence, by (2), we have

$$(3) \quad \begin{aligned} f([y_k^n, b_n]) &= \bigcup_{j=k}^{\infty} f([y_j^n, y_{j+1}^n]) \cup f(\{b_n\}) \\ &\subset \bigcup_{j=k}^{\infty} h([y_j^n, y_{j+1}^n]) \cup h(\{b_n\}) = h([y_k^n, b_n]) \\ &\subset \bigcup_{j=k}^{\infty} \overline{f([y_j^n, y_{j+1}^n])} \cup f(\{b_n\}) \\ &\subset \overline{\bigcup_{j=k}^{\infty} f([y_j^n, y_{j+1}^n]) \cup f(\{b_n\})} = \overline{f([y_k^n, b_n])}. \end{aligned}$$

As  $f$  has the Darboux property, the set  $h([y_k^n, b_n])$  is connected.

The function  $h$  is continuous on  $[x', y_k^n]$ ,  $h([x', b_n])$  is a union of two intervals which have common point, so  $h([x', b_n])$  is connected.

Analogously the interval  $[\max([x', x''] \cap E), x'']$  is a part of a component  $(a_m, b_m)$  with an attached left end, hence

$$[\max([x', x''] \cap E), x''] = [a_m, x'']$$

and, as previously, we can show that the set  $h([a_m, x''])$  is connected, too.

It follows easily that

$$[\min([x', x''] \cap E), \max([x', x''] \cap E)] = [b_n, a_m].$$

Let

$$M = \{i \in \mathbb{N} : (a_i, b_i) \subset [b_n, a_m]\}.$$

Hence we have

$$[b_n, a_m] = (E \cap [b_n, a_m]) \cup \bigcup_{i \in M} \bigcup_{j \in \mathbb{Z}} [y_j^i, y_{j+1}^i].$$

So, from (2), we obtain

$$\begin{aligned} f([b_n, a_m]) &= f([b_n, a_m] \cap E) \cup \bigcup_{i \in M} \bigcup_{j \in \mathbb{Z}} f([y_j^i, y_{j+1}^i]) \\ &\subset h([b_n, a_m] \cap E) \cup \bigcup_{i \in M} \bigcup_{j \in \mathbb{Z}} h([y_j^i, y_{j+1}^i]) = h([b_n, a_m]) \\ &\subset f([b_n, a_m] \cap E) \cup \bigcup_{i \in M} \bigcup_{j \in \mathbb{Z}} \overline{f([y_j^i, y_{j+1}^i])} \\ &\subset \overline{f([b_n, a_m] \cap E) \cup \bigcup_{i \in M} \bigcup_{j \in \mathbb{Z}} f([y_j^i, y_{j+1}^i])} = \overline{f([b_n, a_m])}. \end{aligned}$$

As  $f$  has the Darboux property, the set  $h([b_n, a_m])$  is connected.

Hence  $h([x', x''])$  is a union of three connected sets  $h([x', b_n])$ ,  $h([b_n, a_m])$  and  $h([a_m, x''])$ , such that the first and the second, also the second and the third sets are not disjoint, so the set  $h([x', x''])$  is connected, too.

Let us show that  $h$  has the  $q$ -property. Let  $(a, b)$  be an interval on which  $h$  is not constant and let  $(C, D) \subset h((a, b))$ ,  $C < D$ . We will show that there exists an open nondegenerate interval  $(c, d) \subset (a, b)$  such that  $h((c, d)) \subset (C, D)$ .

Fix  $y \in (C, D)$ . Then we can find a point  $x \in (a, b)$  such that  $h(x) = y$ .

There are possible cases:

1. there exists a component interval  $(a_n, b_n)$  of complement of  $E$  with  $x \in (a_n, b_n)$ .  
Hence  $h$  is continuous at  $x$  and we can find a number  $\delta > 0$  such that

$$(x - \delta, x + \delta) \subset (a, b) \quad \text{and} \quad h((x - \delta, x + \delta)) \subset (C, D).$$

Put  $(c, d) = (x - \delta, x + \delta)$ .

2. there exists a component interval  $(a_n, b_n)$  of complement of  $E$  with  $x = a_n$  (analogously if there exists a component interval  $(a_n, b_n)$  of complement of  $E$  satisfying  $x = b_n$ ). If  $h$  is constant on the interval  $[x, d']$ , where  $d' \in (x, b)$ , then put  $(c, d) = (x, d')$ .

Otherwise let  $x_1 \in (a_n, b) \cap (a_n, b_n)$  be a point at which  $h(x_1) \neq h(x)$ . As  $h$  is Darboux function, there exists a point  $x_2 \in (x, x_1)$  such that  $h(x_2) \in (C, D) \cap h((x, x_1))$ . Clearly  $x_2 \in C(h) \cap (a, b)$ , i.e. we can find a number  $\delta > 0$  satisfying  $(x_2 - \delta, x_2 + \delta) \subset (a, b)$  and  $h((x_2 - \delta, x_2 + \delta)) \subset (C, D)$ . Put  $(c, d) = (x_2 - \delta, x_2 + \delta)$ .

3.  $x \notin \bigcup_{n=1}^{\infty} [a_n, b_n]$ . We can assume that  $h$  is not constant on each interval  $[x, d']$ , where  $d' \in (x, b)$ , and on each interval  $[c', x]$ , where  $c' \in (a, x)$  (otherwise put  $(c, d) = (x, d')$  or  $(c, d) = (c', x)$ ).

It is clear that  $h(x) = f(x)$ , as  $x \in E$ .

Observe that for each  $t \in (x, b) \cap E$  the set  $h([x, t] \cap (\mathbb{R} \setminus E))$  is dense on the interval  $h([x, t])$ . Suppose on the contrary. Then there exists a point  $x_1 \in (x, t) \cap E$  such that

$$(4) \quad \text{dist}(h(x_1), h([x, t] \cap (\mathbb{R} \setminus E))) > 0.$$

Observe that

$$(5) \quad f((x, t) \cap (\mathbb{R} \setminus E)) \subset h((x, t) \cap (\mathbb{R} \setminus E)).$$

Indeed, as  $x, t \in E$  and  $x$  is an accumulation point of  $E$ , there exists a subsequence  $\{(a_{n_k}, b_{n_k})\}_{n \in \mathbb{N}}$  of the sequence  $\{(a_n, b_n)\}_{k \in \mathbb{N}}$  such that

$$(x, t) \cap (\mathbb{R} \setminus E) = \bigcup_{k=1}^{\infty} (a_{n_k}, b_{n_k}).$$

Hence, by (2) and from the construction of  $h$ , we have

$$\begin{aligned} f((x, t) \cap (\mathbb{R} \setminus E)) &= \bigcup_{k=1}^{\infty} f((a_{n_k}, b_{n_k})) \\ &= \bigcup_{k=1}^{\infty} \bigcup_{j \in \mathbb{Z}} f([y_j^{n_k}, y_{j+1}^{n_k}]) \\ &\subset \bigcup_{k=1}^{\infty} \bigcup_{j \in \mathbb{Z}} h([y_j^{n_k}, y_{j+1}^{n_k}]) = h((x, t) \cap (\mathbb{R} \setminus E)). \end{aligned}$$

Put

$$\epsilon = \text{dist}(f(x_1), f((x, t) \cap (\mathbb{R} \setminus E))).$$

As  $f(x_1) = h(x_1)$ , by (5) and (4) we obtain that  $\epsilon > 0$ . Hence we have

$$\left(f(x_1) - \frac{\epsilon}{2}, f(x_1) + \frac{\epsilon}{2}\right) \cap f((x, t) \cap (\mathbb{R} \setminus E)) = \emptyset.$$

The set  $E$  is nowhere dense, hence in the neighbourhood  $(x, t)$  of  $x_1$  there is no interval which image is contained in

$$\left(f(x_1) - \frac{\epsilon}{2}, f(x_1) + \frac{\epsilon}{2}\right).$$

So there exists an interval  $(x, t)$  such that  $f$  is not constant on  $(x, t)$ . Put

$$(C, D) = \left(f(x_1) - \frac{\epsilon}{2}, f(x_1) + \frac{\epsilon}{2}\right) \subset f((x, t)).$$

Then for each interval  $(c, d) \subset (x, t)$  condition  $f((c, d)) \not\subset (C, D)$  is satisfied.

It means that  $f$  does not have the q-property. Hence by lemma 1 in [6] the function  $f$  is not quasi-continuous, which contradicts our assumption.

So for each  $t \in (x, b) \cap E$  the set  $h([x, t] \cap (\mathbb{R} \setminus E))$  is dense in  $h([x, t])$ .

Now we will prove that there exists a sequence  $\{x_i\}_{i \in \mathbb{N}}$ ,  $x_i \searrow x$ , such that

$$h(x_i) \xrightarrow{i \rightarrow \infty} h(x).$$

Consider the interval  $(x, x+1)$ . Then we can find a point  $x_0 \in (x, x+1)$  with  $h(x_0) \neq h(x)$ . Assume that  $h(x_0) > h(x)$  (if  $h(x_0) < h(x)$  the proof is analogous). As  $h$  has the Darboux property, we can find a point  $x_1 \in (x, x_0)$  such that

$$h(x_1) \in (h(x), h(x) + 1).$$

Using the Darboux property of  $h$  once more we find a point

$$x_2 \in \left( x, \min \left\{ x + \frac{1}{2}, x_1 \right\} \right)$$

such that

$$h(x_2) \in \left( h(x), h(x) + \frac{1}{2} \right).$$

Assume that we have a point  $x_{i-1}$  satisfying

$$h(x_{i-1}) \in \left( h(x), h(x) + \frac{1}{i-1} \right).$$

In the interval  $(x, \min \{x + \frac{1}{i}, x_{i-1}\})$  we can find by Darboux property a point  $x_i$  such that

$$h(x_i) \in \left( h(x), h(x) + \frac{1}{i} \right).$$

Hence we obtain a sequence of points  $\{x_i\}_{i \in \mathbb{N}}$ ,  $x_i \searrow x$ , satisfying

$$h(x_i) \xrightarrow{i \rightarrow \infty} h(x).$$

We can assume that  $x_i \in (a, b)$  for all  $i \in \mathbb{N}$ .

Let  $i \in \mathbb{N}$ .

As  $h$  has the Darboux property, we have

$$(h(x), h(x_i)) \subset h([x, x_i]).$$

By virtue of the fact proved above, the set  $h([x, x_i] \cap (\mathbb{R} \setminus E))$  is dense in  $h([x, x_i])$ , so in the interval  $(h(x), h(x_i))$  there exists a point  $y_i$  which belongs to  $h([x, x_i] \cap (\mathbb{R} \setminus E))$ . So we can find a point  $s_i \in [x, x_i] \cap (\mathbb{R} \setminus E)$  such that  $h(s_i) = y_i \in (h(x), h(x_i))$ .

Hence we obtain a sequence  $\{s_i\}_{i \in \mathbb{N}}$  of points of  $\mathbb{R} \setminus E$  such that

$$s_i \xrightarrow{i \rightarrow \infty} x \quad \text{and} \quad h(s_i) \xrightarrow{i \rightarrow \infty} h(x).$$

As  $x \in (a, b)$  and  $h(x) \in (C, D)$ , there exists a number  $i_0 \in \mathbb{N}$  such that  $s_{i_0} \in (a, b)$  and  $h(s_{i_0}) \in (C, D)$ . As  $h$  is continuous on  $\mathbb{R} \setminus E$ , there exists a neighborhood  $(c, d)$  of  $s_{i_0}$  such that  $(c, d) \subset (a, b)$  and  $h((c, d)) \subset (C, D)$ .

Finally we showed that  $h$  has the q-property. As  $h$  also has the Darboux property, by Lemma 1 in [6], the function  $h$  is quasi-continuous.

Consequently  $h \in \mathcal{DQ}_i$ , as the set  $D(h)$  of discontinuity points of  $h$  is nowhere dense.  $\square$

**Theorem 2.** *The family  $\mathcal{D}_{s_i}$  is dense in  $(\mathcal{DQ}, \rho)$ .*

*Proof.* Let  $f \in \mathcal{DQ}$  and  $\epsilon > 0$ . By Theorem 1 there exists a function

$$g \in K\left(f, \frac{\epsilon}{2}\right) \cap \mathcal{DQ}_i.$$

By Theorem 4 in [10] we can find a function  $h \in \mathcal{D}_s$  and a continuous function  $\alpha$ , such that

$$g = h + \alpha \quad \text{and} \quad |\alpha(x)| \leq \frac{\epsilon}{2} \quad \text{for } x \in \mathbb{R}.$$

It is easy to check that  $D(g) = D(h)$ , so  $h \in \mathcal{D}_{s_i}$ .

Consequently,

$$\rho(f, h) \leq \rho(f, g) + \rho(g, h) < \frac{\epsilon}{2} + \frac{\epsilon}{2} = \epsilon,$$

so  $h \in K(f, \epsilon) \cap \mathcal{D}_{s_i}$ .  $\square$

**Corollary 1.** *If  $\mathcal{A}$  has the  $(*)$ -property, then the family  $\mathcal{D}_{\mathcal{A}i}$  is dense in  $(\mathcal{DQ}, \rho)$ .*

The proof follows from the previous theorem and from the inclusion  $\mathcal{D}_s \subset \mathcal{D}_{\mathcal{A}} \subset \mathcal{DQ}$  (see [6], Theorem 1).

## References

- [1] A. M. Bruckner, J. G. Ceder, and M. L. Weiss, *Uniform limits of Darboux functions*, Colloq. Math. **15**, no. 1 (1966) 65–77.
- [2] K. Ciesielski, L. Larson, and K. Ostaszewski, *I-Density Continuous Functions*, Mem. Amer. Math. Soc. **515**, Providence, Rhode Island 1994.
- [3] Z. Grande, *On a subclass of the family of Darboux functions*, Colloq. Math. **117**, no. 1 (2009), 95–104.
- [4] G. Ivanova, *Remarks on some modification of the Darboux property*, Bull. Soc. Sci. Lett. Łódź Sér. Rech. Déform. **72**, no. 3 (2014), 91–100.
- [5] G. Ivanova and E. Wagner-Bojakowska, *On some modification of Darboux property*, Math. Slovaca (to appear).
- [6] G. Ivanova and E. Wagner-Bojakowska, *On some modification of Świątkowski property*, Tatra Mt. Math. Publ. **58** (2014), 101–109.
- [7] A. Kuratowski and A. Mostowski, *Set theory with an introduction to descriptive set theory*, PWN, Warszawa 1976.

- [8] E. Łazarow, R. A. Johnson, and W. Wilczyński, *Topologies related to sets having the Baire property*, Demonstratio Math. **21** (1989) no. 1, 179–191.
- [9] N. Levine, *Semi-open sets and semi-continuity in topological spaces*, Amer. Math. Monthly **70** (1963), 36–41.
- [10] A. Maliszewski, *On the limits of strong Świątkowski functions*, Zeszyty Nauk. Politech. Łódź. Mat. **27**, no. 719 (1995), 87–93.
- [11] T. Mańk and T. Świątkowski, *On some class of functions with Darboux's characteristic*, Zeszyty Nauk. Politech. Łódź. Mat. **11**, no. 301 (1977), 5–10.
- [12] A. Neubrunnová, *On certain generalizations of the notion of continuity*, Matematický Časopis **23**, no. 4 (1973), 374–380.
- [13] W. Poreda, E. Wagner-Bojakowska, and W. Wilczyński, *A category analogue of the density topology*, Fund. Math. **125** (1985), 167–173.
- [14] W. Poreda, E. Wagner-Bojakowska, and W. Wilczyński, *Remarks on  $\mathcal{I}$ -density and  $\mathcal{I}$ -approximately continuous functions*, Comm. Math. Univ. Carolinae **26**, no. 3 (1985), 553–563.
- [15] P. Szczuka and M. Marciniak, *Products of internally quasi-continuous functions*, Tatra Mt. Math. Publ. **55** (2013), 17–25.
- [16] R. Wiertelak, *A generalization of density topology with respect to category*, Real Anal. Exchange **32**, no. 1 (2006/2007), 273–286.
- [17] W. Wilczyński, *A generalization of the density topology*, Real Anal. Exchange **8**, no. 1 (1982/1983), 16–20.
- [18] W. Wilczyński, *A category analogue of the density topology, approximate continuity and the approximate derivative*, Real Anal. Exchange **10**, no. 2 (1984/1985), 241–265.

Faculty of Mathematics and Computer Science  
Łódź University  
Stefana Banacha 22, PL-90-238 Łódź, Poland  
e-mail: gertruda@math.uni.lodz.pl

Presented by Władysław Wilczyński at the Session of the Mathematical-Physical Commission of the Łódź Society of Sciences and Arts on December 4, 2014

## O PEWNYCH PODRODZINACH FUNKCJI DARBOUX QUASI-CIĄGŁYCH

### S t r e s z c z e n i e

Niniejsza praca jest poświęcona uogólnieniu silnej własności Świątkowskiego. Dowodzi się, że rodzina funkcji mających silną własność Świątkowskiego o nigdzie gęstym zbiorze punktów nieciągłości jest zbiorem gęstym w przestrzeni  $\mathcal{DQ}$  funkcji quasi-ciągłych o własności Darboux. W pracy podane są też warunki, dla których rodzina funkcji mających  $\mathcal{A}$ -własność Darboux o nigdzie gęstym zbiorze punktów nieciągłości jest podzbiorem gęstym rodziny  $\mathcal{DQ}$ .

*Słowa kluczowe:* własności Darboux, mocna własność Świątkowskiego, quasi-ciągłość



## B U L L E T I N

DE LA SOCIÉTÉ DES SCIENCES ET DES LETTRES DE ŁÓDŹ

2014

Vol. LXIV

Recherches sur les déformations

no. 3

pp. 45–54

*In memory of  
Professor Zygmunt Charzyński (1914–2001)*

*Nikolaos Skoulidis and Hariton M. Polatoglou*

**DEPENDENCE OF THE CURVATURE OF SI/GE CANTILEVERS ON THE SIZE, COMPOSITION, AND TEMPERATURE****Summary**

Mirrors are very important in controlling electromagnetic radiation, with applications such as radiation guiding, lithography, modulation, sensors and filtering. Especially in our days the needs of this control is concentrated in the micro and sub-micro scale. But the trend in technology is to create and use structures in the nanometre range. Therefore is necessary to study the possibilities of using new materials that could be used for the formation and the control of mirrors at that scale. In this work we studied the nanometre sized structures consisting of Si and Ge, forming bilayer cantilevers using atomistic modelling and molecular dynamics. We found that the atomistic modelling can shows phenomena that are not possible to be shown utilizing the methodology of continuum mechanics. We found that the strains are localized mainly near the interface of the two materials and the radius of curvature is depended on the distance from the interface. The experimental observation that the radius of the curvature is slightly smaller than the calculated with the continuum mechanics methodology was reproduced here. This modelling also showed a higher dependence on linear expansion coefficient and the results of strains distribution can be extended to larger structures because the effect of the free surface and the interface is limited to about 6 lattice units or 3.5 nm depth.

*Keywords and phrases:* cantilever, mirror, electromagnetic radiation, atomic modelling, molecular dynamics

**1. Introduction**

The integration of electronics with micromechanical components on a common substrate is a technology for creating microelectromechanical systems (MEMS). These devices can find applications as sensors or actuators. As actuators can guide mirrors which are very important in controlling electromagnetic radiation, with applications

such as radiation guiding, lithography, modulation, sensors and filtering. In our days the needs of this control is concentrated in the micro and sub-micro scale [intro\_1, 2, 3]. The trend in technology is to use smaller device falling in the scale of few nanometres. Some of the advantages of the nanometre scale nanostructures are the possibility of using the fabrication methods of semiconductor chips that leads to the precise and reproducible control of properties, geometry and positioning, the possibility of using a large variety of materials such as Si, Ge, SiGe alloys, InAs, GaAs, InGaAs alloys, polypyrrole, gold (PPy-Au) etc. SiGe, Si and Cr trilayer nanotubes were produced using the molecular-beam epitaxy (MBE) or the ultrahigh-vacuum chemical vapour deposition (UHV-CVD) with wall thickness in the range of few nanometres [nanotubes] and found the radius of curvature to fall in the submicron range. The case of PPy-Au has been studied theoretically and experimentally in [ppy-bi]. The high stress in the interface of the PPy-Au can cause the delamination of the materials and an alternate technique has been proposed with the addition of a third intermediate layer. This case has been modelled and found that the additional layer does not lead to the loss of curvature [ppy-tri].

Another possible application of the bilayer nanostructures is the formation of nanohelices. These structures can find applications as nano-springs, nano-coils for the detection or creation of magnetic field or as temperature sensors with the advantage of the large surface and small mass. Such structures have been produced and their properties investigated recently by Zhang et al [helices].

The effect of uncapped Ge quantum dots (QD) grown on Si films on the bending of the structure has been studied by Huang and al [bending\_qd]. And found that the shape of QD is largely affecting this bending.

The aim of the present work is to study the possibilities of a nano sized composite material to be used as an actuator for the control of a similarly sized mirror. The material we study is a bilayer Si/Ge cantilever measuring up to a few of nanometres and the properties we study are the curvature of the cantilevers and its dependence on the size, composition and temperature. Also we compare our results to the continuum mechanics analysis.

## 2. Method

For this study we created atomistic models of cantilevers of different size and composition and applied molecular dynamics to investigate their structural properties, and particularly the radius of the curvatures and their dependence on different factors. The models we used were, measuring few nanometres and consist from two layers, one from Si and the other from Ge, hypothetically grown on the Si along the z direction. In this way we simulate dual material cantilevers. The thickness of the created structures is 10 to 20 lattice units (LU) and the length is 20 LU. The thickness ratio (composition) of Ge and Si in the models takes the values of 1:3 (25% Ge), 1:1 (50% Ge) and 3:1 (75% Ge). A 50% Ge cantilever model, with thickness of 10 LU

before any relaxation, is shown in Fig. 1 where the lower part or dark grey is the Si region and the upper part or light grey is the Ge region. On these structures we applied periodic boundary conditions on the  $y$  direction only (perpendicular to the plane of figure). We have applied the simulated annealing method which leads to the global minimum of the energy of the structure and tested a variety of integration methods e.g. the Verlet (classical and velocity) [Verl] and Beeman [Bee], and we found to have similar results.

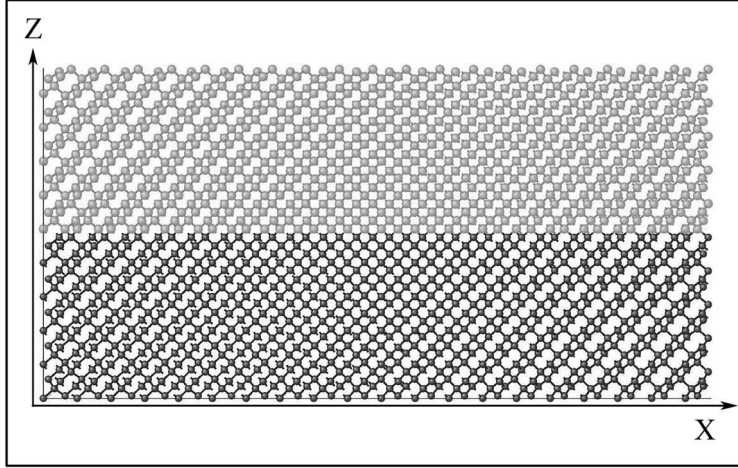


Fig. 1: Unrelaxed cantilever atomistic model. Si are the dark grey atoms, Ge are the light grey atoms.

For the calculation of the forces we used the Stillinger-Weber interatomic potential model [SW]. This model has been proven to describe very well the studied compounds [SW\_SIGE]. Also it describes their interface and free surface [SW\_INTER\_SURF]. It consists of two and three body terms, with the two body term taking into account the bond length of the first order neighbours and the three body term the bond angles of the same order of neighbours penalizing any deviations from the perfect tetrahedral structure. This model works for moderate distortions from the perfect tetrahedral. In the case of Si and Ge the distortions are expected to be less than 7%, the lattice mismatch of the 2 bulks. The atoms that are on the surface of the structure have only one or two neighbours which lie in the interior of the structure. For the calculation of the forces this poses a serious problem as the direction of the calculated force is irrelevant. For this purpose we used an alternative methodology. Instead of calculating the force from the analytical derivative of the potential energy of the atom (Eq. 1), we calculated the derivative arithmetically from the potential energy of the whole structure (Eq. 2).

$$(1) \quad F_i = -\frac{dU_i}{dr_i},$$

$$(2) \quad F_i = - \sum_j \frac{\Delta U_j}{\Delta r_i},$$

where  $U_i$  is the energy of atom  $i$  and  $j$  is the first neighbour of atom  $i$ .

Actually, the sum in this equation runs only for the first neighbours of the atom  $i$  because we assume only interactions over the first neighbours. Thus, the calculated forces have a well defined direction. For the interface we used for the parameters of SW potential the arithmetic mean value for the energies and the geometric mean value for the interatomic distances.

All tasks were performed with the STREL [strel\_1, 2] integrated windows based environment, which is designed for the calculation of the structural and electronic properties of nanostructures. The time step for the relaxation process was 0.1 fs, and the total relaxation time was 20 ps. The estimation of the atomic sites was taken from the average atomic positions over the last 10 ps.

A comparison of the results with that derived from continuum mechanics calculations on bilayer materials used as an evaluation of the correctness of our method. The curvature is given by the Eq. 3, 3a [form, \_2001, 2002, \_last]

$$(3) \quad \frac{1}{R} = \frac{6B_1B_2t_1t_2(t_1 + t_2)}{B_1^2t_1^4 + B_2^2t_2^4 + 2B_1B_2t_1t_2(2t_1^2 + 2t_2^2 + 3t_1t_2)} \varepsilon_0,$$

$$(3a), \quad \varepsilon_0 = \frac{(\alpha_2 - \alpha_1)}{\alpha_2}$$

where  $B_i$  is the bulk modulus,  $t_i$  – the thickness, and  $\alpha_i$  – the lattice constant of compound  $i$ , and  $R$  is the radius of the curvature. In this formula we presume that the widths of the two materials are the same.

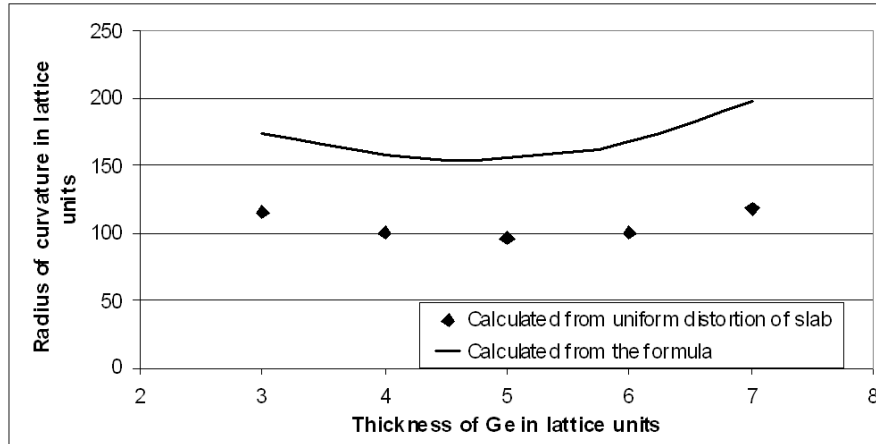


Fig. 2: Radius of curvature relative to the thickness of Ge for uniform distribution of strains (rhombuses) and from the formula (line).

At first we tested a uniform strain distribution on a curved structure without applying any molecular dynamics. The calculated curvature for the minimum energy of a structure 10 LU thick with material properties for 300 K is shown in the Fig. 2. The radius is calculated at the interface. On the same figure is plotted the curvature calculated from the Eq. 3 for the same structure. For the Eq. 3 the parameters of lattice constant and bulk modulus are also for  $T = 300$  K. We see that the uniform distribution of strains gives about 40% smaller radius of the curvature than the calculated from the Eq. 3 although the form of curvature is the same. Reference [form\_2002\_nano] also shows experimentally that the radius is smaller than the predicted but the difference is not so large. So this method is not adequate to describe that property and a full relaxation is necessary to be performed.

### 3. Results

#### 3.1. Energy of structures

In Fig. 3 we plot the energy of structures per atom for the temperature range 100–600 K. The studied structure has a length of 20 (LU) or about 10.8 nm and height 10 LU or 5.4 nm and consist of 50% Si and 50% Ge. We see that the kinetic energy curve follows the Boltzmann law as expected. This is a good indication that the applied methodology is properly working.

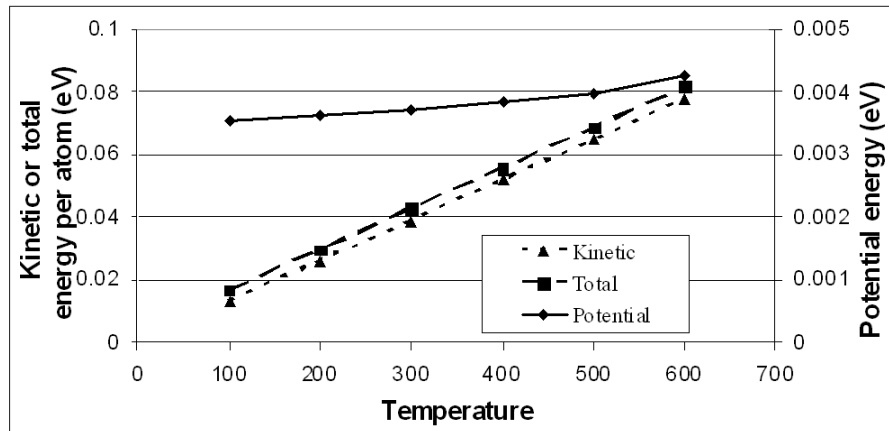


Fig. 3: Energy of structures vs temperature. The studied structures are consisted of 50% Ge.

#### 3.2. Effect of temperature

In Fig. 4 we plot the dependence of the radius of curvature vs the temperature for the upper layer of Ge and the lower layer of Si and the interface layer (as can be seen

in Fig. 1) of a structure similar to the previous. We see that the lower layer of the Si has a bigger radius and this is explained by the larger value of the bulk modulus of Si (98 GPa) compared to the Ge (75 GPa) at 300 K [SiGeBulk]. The decrease of radius of the top of the Ge and the increase of radius of the bottom of Si is explained by the larger linear expansion coefficient of Ge ( $5.9 \times 10^{-6} \text{ K}^{-1}$ ) [Ge\_e\_c] compared to Si ( $2.6 \times 10^{-6} \text{ K}^{-1}$ ) [Si\_e\_c]. In general the calculated radius is in good agreement with that calculated from the Eq. 3 but this method can distinguish the radius at different positions of the structure. The changes we observed are bigger than one would expect to arise solely from the expansion coefficient through the Eq. 3. This equation gives for the same temperature range only a 1% change for the radius of curvature.

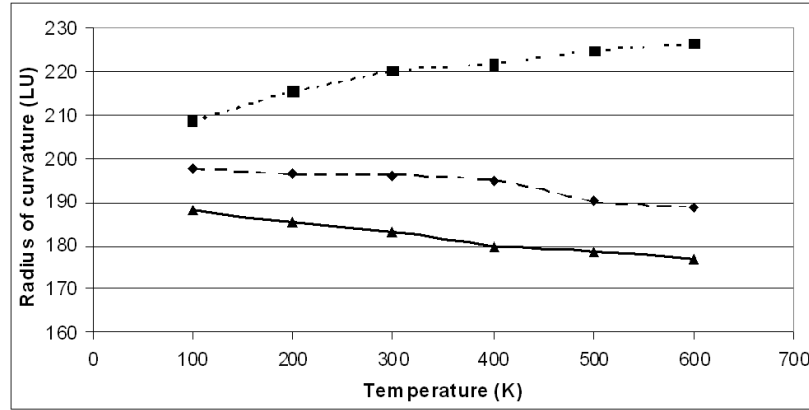


Fig. 4: Temperature dependence of radius for top of Ge (triangles), bottom of Si (squares) and interface (rhombuses).

### 3.3. Effect of composition

In Fig. 5 we plot the radius of curvature vs temperature for the three compositions 25%, 50% and 75% Ge and for the top layer of Ge and the interface layer. The diagram for the bottom layer of Si is similar to that of the top of Ge but with curves in reverse order. The structure here has the same length along the  $x$  axis but the thickness is now 20 LU. We see that at the interface layer the calculated radius is slightly smaller than that deriving from Eq. 3 which gives a radius of 312 LU for the 50% Ge at 200 K. The previous observation that the radius of curvature is depended on the position within the cantilever is more obvious here especially for the cases of 25 and 75% content of Ge and shows that the radius at the free surface of the material with the highest content tends to become infinitive.

An interesting feature of the relaxed structures in the case of thick cantilever is observed in Fig. 6. We notice firstly that away from the interface the material which

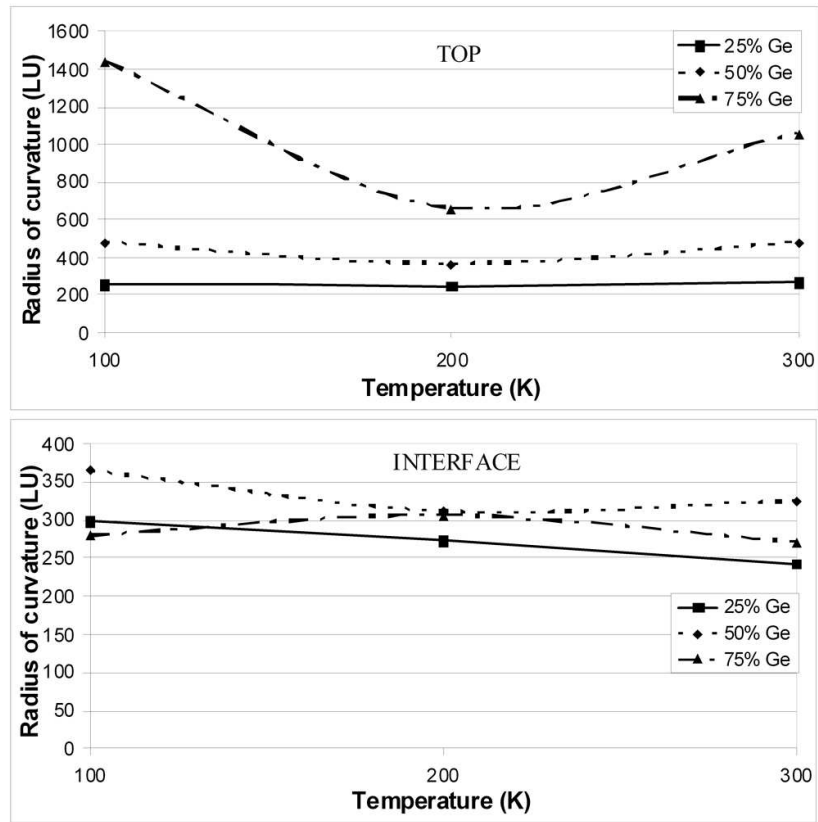


Fig. 5: Temperature dependence of curvature for a structure with 20 LU height at top of Ge and interface.

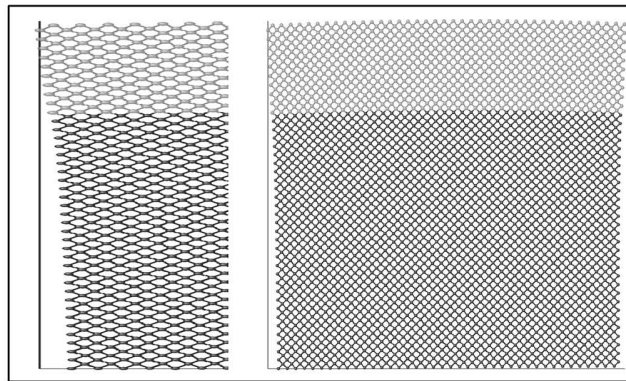


Fig. 6: Distorted cantilever containing 25% Ge (top) and 75% Si (bottom). The left image is the extended left part of the cantilever by  $x$  axis only.

is thick (one shown only in Fig.) relaxes to its lattice parameter and therefore the radius of curvature tends to be infinite and secondly that the radius of curvature close to the interface is the smaller. Because of that there is a transition region around the interface with width of about 6 LU in each material, where the unavoidable strains are present. In Fig. 7 we plot the strain tensor components  $\varepsilon_{xx}$  and  $\varepsilon_{zz}$ . The previous observation is shown here for the strains at atomic level.

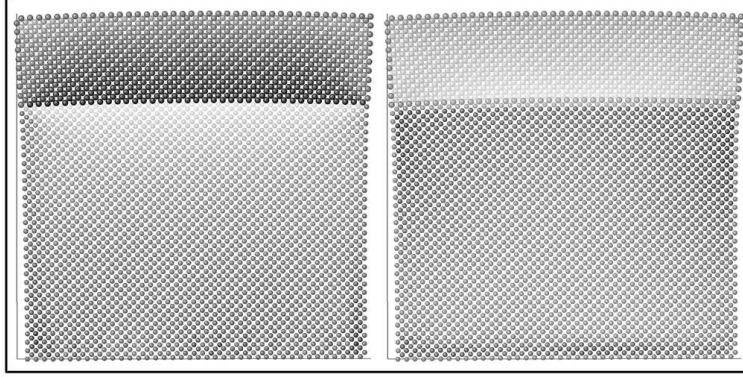


Fig. 7: Strains for a 25% Ge (top) and 75% Si (bottom). Left the  $\varepsilon_{xx}$  and right the  $\varepsilon_{zz}$  tensors. Dark color shows the negative strain and light color the positive strain.

The Si is expanded along the horizontal  $-x$  axis ( $\varepsilon_{xx} > 0$ ) and compressed along the vertical  $-z$  axis ( $\varepsilon_{zz} < 0$ ) for about 6 LU from the interface. Similar is the situation in the Ge area but with inversed strains. We observe that 6 LU away the interface the values of tensors become almost zero. Also, the effect of the free surface at minimum and maximum  $z$  is obvious near the interface. But in the internal area (again 6 LU away from the free surface) the strains look quite uniform, predicting that the longer cantilever will not show different behavior, regarding the curvature and/or the strains distribution

#### 4. Conclusion

The study of nanosized bilayer cantilevers with atomistic models reveals phenomena that are not possible to be shown with the study of continuum mechanics, such as that the strains are localized mainly near the interface of the two materials and the radius of curvatures is depended on the distance from the interface. The calculated radius is slightly smaller than the predicted with the continuum mechanics, which is also observed and experimentally and the atomistic models show a higher dependence on linear expansion coefficient. Finally, the strains distribution show that the free surface and the interface affect only a small part of the total structure with a depth of 6 LU, making possible to extend our results on them and on curvature for longer and thicker structures.

## References

- [1] S. Chang and S. Sivoththaman, *J. Micromech. Microeng.* **16** (2006), 1307–1313.
- [2] K. Jongbaeg, C. Hyuck, L. Liwei and R. S. Muller, in: *Proceedings, 12th International Conference Solid-State Sensors, Actuators and Microsystems, Boston 2003*, vol. 2 (IEEE, 2003), 1015–1018.
- [3] S. Sedky, A. Witvrouw, and K. Baert, *Sensors and Actuators A* **97-98** (2002), 503–511.
- [4] S. V. Golod, V. Ya. Prinz, P. Wagli, L. Zhang, O. Kirfel, E. Deckhardt, F. Glaus, C. David, and D. Grutzmacher, *Appl. Phys. Lett.* **84** (2004), 3391–3393.
- [5] M. Christophersen, B. Shapiro, and E. Smela, *Sensors and Actuators B* **115** (2006), 596–609.
- [6] B. Shapiro and E. Smela, *J. of Intell. Mat. Sys. and Struct.* **0** (2006), 1–6.
- [7] L. Zhang, E. Ruh, D. Grutzmacher, L. Dong, D. J. Bell, B. J. Nelson, and C. Schonberger, *Nano Letters* **6** (2006), 1311–1317.
- [8] M. Huang, P. Rugheimer, M. G. Lagally, and F. Liu<sup>1</sup>, *Phys. Rev. B* **72** (2005), 085450.
- [9] C. Deneke, C. Muller, N. Y. Jin-Phillipp, and O. G. Schmidt, *Semicond. Sci. Technol.* **17** (2002), 1278–1281.
- [10] L. Verlet, *Phys. Rev.* **159** (1967), 98–103.
- [11] D. Beeman, *J. Comp. Phys.* **20** (1976), 130–139.
- [12] F. H. Stillinger and T. A. Weber, *Phys. Rev. B* **31** (1985), 5262–5271.
- [13] Z. Q. Wang and D. Stroud, *Phys. Rev. B* **38** (1988), 1384–1391.
- [14] P. Dluzewski and P. Traczykowski, *Arch. Mech.* **55** (2003), 501–514.
- [15] N. Skoulidis and H. M. Polatoglou, *Int. J. Nanotechnology* **2** (2005), 271–279.
- [16] N. Skoulidis and H. M. Polatoglou, *J. of Materials Education* **29** (2007), 117–132.
- [17] Wen-Hwa Chut, M. Mehregany, and R. L. Mullen, *J. Micromech. Microeng.* **3** (1993), 4–7.
- [18] P. O. Vaccaro, K. Kubota, and T. Aida, *App. Phys. Lett.* **78** (2001), 2852–2854.
- [19] G. P. Nikishkov, I. Khmyrova, and V. Ryzhii, *Nanotechnology* **14** (2003), 820–823.
- [20] S. I. Novikova, *Sov. Phys. Solid State* **2** (1960), 37.
- [21] Y. Okada and Y. Tokumaru, *J. Appl. Phys.* **56** (1984), 314.
- [22] F. Schaffler, in: *Properties of Advanced Semiconductor Materials GaN, AlN, InN, BN, SiC, SiGe*, ed. M. E. Levinshtein, S. L. Rumyantsev, M. S. Shur, John Wiley and Sons, Inc., New York 2001, pp. 149–188.

Physics Department  
Solid State Physics Section  
Aristotle University of Thessaloniki  
Gr-54124 Thessaloniki  
Greece  
e-mail: hariton@auth.gr

Presented by Ilona Zasada at the Session of the Mathematical-Physical Commission of the Łódź Society of Sciences and Arts on December 4, 2014

## ZALEŻNOŚĆ KSZTAŁTU BELECZEK POMIAROWYCH Si/Ge OD ICH ROZMIARU, SKŁADU I TEMPERATURY

### S t r e s z c z e n i e

Zwierciadła są bardzo ważnym elementem kontrolnym promieniowania elektromagnetycznego używanym do prowadzenia wiązki w litografii, jej modulacji i filtracji. Powszechnie używa się układów kontrolnych w skali mikrometrycznej, ale wyzwania nowoczesnych technologii idą w kierunku tworzenia i wykorzystywania układów o rozmiarach nanometrycznych. W tym kontekście konieczne są badania dotyczące nowych struktur, które mogłyby zostać wykorzystane w układach kontrolujących zwierciadła w skali nano. W pracy został przedstawiony teoretyczny opis struktur nanometrycznych tworzących dwuwarstwowe belecзки pomiarowe wykonane z Si i Ge. Do opisu zastosowano dwie metody: modelowanie atomowe oraz dynamikę molekularną. Pokazano, że podejście atomowe pozwala na opis zjawisk w sposób niedostępny przy zastosowaniu mechaniki ośrodków ciągłych. Przeanalizowano między innymi rozkład naprężeń i krzywizny belecзки w funkcji odległości od powierzchni Si/Ge. Uzyskane wyniki są zgodne z dostępnymi danymi doświadczalnymi.

*Słowa kluczowe:* belecзка pomiarowa, zwierciadło, promieniowanie elektromagnetyczne, modelowanie atomowe, dynamika molekularna

## B U L L E T I N

DE LA SOCIÉTÉ DES SCIENCES ET DES LETTRES DE ŁÓDŹ

2014

Vol. LXIV

Recherches sur les déformations

no. 3

pp. 55–68

*In memory of  
Professor Zygmunt Charzyński (1914–2001)*

*Stawomir Szumiński*

## SEMI-MAGIC SQUARES AND KIRCHHOFF'S VOLTAGE LAW

**Summary**

We consider bases of the vector spaces of semi-magic squares consisting only of permutation matrices. We show a relation between such bases and the maximal sets of linearly independent equations of some system. Using this relation we prove the existence of some particular types of bases consisting of the unit matrix and cyclic permutation matrices. In most cases the bases correspond to sets of permutations including as many cycles of the same length as possible. We give examples of all considered types of bases and we show some connections between our results and the maximal sets of independent loops in some particular graphs of electric circuits.

*Keywords and phrases:* semi-magic square, permutation matrix, cyclic permutation, Kirchhoff's voltage law

**1. Introduction**

We call a matrix  $[a_{ij}]_{n \times n}$  of real numbers a *semi-magic square* if there exists a real number  $m$  for which the matrix satisfies the conditions:

$$\sum_{j=1}^n a_{ij} = m \quad \text{for } 1 \leq i \leq n \quad (\text{the entries in each row add up to } m),$$

$$\sum_{i=1}^n a_{ij} = m \quad \text{for } 1 \leq j \leq n \quad (\text{the entries in each column add up to } m).$$

The number  $m$  is called the *magic constant* of the semi-magic square. The set of all semi-magic squares of a given order  $n$  is a vector space which dimension is equal to  $(n-1)^2 + 1$  (see [1]). We denote this space by  $\mathcal{SM}(n)$ .

We denote by  $S_n$  the permutation group of the set  $\{1, 2, \dots, n\}$  and by  $e$  its unit element. By the *permutation matrix* of  $\nu \in S_n$  we mean the matrix  $M(\nu) = [a_{ij}]_{n \times n}$ , where

$$a_{ij} = \begin{cases} 1, & j = \nu(i) \\ 0, & j \neq \nu(i) \end{cases} \quad \text{for } 1 \leq i, j \leq n.$$

We call  $\nu \in S_n$  a *p-cycle* or a *cycle of length p* if  $\nu(i_1) = i_2, \nu(i_2) = i_3, \dots, \nu(i_p) = i_1$  for some  $\{i_1, i_2, \dots, i_p\}$  and  $\nu(j) = j$  for any  $j \notin \{i_1, i_2, \dots, i_p\}$ . Then we denote  $\nu$  by  $(i_1, i_2, \dots, i_p)$ . It is worth noting that this *p-cycle* notation is ambiguous, i.e. we have also  $\nu = (i_k, i_{k+1}, \dots, i_p, i_1, \dots, i_{k-1})$  for any  $2 \leq k \leq p$ . The inverse of  $\nu$  is the *p-cycle*  $\nu^{-1} = (i_p, i_{p-1}, \dots, i_1)$ . A permutation matrix of a cycle of length  $p$  we call briefly a *p-cycle matrix* or a *matrix of p-cycle*. We write  $M(\nu)$  or  $M(i_1, i_2, \dots, i_p)$ .

Each permutation matrix is a semi-magic square with the magic constant  $m = 1$ . Moreover, the set of all such matrices of a given size  $n \times n$  spans  $\mathcal{SM}(n)$ . If  $n < 3$  then the set of all permutation matrices of order  $n$  is the basis of this space. For the trivial case  $n = 1$  it is  $\{M(e)\}$  and for  $n = 2$  it is  $\{M(e), M(1, 2)\}$ . For any  $n \geq 3$  the set

$$(1) \quad \{M(e)\} \cup \{M(1, k) : 2 \leq k \leq n\} \cup \{M(1, k, l) : 2 \leq k, l \leq n, k \neq l\}$$

is an example of such basis (see [1]). In Section 3 we prove that for any  $4 \leq p \leq n$  it is possible to obtain another basis from (1) by replacing the set of 3-cycle matrices with some set of *p-cycle* matrices. Moreover, we give some constraints for the existence of bases consisting only of the unit matrix and *p-cycle* matrices for some fixed  $p$ . Next, in Section 4 we give examples of all previously considered types of bases. Finally, in Section 5 we show some connections between our results and maximal sets of linearly independent Kirchhoff's voltage equations.

## 2. Connections with some system of equations

Let  $\mathbb{X} = [x_{ij}]$  be a square matrix of order  $n$ , where for any  $1 \leq i, j \leq n$  the element  $x_{ij}$  is a real variable. The system of all equations

$$(2) \quad \sum_{k=1}^n x_{k, \nu(k)} = 0,$$

where  $\nu \in S_n$ , we can write as

$$(3) \quad \mathbb{A} \curvearrowright = \mathcal{K},$$

where  $\curvearrowright$  is the column vector whose elements are taken row-wise from  $\mathbb{X}$ , i.e.

$$\curvearrowright = [x_{11}, x_{12}, \dots, x_{1n}, x_{21}, x_{22}, \dots, x_{2n}, \dots, x_{n1}, x_{n2}, \dots, x_{nn}]^T,$$

and elements of each row of the matrix  $\mathbb{A}$  are taken row-wise from the matrix of  $\nu$  which occurs in the corresponding equation. From (3) we see that the maximum number of linearly independent equations is equal to the maximum number of linearly independent permutation matrices of order  $n$ . Moreover, any subset of equa-

tions from (3) is linearly independent if and only if so is the corresponding subset of permutation matrices. To simplify notation, we write the sum in (2) as  $y(\nu)$ , e.g.

$$y(e) = \sum_{i=1}^n x_{ii}.$$

If  $\nu = (i_1, i_2, \dots, i_p)$ , then we write also  $y(i_1, i_2, \dots, i_p)$ . Now, we can give at once the maximal set of linearly independent equations of the system (3) corresponding to the basis (1):

$$(4) \quad \{y(e) = 0\} \cup \{y(1, k) = 0: 2 \leq k \leq n\} \cup \{y(1, k, l) = 0: 2 \leq k, l \leq n, k \neq l\}.$$

In the remainder of this paper, we use the following three properties and two lemmas about sums of variables occurring in the system (3).

If  $\nu = (i_1, i_2, \dots, i_p) \in S_n$ , where  $4 \leq p \leq n$ , then

$$(5) \quad y(\nu) = \sum_{k=2}^{p-1} y(i_1, i_k, i_{k+1}) - \sum_{k=3}^{p-1} y(i_1, i_k).$$

If  $\nu \in S_n$  is a  $p$ -cycle, where  $3 \leq p \leq n-1$  and  $j = \nu(j)$ , then

$$(6) \quad y(\nu) = y(e) + \sum_{i \neq \nu(i)} y(j, i, \nu(i)) - \sum_{i \neq \nu(i)} y(j, i).$$

If  $\nu \in S_n$  is a  $p$ -cycle, where  $3 \leq p \leq n$ , then

$$(7) \quad y(\nu) + y(\nu^{-1}) + (p-2)y(e) = \sum_{i \neq \nu(i)} y(i, \nu(i)).$$

**Lemma 1.** *Let  $4 \leq p \leq n$ . If  $y(\nu) = 0$  for any  $p$ -cycle  $\nu \in S_n$ , then*

$$y(i, j, k) - y(i, k, l) = y(i, j) - y(i, l)$$

*for any distinct  $1 \leq i, j, k, l \leq n$ .*

**Lemma 2.** *Let  $3 \leq p \leq n-1$ . If  $y(\nu) = 0$  for any  $p$ -cycle  $\nu \in S_n$ , then  $y(\nu_1) = y(\nu_2)$  for any 3-cycles  $\nu_1, \nu_2 \in S_n$ . If  $n \geq 5$ , this is also true for any 2-cycles  $\nu_1, \nu_2 \in S_n$ .*

Property (5) for  $i_1 = 1$  and property (6) for  $j = 1$  correspond to linear combinations of  $M(\nu)$  in the basis (1). In [1] a linear combination of any semi-magic matrix in this basis is derived. In the same paper the formula corresponding to property (7) in case  $\nu = (1, 2, \dots, p)$  is used. Direct proofs of all these properties and lemmas are in the appendix.

Throughout the paper, we use the following reasoning. Let  $P \subset S_n$  and  $\lambda \in S_n$ . To prove that  $M(\lambda)$  is a linear combination of the set  $\{M(\nu): \nu \in P\}$  we assume implicitly that for any  $\nu \in P$  the equality  $y(\nu) = 0$  holds and next we show that this implies  $y(\lambda) = 0$ . For example, let us consider the set

$$(8) \quad \{M(e)\} \cup \{M(k, l): 1 \leq k < l \leq n\} \cup \{M(1, k, l): 2 \leq k < l \leq n\}.$$

This set and the basis (1) have the same number of elements. Let  $2 \leq k < l \leq n$ . Since the relation

$$y(e) = y(1, k) = y(k, l) = y(l, 1) = y(1, k, l) = 0$$

holds, we have by property (7) the following equality

$$0 = y(1, k, l) + y(l, k, 1) + (p-2)y(e) - y(1, k) - y(k, l) - y(l, 1) = y(1, l, k).$$

So any element of the basis (1) is a linear combination of the set (8). Hence this set is also a basis of  $\mathcal{SM}(n)$ .

### 3. Existence of bases

**Theorem 1.** *For any  $3 \leq p \leq n$  there exists a basis of  $\mathcal{SM}(n)$  consisting of  $M(e)$ , some  $(n-1)$  matrices of 2-cycles, and some  $(n-1)(n-2)$  matrices of  $p$ -cycles.*

*Proof.* The basis (1) consists of  $M(e)$ ,  $(n-1)$  matrices of 2-cycles, and  $(n-1)(n-2)$  matrices of 3-cycles. So the theorem is true in case  $p = 3$ .

For  $4 \leq p \leq n$  it suffices to show that any 3-cycle matrix from (1) is a linear combination of the set consisting of  $M(e)$ ,  $(n-1)$  matrices of 2-cycles from (1), i.e. matrices  $M(1, k)$  for  $2 \leq k \leq n$ , and all  $p$ -cycle matrices. Since  $y(1, k) = 0$  for  $2 \leq k \leq n$ , we have by Lemma 1 that for any distinct  $2 \leq i_1, i_2, i_3 \leq n$  the equality  $y(1, i_1, i_2) = y(1, i_2, i_3)$  holds. Now, for any distinct  $2 \leq j_1, j_2 \leq n$  we can take some  $p$ -cycle  $\nu = (1, j_1, j_2, \dots, j_{p-1})$  for which by property (5) we have

$$0 = y(\nu) = \sum_{k=1}^{p-2} y(1, j_k, j_{k+1}) = (p-2)y(1, j_1, j_2).$$

Hence  $y(1, k, l) = 0$  for any distinct  $2 \leq k, l \leq n$ . □

**Corollary 1.** *For any  $3 \leq p \leq n$  there exists a basis of  $\mathcal{SM}(n)$  consisting of  $M(e)$ , all matrices of 2-cycles, and some  $\frac{1}{2}(n-1)(n-2)$  matrices of  $p$ -cycles.*

*Proof.* The basis (8) consists of  $M(e)$ , all matrices of 2-cycles, and  $\frac{1}{2}(n-1)(n-2)$  matrices of 3-cycles. So the corollary is true in case  $p = 3$ .

For  $4 \leq p \leq n$  it suffices to show that any 3-cycle matrix from (8) is a linear combination of the set consisting of  $M(e)$ , all matrices of 2-cycles, and all  $p$ -cycle matrices, which is true by Theorem 1. □

**Corollary 2.** *For any  $n \geq 3$ , the maximum number of linearly independent  $n$ -cycle matrices equals  $(n-1)(n-2)$ .*

*Proof.* Let us consider a set of  $n$  matrices of  $(n-1)$ -cycles  $M(\nu_k)$  such that  $\nu_k(k) = k$  for  $1 \leq k \leq n$ . This set is linearly independent, because  $M(\nu_k)$  is its only element with non-zero element in row  $k$ , column  $k$ . Moreover, any non-zero linear combination of its elements must have at least one non-zero diagonal element. But any linear combination of all  $n$ -cycle matrices has all diagonal elements equal zero. This means

that the intersection of the subspaces generated by these two sets consists only of the zero matrix. Since the dimension of  $\mathcal{SM}(n)$  equals  $(n-1)^2 + 1$ , the maximum number of independent  $n$ -cycle matrices is not greater than

$$(n-1)^2 + 1 - n = (n-1)(n-2).$$

By Theorem 1 there exists a linearly independent set of  $(n-1)(n-2)$  matrices of  $n$ -cycles.  $\square$

**Theorem 2.** *If  $n \geq 5$ , then for any  $3 \leq p \leq n-1$  there exists a basis of  $\mathcal{SM}(n)$  which consists of  $M(e)$  and some  $(n-1)^2$  matrices of  $p$ -cycles.*

*Proof.* Since the dimension of  $\mathcal{SM}(n)$  equals  $(n-1)^2 + 1$ , it remains to show that any 2-cycle and 3-cycle matrix from the basis (1) is a linear combination of the set consisting of  $M(e)$  and all  $p$ -cycle matrices. Let  $2 \leq k, l \leq n$ ,  $k \neq l$ . Because  $p < n$ , there exists a  $p$ -cycle  $\nu = (k, l, i_1, i_2, \dots, i_{p-2})$  such that  $\nu(1) = 1$ . Since  $y(e) = 0$ , by property (6) and Lemma 2 we have

$$0 = y(\nu) = py(1, k, l) - py(1, k),$$

hence  $y(1, k, l) = y(1, k)$ . If  $4 \leq p \leq n-1$ , then by property (5) we have

$$0 = y(1, k, l, i_1, i_2, \dots, i_{p-3}) = (p-2)y(1, k, l) - (p-3)y(1, k) = y(1, k, l).$$

For  $p = 3$  the equality  $y(1, k, l) = 0$  holds by assumption. We have just shown that

$$y(1, k, l) = y(1, k) = 0$$

for any distinct  $2 \leq k, l \leq n$ .  $\square$

**Remark 1.** *Theorem 2 is not true in case  $p = 3, n = 4$ , because then the number of all 3-cycle matrices equals 8 which is less than  $(n-1)^2 = 9$ .*

**Remark 2.** *It is not possible to construct a basis of  $\mathcal{SM}(n)$  consisting only of  $p$ -cycle matrices for some  $2 \leq p \leq n$ . This is because for any  $p$ -cycle matrix  $d = (n-p)m$ , where  $d$  is the sum of all its diagonal elements and  $m$  is its magic constant. Hence any linear combination of all  $p$ -cycle matrices must have the same property. But for  $2 \leq q \leq n$ ,  $q \neq p$  any  $q$ -cycle matrix does not have this property. This also means that in Theorem 2 we may replace  $M(e)$  by any  $q$ -cycle matrix, where  $q \neq p$ .*

#### 4. Examples of bases

Let

$$4 \leq p \leq n, \quad \pi = (2, 3, \dots, p), \quad \text{and} \quad \tau = (2, 3, 4, 5).$$

Since  $\pi$  is a  $(p-1)$ -cycle,  $2 \leq \pi^k(i) \leq p$  and  $\pi^{p-1}(i) = i$  for any  $k = 0, 1, 2, \dots$  and  $2 \leq i \leq p$ . Similarly,  $2 \leq \tau^k(i) \leq 5$  and  $\tau^4(i) = i$  for any  $k = 0, 1, 2, \dots$  and  $2 \leq i \leq 5$ . We use these facts implicitly. Let us denote

$$\delta_i = \begin{cases} (1, \pi(i), \pi^2(i), \dots, \pi^{p-1}(i)), & 2 \leq i \leq p \\ (1, i - p + 2, \dots, i - 1, i), & p + 1 \leq i \leq n \end{cases},$$

$$\gamma_i = \begin{cases} (\tau(i), \tau^2(i), \tau^3(i)), & 2 \leq i \leq 5 \\ (2, 3, i), & 6 \leq i \leq n \end{cases},$$

$$\zeta_i = \begin{cases} (1, \pi(i), \pi^2(i), \dots, \pi^{p-3}(i), p + 1, \pi^{p-2}(i)), & 2 \leq i \leq p \\ (2, 3, \dots, p, i), & p + 1 \leq i \leq n \end{cases},$$

for  $2 \leq i \leq n$ . Moreover, for any  $2 \leq i \leq n - 2$ ,  $i + 2 \leq j \leq n$  let us denote

$$\rho_{ij} = \begin{cases} (1, \pi^K(i), \dots, \pi(i), i, j, \pi(j), \dots, \pi^L(j)), & 2 \leq i \leq p - 2, i + 2 \leq j \leq p \\ (1, \pi^2(i), \pi^3(i), \dots, \pi^{p-2}(i), i, j), & 2 \leq i \leq p - 1, p + 1 \leq j \leq n, \\ (1, i - p + 3, \dots, i - 1, i, j), & p \leq i \leq n - 2, i + 2 \leq j \leq n \end{cases}$$

where  $K = (j - i) - 1$  and  $L = (p - 1) - (j - i) - 1$ . Using property (5) we obtain the following equalities:

$$(9a) \quad y(\delta_{\pi(i)}) - y(\delta_i) = y(1, i, \pi(i)) - y(1, \pi(i), \pi^2(i)) - y(1, i) + y(1, \pi^2(i)),$$

$$(9b) \quad y(\delta_{\pi(i)}^{-1}) - y(\delta_i^{-1}) = y(1, \pi(i), i) - y(1, \pi^2(i), \pi(i)) - y(1, i) + y(1, \pi^2(i)),$$

which are true for any  $2 \leq i \leq p$ .

To construct all our examples in cases  $4 \leq p \leq n$  we use the set of  $p$ -cycles

$$(10) \quad A = \{\delta_i : 2 \leq i \leq n\} \cup \{\rho_{ij} : 2 \leq i \leq n - 2, i + 2 \leq j \leq n\} \setminus \{\rho_{2p}\}$$

which has  $\frac{1}{2}(n-1)(n-2)$  elements. The sets  $\{\gamma_i : 2 \leq i \leq n\}$  and  $\{\zeta_i : 2 \leq i \leq n\}$  are used to construct examples to Theorem 2 for  $p = 3$  and  $4 \leq p \leq n - 1$  respectively. To prove that a given set is a basis of  $\mathcal{SM}(n)$  we show that it generates another basis. Checking that the cardinality of the set equals the dimension of  $\mathcal{SM}(n)$  is left to the reader.

#### 4.1. Examples to Theorem 1

The basis (1) is an example to Theorem 1 in case  $p = 3$ . For  $4 \leq p \leq n$ , the set

$$(11) \quad \{M(e)\} \cup \{M(1, k) : 2 \leq k \leq n\} \cup \{M(\nu) : \nu \in A\} \cup \{M(\nu^{-1}) : \nu \in A\},$$

where  $A$  is the set defined in (10), is such an example. To prove this, it suffices to show that any 3-cycle matrix from the basis (1) is a linear combination of matrices from the set (11).

We have  $y(e) = 0$ ,  $y(1, k) = 0$  for any  $2 \leq k \leq n$ , and  $y(\nu) = y(\nu^{-1}) = 0$  for any  $p$ -cycle  $\nu \in A$ . By (9a) we get  $y(1, i, \pi(i)) = y(1, \pi(i), \pi^2(i))$  for  $2 \leq i \leq p$ . From this and property (5) we get

$$0 = y(\delta_i) = \sum_{k=1}^{p-2} y(1, \pi^k(i), \pi^{k+1}(i)) = (p-2)y(1, i, \pi(i)),$$

hence  $y(1, i, i+1) = y(1, p, 2) = 0$  for any  $2 \leq i \leq p-1$ . If  $p+1 \leq i \leq n$  and  $y(1, j, j+1) = 0$  for any  $2 \leq j \leq i-2$ , then by property (5) we have

$$0 = y(\delta_i) = \sum_{j=i-p+2}^{i-2} y(1, j, j+1) + y(1, i-1, i) = y(1, i-1, i),$$

and by induction on  $i$  we get  $y(1, i, i+1) = y(1, p, 2) = 0$  for  $2 \leq i \leq n-1$ . Using (9b) we can prove analogously that  $y(1, i+1, i) = y(1, 2, p) = 0$  for  $2 \leq i \leq n-1$ .

For any  $2 \leq i \leq n-2$ ,  $i+2 \leq j \leq n$  such that  $i \neq 2$  or  $j \neq p$ , by the above and property (5) we have  $0 = y(\rho_{ij}) = y(1, i, j)$  and  $0 = y(\rho_{ij}^{-1}) = y(1, j, i)$ .

We have shown that  $y(1, k, l) = 0$  for any distinct  $2 \leq k, l \leq n$ .

#### 4.2. Examples to Corollary 1

The basis (8) is an example to Corollary 1 in case  $p = 3$ . For  $4 \leq p \leq n$ , the set

$$(12) \quad \{M(e)\} \cup \{M(k, l): 1 \leq k < l \leq n\} \cup \{M(\nu): \nu \in A\},$$

where  $A$  is the set defined in (10), is such an example. Since by property (7) we have

$$y(\nu^{-1}) = \sum_{i \neq \nu(i)} y(i, \nu(i)) - y(\nu) - (p-2)y(e) = 0,$$

for any  $\nu \in A$ , the set (12) generates the basis (11).

#### 4.3. Examples to Theorem 2

For  $p = 3$  the set

$$(13) \quad \{M(e)\} \cup \{M(\gamma_i): 2 \leq i \leq n\} \cup \{M(1, k, l): 2 \leq k, l \leq n, k \neq l\}$$

is an example to Theorem 2. To prove this, it suffices to show that any 2-cycle matrix from the basis (1) is a linear combination of this set.

We have  $y(e) = 0$ ,  $y(\gamma_i) = 0$  for any  $2 \leq i \leq n$ , and  $y(1, k, l) = 0$  for any distinct  $2 \leq k, l \leq n$ . By property (6) we get

$$\begin{aligned} 0 = y(\gamma_{\tau(i)}) - y(\gamma_i) &= -y(1, \tau^2(i)) - y(1, \tau^3(i)) - y(1, \tau^4(i)) \\ &\quad + y(1, \tau(i)) + y(1, \tau^2(i)) + y(1, \tau^3(i)) \\ &= y(1, \tau(i)) - y(1, i), \end{aligned}$$

and hence  $y(1, i) = y(1, \tau(i))$ , for any  $2 \leq i \leq 5$ . Now, by property (6) we have

$$0 = y(\gamma_i) = -\sum_{k=1}^3 y(1, \tau^k(i)) = -3y(1, i)$$

for  $2 \leq i \leq 5$ , and since  $y(1, 2) = y(1, 3) = 0$ , we have also

$$0 = y(\gamma_i) = -y(1, 2) - y(1, 3) - y(1, i) = -y(1, i)$$

for  $6 \leq i \leq n$ . So the equality  $y(1, i) = 0$  holds for any  $2 \leq i \leq n$ .

For  $3 < p < n$  the set

$$(14) \quad \{M(e)\} \cup \{M(\zeta_i): 2 \leq i \leq n\} \cup \{M(\nu): \nu \in A\} \cup \{M(\nu^{-1}): \nu \in A\},$$

where  $A$  is the set defined in (10), is an example to Theorem 2. To prove this, it suffices to show that any 2-cycle matrix from the basis (11) is a linear combination of matrices from the set (14).

We have  $y(e) = 0$ ,  $y(\zeta_i) = 0$  for any  $2 \leq i \leq n$ , and  $y(\nu) = y(\nu^{-1}) = 0$  for any  $p$ -cycle  $\nu \in A$ . By subtracting (9b) from (9a) we get

$$y(1, i, \pi(i)) - y(1, \pi(i), i) = y(1, \pi(i), \pi^2(i)) - y(1, \pi^2(i), \pi(i))$$

for  $2 \leq i \leq p$ . From this and property (5) we have

$$\begin{aligned} 0 &= y(\delta_{\pi(i)}) - y(\delta_{\pi(i)}^{-1}) = \sum_{k=2}^{p-1} \left[ y(1, \pi^k(i), \pi^{k+1}(i)) - y(1, \pi^{k+1}(i), \pi^k(i)) \right] \\ &= (p-2) \left[ y(1, i, \pi(i)) - y(1, \pi(i), i) \right], \end{aligned}$$

hence  $y(1, i, \pi(i)) = y(1, \pi(i), i)$  for  $2 \leq i \leq p$ . Since by property (5) we have also

$$\begin{aligned} 0 &= y(\delta_{\pi(i)}) - y(\rho_{i, p+1}) = y(1, i, \pi(i)) - y(1, i, p+1), \\ 0 &= y(\delta_{\pi(i)}^{-1}) - y(\rho_{i, p+1}^{-1}) = y(1, \pi(i), i) - y(1, p+1, i), \end{aligned}$$

for  $2 \leq i \leq p-1$ , and

$$\begin{aligned} 0 &= y(\delta_{\pi(p)}) - y(\delta_{p+1}) = y(1, p, 2) - y(1, p, p+1), \\ 0 &= y(\delta_{\pi(p)}^{-1}) - y(\delta_{p+1}^{-1}) = y(1, 2, p) - y(1, p+1, p), \end{aligned}$$

the following relation holds

$$y(1, i, p+1) = y(1, i, \pi(i)) = y(1, \pi(i), i) = y(1, p+1, i)$$

for  $2 \leq i \leq p$ . From this and property (5) we obtain

$$\begin{aligned} 0 &= y(\zeta_{\pi(i)}) - y(\delta_{\pi(i)}) \\ &= y(1, \pi^{p-2}(i), p+1) - y(1, \pi^{p-2}(i), \pi^{p-1}(i)) \\ &\quad + y(1, p+1, \pi^{p-1}(i)) - y(1, \pi^{p-1}(i), \pi^p(i)) + y(1, \pi^{p-1}(i)) - y(1, p+1) \\ &= y(1, i) - y(1, p+1), \end{aligned}$$

hence  $y(1, i) = y(1, p+1)$  for  $2 \leq i \leq p$ . By the above and (9a) we get

$$y(1, i, \pi(i)) = y(1, p, p+1) = y(1, p+1, 2)$$

for any  $2 \leq i \leq p$ . Now, by property (6) we have

$$0 = y(\zeta_{p+1}) = p y(1, p, p+1) - p y(1, p+1),$$

hence  $y(1, p+1) = y(1, p, p+1)$ , and by property (5) we have

$$0 = y(\delta_{p+1}) = (p-2)y(1, p, p+1) - (p-3)y(1, p+1) = y(1, p+1),$$

hence  $y(1, p+1) = y(1, p, p+1) = 0$ . It follows that

$$y(1, i, i+1) = y(1, p, 2) = y(1, i+1, i) = y(1, 2, p) = 0$$

for  $2 \leq i \leq p$ , the equality  $y(1, i) = 0$  holds for  $2 \leq i \leq p+1$ , and by properties (5) and (6) we obtain

$$0 = y(\rho_{pi}) + y(\rho_{2i}^{-1}) - y(\zeta_i) = y(1, i)$$

for  $p+2 \leq i \leq n$ . So the equality  $y(1, i) = 0$  holds for any  $2 \leq i \leq n$ .

## 5. Connections with Kirchhoff's voltage law

Let  $\{\nu_k : 1 \leq k \leq M\}$  be a set of permutations from  $S_n$  such that the corresponding set of equations in the system (3) is linearly independent and the equation  $y(e) = 0$  is not a linear combination of this set of equations. In the remainder of this section we use implicitly the fact that then the set of equations

$$\sum_{i \neq \nu_k(i)} x_{i, \nu_k(i)} = 0 \quad \text{for } 1 \leq k \leq M$$

is also linearly independent. This is because otherwise the set of equations

$$0 = \sum_{i \neq \nu_k(i)} (x_{i, \nu_k(i)} - x_{i, i}) = \sum_{i \neq \nu_k(i)} x_{i, \nu_k(i)} + \sum_{i = \nu_k(i)} x_{i, i} - \sum_{i=1}^n x_{i, i} = y(\nu_k) - y(e)$$

for  $1 \leq k \leq M$  would be linearly dependent, which is not true.

### 5.1. Graphs with one branch between each pair of nodes

Let us consider a graph of an electric circuit with  $n \geq 4$  nodes such that each two of them are connected by one branch. We can create the matrix  $\mathbb{U} = [u_{ij}]_{n \times n}$ , where each entry  $u_{ij}$  is the node voltage at node  $i$  with respect to node  $j$ . Since  $u_{ij} = -u_{ji}$  for any  $1 \leq i, j \leq n$ , it follows that the matrix  $\mathbb{U}$  is antisymmetric. In particular,  $u_{ii} = 0$  for  $1 \leq i \leq n$ . Let us assume that for any  $1 \leq i < j \leq n$  the branch between node  $i$  and node  $j$  is directed from  $i$  to  $j$ , which means that  $u_{ij}$  is the branch voltage and  $u_{ji}$  is its negation. It follows from Kirchhoff's voltage law that for any  $p$ -cycle  $\nu$ , where  $3 \leq p \leq n$ , the following equality holds

$$\sum_{i < \nu(i)} u_{i, \nu(i)} - \sum_{i > \nu(i)} u_{\nu(i), i} = 0.$$

The set of all branches corresponding to the terms in the equality above we call a *loop of length  $p$* . The  $p$ -cycle  $\nu$  determines the loop direction in the obvious way. We say that some loops are independent if the corresponding Kirchhoff's voltage equations are linearly independent. From electric circuit theory we know that the maximum number of independent loops in a connected graph equals

$$N = b - \alpha + 1,$$

where  $b$  is the number of its branches and  $\alpha$  is the number of its nodes (see for instance [3]). In our case this number equals

$$N_1 = \binom{n}{2} - n + 1 = \frac{1}{2}n(n-1) - (n-1) = \frac{1}{2}(n-1)(n-2),$$

and electric circuit theory gives an easy way to find the maximal set of independent loops which consists only of loops of length 3. In [2] it is proved that we can do the same for the loops of length  $n$  and it is shown how to do it. We have shown in Section 3 that it is possible for any  $3 \leq p \leq n$ . Indeed, by Corollary 1 there exists a set of  $p$ -cycles  $\{\nu_k : 1 \leq k \leq N_1\}$  such that the corresponding set of equations

$$0 = \sum_{i \neq \nu_k(i)} u_{i, \nu_k(i)} - \sum_{i > \nu_k(i)} (u_{i, \nu_k(i)} + u_{\nu_k(i), i}) = \sum_{i < \nu_k(i)} u_{i, \nu_k(i)} - \sum_{i > \nu_k(i)} u_{\nu_k(i), i}$$

is linearly independent. To obtain examples of such sets of equations it suffices to take all equations corresponding to  $p$ -cycles occurring in (8) for  $p = 3$  and in (12) for  $4 \leq p \leq n$  respectively.

## 5.2. Graphs with two branches between each pair of nodes

Now, let us consider a graph of an electric circuit with  $n \geq 3$  nodes such that each two of them are connected by two branches. Then, the maximum number of linearly independent loops equals

$$N_2 = N_1 + \binom{n}{2} = 2 \binom{n}{2} - n + 1 = n(n-1) - (n-1) = (n-1)^2.$$

We can create the same matrix  $\mathbb{U}$  as in the previous subsection. Now, let us assume that each pair of branches have opposite directions. Then, any  $p$ -cycle,  $2 \leq p \leq n$ , corresponds to exactly one loop consisting only of branches with the same direction as the loop direction. The set of all such loops contains the maximal set of independent loops consisting only of loops of the same length if and only if the number of nodes  $n \geq 5$  and the length of loops  $3 \leq p \leq n-1$ . Indeed, the number of all 2-cycles is too small and by Remark 1 the number of all 3-cycles is too small in case  $n = 4$ . By Corollary 2 the maximum number of linearly independent loops of length  $n$  is too small. Finally, by Theorem 2, for  $n \geq 5$  and  $3 \leq p \leq n-1$  there exists a set of  $p$ -cycles  $\{\nu_k : 1 \leq k \leq N_2\}$  such that the corresponding set of equations

$$\sum_{i \neq \nu_k(i)} u_{i, \nu_k(i)} = 0$$

is linearly independent. To obtain examples of such sets of equations it suffices to take all equations corresponding to  $p$ -cycles occurring in (13) for  $p = 3$  and in (14) for  $4 \leq p \leq n-1$  respectively.

## 6. Appendix

### 6.1. Proofs of the properties

First, let us notice that

$$\begin{aligned} y(\nu) &= \sum_{i=1}^n x_{i,\nu(i)} = \sum_{i \neq \nu(i)} x_{i,\nu(i)} + \sum_{i=\nu(i)} x_{i,i} = \sum_{i \neq \nu(i)} x_{i,\nu(i)} - \sum_{i \neq \nu(i)} x_{i,i} + \sum_{i=1}^n x_{i,i} \\ &= \sum_{i \neq \nu(i)} x_{i,\nu(i)} - \sum_{i \neq \nu(i)} x_{i,i} + y(e) \end{aligned}$$

for any  $\nu \in S_n$ .

*Proof.* [Proof of property (5)]

$$\begin{aligned} y(i_1, i_2, \dots, i_p) &= x_{i_1, i_2} + \sum_{k=2}^{p-1} x_{i_k, i_{k+1}} + x_{i_p, i_1} - \sum_{k=1}^p x_{i_k, i_k} + y(e) \\ &= \sum_{k=2}^{p-1} (x_{i_1, i_k} + x_{i_k, i_{k+1}} + x_{i_{k+1}, i_1}) - \sum_{k=3}^{p-1} (x_{i_1, i_k} + x_{i_k, i_1}) \\ &\quad - \sum_{k=1}^p x_{i_k, i_k} + y(e) \\ &= \sum_{k=2}^{p-1} (y(i_1, i_k, i_{k+1}) + x_{i_1, i_1} + x_{i_k, i_k} + x_{i_{k+1}, i_{k+1}} - y(e)) \\ &\quad - \sum_{k=3}^{p-1} (y(i_1, i_k) + x_{i_1, i_1} + x_{i_k, i_k} - y(e)) - \sum_{k=1}^p x_{i_k, i_k} + y(e) \\ &= \sum_{k=2}^{p-1} y(i_1, i_k, i_{k+1}) - \sum_{k=3}^{p-1} y(i_1, i_k) \end{aligned}$$

□

*Proof.* [Proof of property (6)]

$$\begin{aligned} y(\nu) &= \sum_{i \neq \nu(i)} x_{i,\nu(i)} - \sum_{i \neq \nu(i)} x_{i,i} + y(e) \\ &= \sum_{i \neq \nu(i)} (x_{j,i} + x_{i,\nu(i)} + x_{\nu(i),j}) - \sum_{i \neq \nu(i)} x_{j,i} - \sum_{i \neq \nu(i)} x_{\nu(i),j} - \sum_{i \neq \nu(i)} x_{i,i} + y(e) \\ &= \sum_{i \neq \nu(i)} (x_{j,i} + x_{i,\nu(i)} + x_{\nu(i),j}) - \sum_{i \neq \nu(i)} (x_{j,\nu(i)} + x_{\nu(i),j}) - \sum_{i \neq \nu(i)} x_{i,i} + y(e) \\ &= \sum_{i \neq \nu(i)} (y(j, i, \nu(i)) + x_{j,j} + x_{i,i} + x_{\nu(i),\nu(i)} - y(e)) \\ &\quad - \sum_{i \neq \nu(i)} (y(j, \nu(i)) + x_{j,j} + x_{\nu(i),\nu(i)} - y(e)) - \sum_{i \neq \nu(i)} x_{i,i} + y(e) \end{aligned}$$

$$\begin{aligned}
&= \sum_{i \neq \nu(i)} y(j, i, \nu(i)) - \sum_{i \neq \nu(i)} y(j, \nu(i)) + y(e) \\
&= y(e) + \sum_{i \neq \nu(i)} y(j, i, \nu(i)) - \sum_{i \neq \nu(i)} y(j, i).
\end{aligned}$$

□

*Proof.* [Proof of property (7)]

$$\begin{aligned}
\sum_{i \neq \nu(i)} y(i, \nu(i)) &= \sum_{i \neq \nu(i)} \left( y(i, \nu(i)) - y(e) \right) + p y(e) \\
&= \sum_{i \neq \nu(i)} \left( x_{i, \nu(i)} + x_{\nu(i), i} - x_{i, i} - x_{\nu(i), \nu(i)} \right) + p y(e) \\
&= \sum_{i \neq \nu(i)} \left( x_{i, \nu(i)} + x_{\nu(i), i} \right) - \sum_{i \neq \nu(i)} x_{i, i} - \sum_{i \neq \nu(i)} x_{\nu(i), \nu(i)} + p y(e) \\
&= \sum_{i \neq \nu(i)} x_{i, \nu(i)} + \sum_{i \neq \nu(i)} x_{\nu(i), i} - 2 \sum_{i \neq \nu(i)} x_{i, i} + 2 y(e) + (p-2) y(e) \\
&= y(\nu) + y(\nu^{-1}) + (p-2) y(e).
\end{aligned}$$

□

## 6.2. Proofs of the lemmas

First, let us notice that by property (5) we have

$$\begin{aligned}
y(i_1, i_2, \dots, i_r, \dots, i_p) &= \\
&= \sum_{k=2}^{p-1} y(i_1, i_k, i_{k+1}) - \sum_{k=3}^{p-1} y(i_1, i_k) \\
&= \sum_{k=2}^{r-1} y(i_1, i_k, i_{k+1}) + \sum_{k=r}^{p-1} y(i_1, i_k, i_{k+1}) - \sum_{k=3}^{r-1} y(i_1, i_k) - y(i_1, i_r) - \sum_{k=r+1}^{p-1} y(i_1, i_k) \\
&= y(i_1, i_2, \dots, i_r) + y(i_1, i_r, i_{r+1}, \dots, i_p) - y(i_1, i_r)
\end{aligned}$$

for any  $p$ -cycle  $(i_1, i_2, \dots, i_r, \dots, i_p) \in S_n$ , where  $4 \leq p \leq n$  and  $3 \leq r \leq p-1$ .

*Proof.* [Proof of Lemma 1]

If  $p = 4$ , then for any distinct  $1 \leq i, j, k, l \leq 4$  we have

$$\begin{aligned}
0 &= y(i, l, j, k) = y(i, l, j) + y(i, j, k) - y(i, j), \\
0 &= y(i, k, l, j) = y(i, k, l) + y(i, l, j) - y(i, l),
\end{aligned}$$

and by subtracting one equation from the other we get

$$y(i, j, k) - y(i, k, l) = y(i, j) - y(i, l).$$

If  $5 \leq p \leq n$ , then for any distinct  $1 \leq i, j, k, l \leq n$  we can take two  $p$ -cycles

$$\begin{aligned}\sigma_1 &= (j, k, i, l, r_1, r_2, \dots, r_{p-4}), \\ \sigma_2 &= (l, r_1, r_2, \dots, r_{p-4}, j, i, k),\end{aligned}$$

for which we have

$$\begin{aligned}0 &= y(\sigma_1) = y(j, k, i) + y(j, i, l) + y(j, l, r_1, r_2, \dots, r_{p-4}) - y(j, i) - y(j, l), \\ 0 &= y(\sigma_2) = y(l, r_1, r_2, \dots, r_{p-4}, j) + y(l, j, i) + y(l, i, k) - y(l, j) - y(l, i),\end{aligned}$$

and by subtracting one equation from the other we get

$$y(i, j, k) - y(i, k, l) = y(i, j) - y(i, l).$$

□

*Proof.* [Proof of Lemma 2]

If  $4 \leq p \leq n - 1$ , then for any distinct  $1 \leq i, j, k, l \leq n$  we can take two  $p$ -cycles

$$\begin{aligned}\sigma_1 &= (i, k, j, r_1, r_2, \dots, r_{p-3}), \\ \sigma_2 &= (i, l, j, r_1, r_2, \dots, r_{p-3}),\end{aligned}$$

for which we have

$$\begin{aligned}0 &= y(\sigma_1) = y(i, k, j) + y(i, j, r_1, r_2, \dots, r_{p-3}) - y(i, j), \\ 0 &= y(\sigma_2) = y(i, l, j) + y(i, j, r_1, r_2, \dots, r_{p-3}) - y(i, j),\end{aligned}$$

and by subtracting one equation from the other we get  $y(i, k, j) = y(i, l, j)$ . It follows that  $y(\nu_1) = y(\nu_2)$  for any 3-cycles  $\nu_1, \nu_2 \in S_n$ . From this and Lemma 1 the equality  $y(\nu_1) = y(\nu_2)$  holds for any 2-cycles  $\nu_1, \nu_2 \in S_n$ .

If  $p = 3$  and  $n \geq 5$ , then for any distinct  $1 \leq i, j, k, l \leq n$  we have

$$\begin{aligned}0 &= y(i, j, k) + y(i, k, l) = y(i, j, k, l) + y(i, k), \\ 0 &= y(j, k, l) + y(j, l, i) = y(j, k, l, i) + y(j, l),\end{aligned}$$

and by subtracting one equation from the other we get  $y(i, k) = y(j, l)$ . Hence for any distinct  $1 \leq i, j, k, l, m \leq n$  we have

$$y(i, k) = y(j, l) = y(i, m),$$

and it follows that  $y(\nu_1) = y(\nu_2)$  for any 2-cycles  $\nu_1, \nu_2 \in S_n$ . □

## References

- [1] D. B. Leep and G. Myerson, *Marriage, Magic, and Solitaire*, The American Mathematical Monthly, **106**, no. 5 (1999), 419–429.
- [2] P. Migus, *The relationship among the Kirchhoff equations for the loop of electrical circuits*, Recherches sur les déformations, **61**, no. 2 (2011), 95–104.
- [3] M. Tadeusiewicz, *Teoria obwodów, cz. I*, Wydawnictwo Politechniki Łódzkiej, Łódź 1990.

Faculty of Mathematics and Computer Science  
University of Łódź  
Stefana Banacha 22, PL-90-238 Łódź  
Poland  
e-mail: szuminski@math.uni.lodz.pl

Presented by Andrzej Łuczak at the Session of the Mathematical-Physical Commission of the Łódź Society of Sciences and Arts on December 4, 2014

## **KWADRATY PÓLMAGICZNE I NAPIĘCIOWE PRAWO KIRCHHOFFA**

### **S t r e s z c z e n i e**

Rozważamy bazy przestrzeni wektorowych kwadratów półmagicznych składające się tylko z macierzy permutacji. Pokazujemy relację między takimi bazami a maksymalnymi zbiorami liniowo niezależnych równań pewnego układu. Używając tej relacji, dowodzimy istnienia pewnych konkretnych rodzajów baz składających się z macierzy jednostkowej i macierzy permutacji cyklicznych. W większości przypadków bazy te odpowiadają zbiorom permutacji zawierającym tak dużo cykli tej samej długości, jak to jest tylko możliwe. Podajemy przykłady wszystkich rozważanych rodzajów baz i pokazujemy związki między naszymi rezultatami a maksymalnymi zbiorami niezależnych pętli w pewnych konkretnych grafach obwodów elektrycznych.

*Słowa kluczowe:* kwadrat półmagiczny, macierz permutacji, permutacja cykliczna, napięciowe prawo Kirchhoffa

## B U L L E T I N

DE LA SOCIÉTÉ DES SCIENCES ET DES LETTRES DE ŁÓDŹ

2014

Vol. LXIV

Recherches sur les déformations

no. 3

pp. 69–80

*In memory of  
Professor Zygmunt Charzyński (1914–2001)*

*Mariusz Zubert, Marcin Janicki, Tomasz Raszkowski, Agnieszka Samson,  
Piotr Stanisław Nowak, and Krzysztof Pomorski*

**THE HEAT TRANSPORT IN NANO-ELECTRONIC DEVICES  
AND PDEs TRANSLATION INTO HARDWARE DESCRIPTION  
LANGUAGES**

**Summary**

In this paper, the DPL and the MD heat transfer models are implemented in the RESCUER language for thermal simulations of various nanostructures. The application of RESCUER language allows simple and effective description of distributed heat transfer problems using equivalent electrical circuits. In this way, compared to the classic Fourier-Kirchhoff heat equation, more accurate heat transfer models for nanoscale components can be obtained.

*Keywords and phrases:* DPL, MD, SPICE, RESCUER, HDL, Fourier-Kirchhoff equation, dual-phase-lag model, molecular dynamics, heat equation, simulation, equivalent electrical circuit

**1. Introduction**

The electro-thermal analysis is one of the most important development steps in the professional design of analogue submicron electric Integrated Circuits (ICs), power modules design process as well as modern nanostructures. This analysis is useful to power density and operating conditions estimation (e.g. the electric circuit operating point, the temperature dependence of device electric properties as well as the maximum operating circuit temperature). Mostly heat transfer in a thermally conducting solid medium can be correctly described using the classical Fourier law

(1) and the resulting Fourier-Kirchhoff heat equation (2)

$$(1) \quad \vec{q}(x, y, z, t) = -\lambda \nabla T(x, y, z, t)$$

$$(2) \quad \frac{\partial}{\partial t} (c_p \rho T(x, y, z, t)) = -\nabla \cdot \vec{q}(x, y, z, t) + q_{gen}(x, y, z, t)$$

with mixed boundary conditions, where  $T(x, y, z, t)$  represents the temperature distribution in ICs,  $q(x, y, z, t)$  is the heat flux,  $q_{gen}(x, y, z, t)$  is internal generated heat density,  $\lambda$  is thermal conductance,  $c_p$  is specific heat capacity,  $\rho$  is mass density and  $t$  is time variable.

Unfortunately, the Fourier-Kirchhoff equation postulates some nonphysical behaviour assuming that heat propagates with infinite speed and both heat flux and temperature gradient are changing instantaneously, what does not agree with experiments [9,16]. Another problem is associated with the semiconductor fabrication technology whose development brought extreme device size down to 14 nm in case of Metal-Oxide-Semiconductor Field-Effect Transistor (MOSFET), e.g. in the Intel Broadwell CPU family, or 6 nm in the prototype FinFETs technology [10] and in nanowire and nanotube fabrication. In all these cases the dimensionless Knudsen number  $Kn$ , which is defined as the ratio of the mean free path to the structure characteristic length, is much more higher than the unity because for silicon the phonon free path at 300 K is around 41.8 nm [15]. Therefore, the ballistic heat transport should be taken into consideration in the heat transfer mathematical description.

The finite speed of heat propagation has been introduced into the Fourier law by Cattaneo and Vernotte who postulated the following relation between the temperature gradient and the heat flux [2, 17]:

$$(3) \quad \tau_q \frac{\partial \vec{q}(x, y, z, t)}{\partial t} + \vec{q}(x, y, z, t) = -\lambda \nabla T(x, y, z, t)$$

This leads to the hyperbolic heat conduction equation. Further modifications have been introduced by Tzou in the single-phase-lag model (SPL) [3, 4]

$$(4) \quad \vec{q}(x, y, z, t + \tau_q) = -\lambda \nabla T(x, y, z, t)$$

and finally in the dual-phase-lag model (DPL) [5]

$$(5) \quad \vec{q}(x, y, z, t) + \tau_q \frac{\partial \vec{q}(x, y, z, t)}{\partial t} = -\lambda \left( \nabla T(x, y, z, t + \tau_T) + \tau_T \frac{\partial}{\partial t} \nabla T(x, y, z, t + \tau_T) \right)$$

where  $\tau_T$  and  $\tau_q$  are the phase lag of the temperature gradient and the heat flux vector respectively. The DPL model can be used to model heat transfer in IC structures developed in technologies down to 180 nm, introduced before 1999, and for electronic circuits operating at frequency up-to 6.4GHz, i.e. those for which the changes in heat generation processes occur in more than 80 ps.

The results presented in [7,8] and [14] show that the heat transfer in latest ICs and nanostructures (with Knudsen number between  $2 \div 7$ ) should be described using the Boltzmann Transfer Equation (BTE), Ballistic-Diffusive (BD) equation [7, 8, 12] or

Molecular Dynamics (MD) approach depending on the application and the dominant physical phenomena.

## 2. Heat transfer in technology node up-to 180 nm

The equation modelling heat transfer in isotropic solids according to the DPL model can be found by introducing (5) into (2) obtaining the following relation [5, 18]:

$$(6) \quad \frac{1}{\alpha} \frac{\partial T(x, y, z, t)}{\partial t} + \frac{\tau_q}{\alpha} \frac{\partial^2 T(x, y, z, t)}{\partial t^2} = \Delta T(x, y, z, t) + \tau_T \frac{\partial}{\partial t} \Delta T(x, y, z, t) + \frac{1}{\lambda} \left( q_{gen}(x, y, z, t) + \tau_q \frac{\partial q_{gen}(x, y, z, t)}{\partial t} \right)$$

where  $\alpha = \lambda / (c_p \rho)$  is material thermal diffusivity and

$$(7) \quad \Delta T(x, y, z, t) \equiv \Delta T(x, y, z, t + \tau_T)$$

This equation has been already solved analytically in [1] but the solution form is not acceptable for electronic simulation environments. In order to simplify modelling and simulation of recently developed silicon structures, the RESCUER compiler has been proposed [19]. The RESCUER software allows joint analysis of multidomain models described in its internal language and their translation into the Mathematica language or into an equivalent electrical circuit simulator, such as Simulation Program with Integrated Circuit Emphasis (SPICE). Such translated models can be used then simultaneously with electrical circuits and digital systems in various simulation environments. Owing to this solution, the advantages of both the multidomain simulation and a chosen simulation environment can be jointly exploited.

The advantage of the proposed approach consists in the creation of a new generation of compilers, which can translate and optimize specified distributed problems described in the high-level abstraction language into a destination language or an equivalent SPICE circuit. Models written in the RESCUER language can contain the following elements:

- sets of second order algebraic and partial differential equation containing first order space and time derivatives;
- constants coefficients defined by the time invariable scalar fields;
- variables treated as solution fields;
- discretization points used to couple equations, constants and variables.

The decomposed models are converted into differential algebraic equation using no-mesh approximations of the first and the second order partial differential operators based on the Taylor series expansions [19]. Then, the models are symbolically simplified and numerically reduced. The final approximate models are mapped into

structures available in a destination environment. In the case of electrical simulators, the set of equations is converted into equivalent electrical circuit using the method presented in [20]. More information about the model translation, the stability and the convergence of generated models can be found in [19–21].

For example, assuming that  $\tau_q = 3$  ps,  $\tau_T = 60$  ps,  $\rho = 2330$  kg/m<sup>3</sup>,  $c_p = 712$  J/kgK and  $\lambda = 148$  W/mK. a one-dimensional DPL heat transfer problem (6) defined as:

$$(8) \quad \begin{aligned} & (x, t) \in [0, L] \times [0, 10^{-6}], L = 180 \cdot 10^{-9}, \quad q_{gen}(x, t) = 0 \\ & T(x, t)|_{t=0} = 0; \left. \frac{\partial T(x, t)}{\partial t} \right|_{t=0} = 0; T(x, t)|_{x=0} = 1(t); \quad T(x, t)|_{x=L} = 0; \end{aligned}$$

can be described in the RESCUER language as follows:

```

object 1D DPLeExample {
  const tauq=3.0E-9, tauT=60.0E-9, lambda=148,
        alpha=lambda/(712*2330);

  var T=0, Tt=0;

  equ DPLeq1(T): (diff[T,t]+tauq*diff[Tt,t])/alpha==
                laplacian[T]+tauT*laplacian[Tt],
        DPLeq2(Tt): diff[T,t]==Tt;

  point P0(0.0E-11) {--boundary conditions for x=0 nm

  equ
        DPLeq1(T): -lambda*diff[T,x]==q,
        DPLeq2(Tt): diff[T,t]==Tt;
  };

  point P1(2.0E-11); pointP2(4.0E-11);
  --... mesh points ...

  point P1000(180.0E-9){ --boundary conditions for x=200 nm
    equ DPLeq1(T): T==0, DPLeq2(Tt): Tt==0;
  }
}

```

The part of this model translated into an equivalent electric circuit in SPICE format (for the coordinate  $x = 2.0 \cdot 10^{-11}$ ) is presented below:

```

* Variables:
* DPLeExample.P0,T,N1, DPLeExample.P0,x=0

```

```

* DPLExample.P0,Tt,N2, DPLExample.P0,x=0
...
* DPLExample.P1,T,N3, DPLExample.P1,x=2e-011
* DPLExample.P1,Tt,N4, DPLExample.P1,x=2e-011
E1 N9 0 N1 0 1 ;voltage controlled voltage source,
                ;output node: N9, ground, inp. node: N1, ground
R2 N2 0 1 ;resistor 1 ohms, between node N2 and ground
C2 N2 0 -1 ; capacitance -1F, between node N2 and ground
C3 N3 N10 3.3627568e-005
E2 N10 0 N4 0 1
G5 0 N3 N1 0 -2.5e+021 ; voltage controlled current source,
                ; input nodes: N1, ground, output node: N3, ground
                ; coupling coeff. -2.5e+021
G6 0 N3 N5 0 -381208.87
G7 0 N3 N7 0 -2.5e+021
G8 0 N3 N4 0 3e+014
G9 0 N3 N2 0 -1.5e+014
G10 0 N3 N6 0 -0.022872532
G11 0 N3 N8 0 -1.5e+014
R3 N3 0 -2e-022
C4 N3 0 -11209.189
.IC V(N3)= {0} ; initial conditions for node N3
...
* DPLExample.P1000,T,N5, DPLExample.P1000,x=1.8e-007
* DPLExample.P1000,Tt,N6, DPLExample.P1000,1.8e-007
...

```

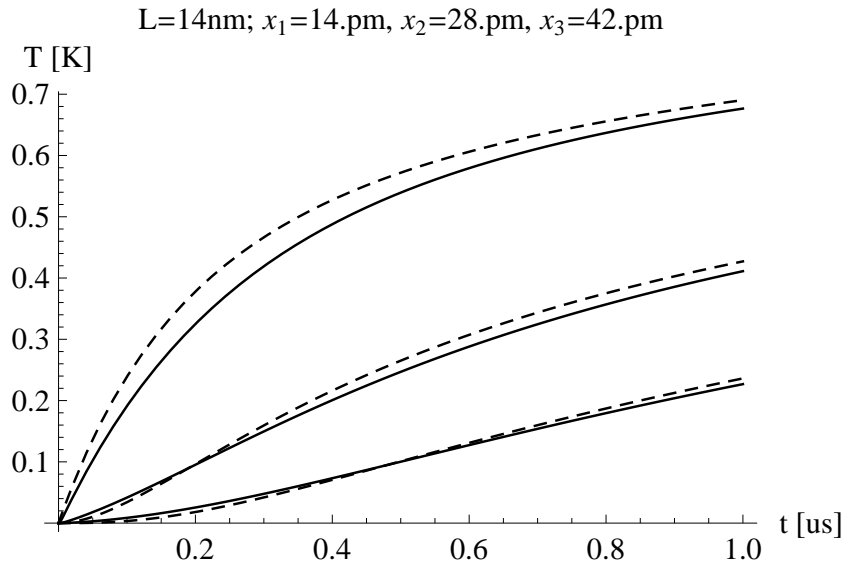
The generated equivalent electric circuit can be used then with electrical simulators for a coupled electro-thermal simulation. An example of simulation results obtained for the DPL (solid line,  $\tau_q = 3$  ps,  $\tau_T = 60$  ps) and the Fourier-Kirchhoff heat transfer models (dashed line,  $\tau_q = \tau_T = 0$ ) have been presented in Fig. 1. As can be seen, for large structures (180 nm in the considered case) the differences between both heat transfer models are negligible. The DPL model is not correct for  $L = 14$  nm ( $Kn \ll 1$ ) therefore the Ballistic-Diffusive Equation [7, 8, 12] or BTE should be used.

### 3. Molecular dynamics simulation of nanowires and nanotubes

Nanowires and nanotubes are defined as nanometre size structures, whose the length is typically much greater than the thickness (eg. 1000:1). These nanostructures are more and more used to manufacture prototype transistors with ultra small gate lengths ( $6 \div 20$  nm =  $11 \div 37 \cdot a$ ). Because the lattice constant ( $a = 0.543$  nm for silicon) is comparable with the nanostructure dimensions, the heat transport can be

effectively simulated using molecular dynamics (MD) approach.

a)



b)

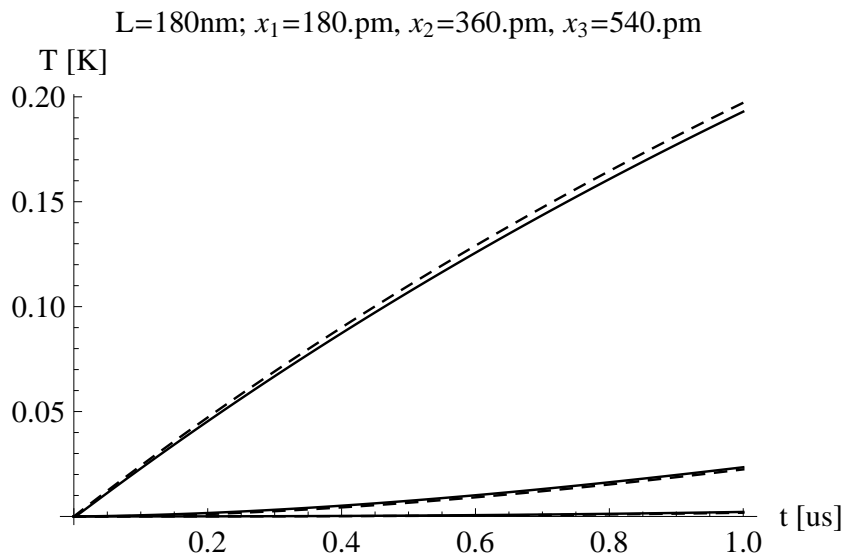


Fig. 1: 1 Simulation results for DPL (solid line,  $\tau_q = 3$  ps,  $\tau_T = 60$  ps) and Fourier-Kirchhoff model ( $\tau_q = \tau_T = 0$ , dashed).  $X$ -axis – time in seconds.  $Y$ -axis – temperature rise for Robin mixed boundary condition at specified nodes.

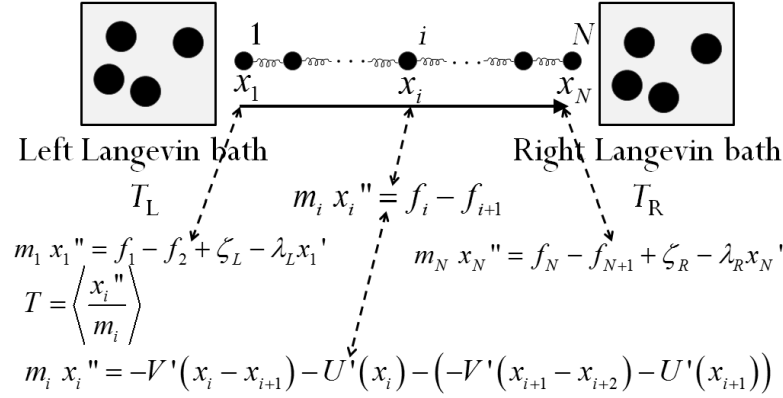


Fig. 2: The 1-D heat MD transport model.

The main problem of microscopic approaches, such as the MD, is related to the insufficient number of particles  $N$  required to estimate the values of thermal conductivity and temperature. Namely, from macroscopic point of view thermal conductivity is defined by the equilibrium time correlation function of the corresponding heat current in Green-Kubo formalism

$$(9) \quad \lambda = \frac{1}{k_B T^2} \lim_{t \rightarrow \infty} \lim_{N \rightarrow \infty} \frac{1}{N} \int_0^t \langle J(t') J(0) \rangle dt'$$

where  $J(t)$ ,  $k_B$ ,  $T$  are the total heat current, Boltzmann coefficient and temperature respectively.

The other problem is associated with the classical temperature definition as the averaged kinetic energy of particles which should be estimated for larger solid regions (grains) using the virial theorem

$$(10) \quad T = \langle [x_1 \quad \dots \quad \frac{p_1^2}{N} \quad \dots] \cdot \nabla H \rangle_\mu = \left\langle \frac{p_i^2}{m_i} \right\rangle_\mu$$

Thus, here the local temperature will be defined as:

$$(11) \quad T_i = \left\langle \frac{\ddot{x}_i}{m_i} \right\rangle$$

One- or many dimensional systems of vibrating lattice particles are placed in the external potential field  $U$  and interact through a nearest neighbour what is modelled by the interaction potential  $V$ . Then, the Hamiltonian can be written as:

$$(12) \quad H = \sum_{i=1}^N \left[ \frac{p_i^2}{2m_i} + V(x_i - x_{i+1}) \right] + \sum_{l=1}^{N-1} U(x_l)$$

where  $m_l$ ,  $x_l$ ,  $p_l = m_l \cdot \dot{x}_l$  for  $l = 1, 2, \dots, N$  denote the particle mass, displacement and moment of the  $l$ -th particle respectively. In the proposed approach, the interaction potential field  $V$  is approximated using the FPU- $\beta$  model [6] (for  $a = 1$ ,  $\beta = 0$  see also [13])

$$(13) \quad V(\Delta x_i) = \frac{(\Delta x_i - a)^2}{2} + \beta \frac{(\Delta x_i - a)^4}{4}$$

The periodic on-site potential for nanostructure-substrate interaction has been described using the FK model [11] (for  $b = 1$ ,  $K = 10\pi$ )

$$(14) \quad U(x_i) = \frac{K}{(2\pi)^2} \cos\left[\frac{2\pi x_i}{b}\right]$$

The motion equation of nanostructure internal particles ( $i = 2, \dots, N - 1$ ) can be described using the following equations:

$$(15) \quad \ddot{x}_i = f_i - f_{i+1}$$

$$(16) \quad f_i = -V(x_i - x_{i+1}) - U'(x_i)$$

Finally, the heat transfer through a nanostructure can be obtained by connecting the Langevin heat reservoirs to the outer particles ( $i = 1$  and  $i = N$ , see Fig. 2).

The description of this problem in the RESCUER language is as follows:

```

object 1D NanoStructure {
  const TL=1.1,TR=0.9, --b.c.
  const m=1, pi= 3.141592653589793;
  const XiL=2,LambdaL=0.1, XiR=1,LambdaR=0.1;
  var xpos=0, p=sqrt[m*(TL+TR)/2], u=0;
  equ eq1(p):diff [p,t]==m*(diff [xpos,x,x]+diff [u,x,x]), --simplified
      eq2(xpos): p==m*diff [xpos,t],
      eq3(u): u==5*cos(2*pi*xpos)/(2*pi);

  point P0(0) { --boundary conditions for x=0 nm
    equ eq1(p): diff [p,t]==m*(diff [xpos,x,x]-
      (XiL-LambdaL*diff [x,t]));
  };
  point P1(1); point P2(2);

  --... mesh points ...
  point P37(37){ --boundary conditions for x=20 nm
    equ eq1(p): diff [p,t]==m*(diff [xpos,x,x]-
      (XiR-LambdaR*diff [x,t]));
  }
}

```

For time instants  $t$  of 0, 5, 10, 15 and 25 seconds, the computed estimates of the local temperature distribution and the total heat current are presented in Fig. 3.

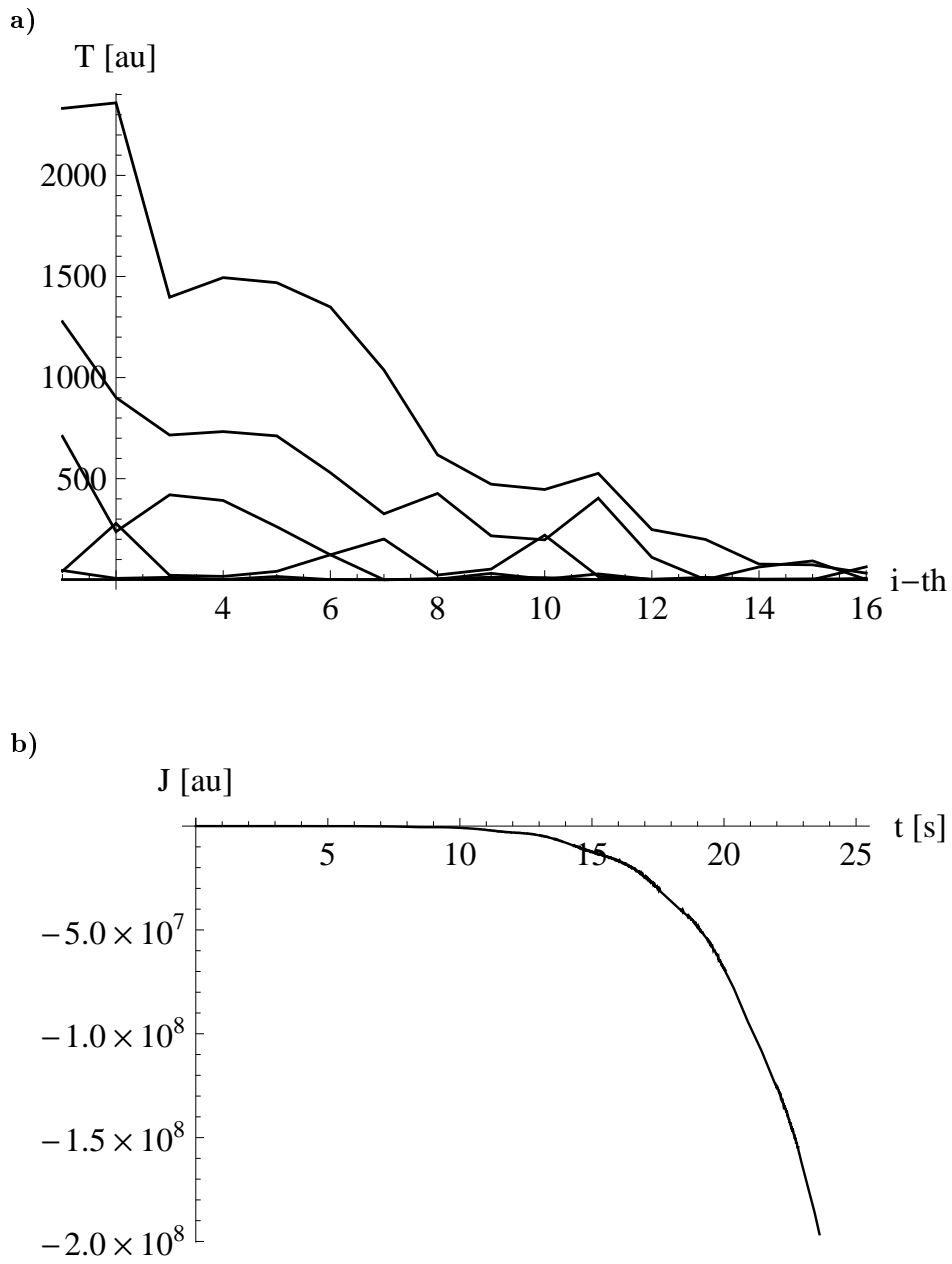


Fig. 3: a) The local temperature distribution estimation for  $t = 0, 5, 10, 15$  and  $25$ s. b) The total heat current estimation.

## 4. Summary

In this paper, the DPL and the MD heat transfer models were implemented in the RESCUER language for thermal simulations of nanostructures. The application of RESCUER language allowed simple and effective description of distributed heat transfer problems using equivalent electrical circuits. Compared to the classic Fourier-Kirchhoff heat equation, more accurate heat transfer models for nanoscale components can be obtained employing BTE, DPL, BD or MD approaches.

## Acknowledgments

This research was supported by the Polish National Science Center project No. 2013/11/B/ST7/01678 and the Internal University Grant K25/DZST/1/2014.

## References

- [1] R. Alkhairey, *Green's function solution for the dual-phase-lag heat equation*, Applied Mathematics **3**, no. 10 (2012), 1170–1178.
- [2] C. Cattaneo, *A form of heat conduction equation which eliminate paradox of instantaneous propagation*, Comptes Rendus **247** (1958), 431–433.
- [3] D. Y. Tzou, *On the thermal shock waves induced by a moving heat source*, ASME J. Heat Transfer **111** (1989), 232–238.
- [4] D. Y. Tzou, *Shock wave formation around a moving heat source in a solid with finite speed of heat propagation*, Int. J. Heat Mass Transfer **32** (1989), 1979–1987.
- [5] D. Y. Tzou, *The generalized lagging response in small-scale and high-rate heating*, Int. J. Heat Mass Transfer **38** (1995), 3231–3240.
- [6] E. Fermi, J. Pasta, and S. Ulam, *Studies of nonlinear problems*, Collected Works of Enrico Fermi II (1965), 978–988.
- [7] G. Chen, *Ballistic-diffusive equations for transient heat conduction from nano to macroscales*, J. Heat Transfer **124** (2001), 320–328.
- [8] G. Chen, *Ballistic-diffusive heat conduction equation*, ASP **86** (2001), 2297–2300.
- [9] S. E. Hebboul and J. P. Wolfe, *Lattice dynamics of insb from phonon imaging*, Zeitschrift für Physik B Condensed Matter **73**, no. 4 (1989), 437–466.
- [10] A. Kaneko, A. Yagishita, K. Yahashi, T. Kubota, M. Omura, K. Matsuo, I. Mizushima, K. Okano, H. Kawasaki, S. Inaba, T. Izumida, T. Kanemura, N. Aoki, K. Ishimaru, H. Ishiuchi, K. Suguro, K. Eguchi, and Y. Tsunashima, *Sidewall transfer process and selective gate sidewall spacer formation technology for sub-15 nm finfet with elevated source/drain extension*, in: *Electron Devices Meeting, IEDM Technical Digest*. IEEE International, 2005, pp. 844–847.
- [11] T. A. Kontorova and Ya. I. Frenkel, *On the theory of plastic deformation and twinning*, Zh. Exp. Teor. Fiz. **8**, no. 12 (1938), 1340–1348.
- [12] G. Lebon, M. Grmela, and Ch. Dubois, *From ballistic to diffusive regimes in heat transport at nano-scales*, Comptes Rendus Mecanique **339** (2011), 324–328.
- [13] S. Lepri, R. Livi, and A. Politi, *Thermal conduction in classical low-dimensional lattices*, Physics Reports **377**, no. 1 (2003), 1–80.

- [14] M. Moghaddam, J. Ghazanfarian, and A. Abbassi, *Implementation of dpl-dd model for the simulation of nanoscale mos devices*, Electron Devices, IEEE Transactions **61** no. 9 (2014), 3131–3138.
- [15] A. Nabovati, D.P. Sellan, and C.H. Amon, *On the lattice boltzmann method for phonon transport*, Journal of Computational Physics **230**, no. 15 (2011), 5864–5876.
- [16] R. J. Gutfeld and A. H. Nethercot, *Heat pulses in quartz and sapphire at low temperatures*, Phys. Rev. Lett. **12** (1964), 641.
- [17] P. Vernotte, *Some possible computations in the phenomena of thermal conduction*, Comptes Rendus **252** (1961), 2190–2191.
- [18] Mingtian Xu and Liqiu Wang, *Dual-phase-lagging heat conduction based on Boltzmann transport equation*, International Journal of Heat and Mass Transfer **48**, no. 25–26 (2005), 5616–5624.
- [19] M. Zubert, *The Multidimensional and Multidomain Modelling and Simulation of Physical Phenomena in Modern Silicon Structures*, PhD thesis, Łódź University of Technology, Łódź 1999, in Polish.
- [20] M. Zubert, M. Napieralska, and A. Napieralski, *Rescuer – the new solution in multidomain simulations*, Microelectronics journal **31**, no. 11 (2000), 945–954.
- [21] M. Zubert, A. Napieralski, and M. Napieralska, *The application of rescuer software to effective mems design and simulation*, Bulletin of the Polish Academy of Sciences. Technical sciences **49**, no. 4 (2001), 595–610.

Department of Microelectronics  
and Computer Science  
Łódź University of Technology  
Wólczańska 221/223, PL-90-924 Łódź  
Poland  
e-mail: mariuszz@dmcs.p.lodz.pl

Faculty of Physics, Astronomy  
and Applied Computer Science  
Jagiellonian University  
St. Lojasiewicza 11, PL-30-348 Kraków  
and  
Faculty of Physics  
University of Warsaw  
Pasteura 5, PL-02-093 Warszawa  
Poland

Presented by Marek Moneta at the Session of the Mathematical-Physical Commission of the Łódź Society of Sciences and Arts on November 20, 2014

## PRZEPIŃY W NANOSTRUKTURACH I AUTOMATYCZNA TRANSLACJA MODELI OPISANYCH RÓWNANIAMI PDE DO ELEKTRYCZNEJ POSTACI OBWODOWEJ I JĘZYKÓW OPISU SPRZĘTU

### Streszczenie

W niniejszej pracy przedstawiono sposoby modelowania nowoczesnych struktur półprzewodnikowych przy użyciu niefurierowskiego opisu przepływu ciepła z wykorzystaniem makroskopowego modelu o niesymetrycznym opóźnieniu zmian temperatury i strumienia

ciepłego (DPL) oraz mikroskopowego modelu dynamiki molekularnej (MD). Zaproponowane modele zostały przekształcone do równoważnej elektrycznej postaci obwodowej i języków opisu sprzętu za pomocą opracowanego kompilatora RESCUER. W publikacji przedstawiono również główne ograniczenia i zakresy stosowania tych sposobów modelowania.

*Słowa kluczowe:* DPL, MD, SPICE, RESCUER, HDL, Fourier-Kirchhoff equation, dynamika molekularna, równanie przepływu ciepła, symulacja, elektryczny model obwodowy

## B U L L E T I N

DE LA SOCIÉTÉ DES SCIENCES ET DES LETTRES DE ŁÓDŹ

2014

Vol. LXIV

Recherches sur les déformations

no. 3

pp. 81–90

*In memory of*  
*Professor Zygmunt Charzyński (1914–2001)*

*Małgorzata Nowak-Kępczyk*

**AN ALGEBRA GOVERNING REDUCTION OF QUATERNARY  
STRUCTURES TO TERNARY STRUCTURES II**  
A STUDY OF THE MULTIPLICATION TABLE FOR THE RESULTING  
ALGEBRA GENERATORS

**Summary**

By applying the reduction matrices of Part I we analyze the multiplication tables of generators of the cubic and nonion algebras and deduce the remaining  $3 \times 3$  subtables for the resulting algebra. We determine the remaining 9 generators and study the corresponding multiplication tables. The problem of linear independence of the resulting generators is left to Part III.

*Keywords and phrases:* noncommutative Galois extensions, finite-dimensional algebras, associative rings and algebras, matrix rings

**9. Six characteristic triples of the  $3 \times 3$ -matrices applied in the  
reduction matrices**

We observe a special form of the matrices involved in the reduction relations (8)–(13) of Part I [4].

$$(a_{jk}) = \begin{pmatrix} a_1 & a_2 & a_3 \\ a_3 & a_1 & a_2 \\ a_2 & a_3 & a_1 \end{pmatrix} \quad \text{or} \quad \begin{pmatrix} a_1 & a_2 & a_3 \\ -a_3 & a_1 & a_2 \\ -a_2 & -a_3 & a_1 \end{pmatrix}$$

where

$$a_1 = \begin{pmatrix} x_1 & x_2 \\ -x_2 & x_1 \end{pmatrix}, \quad a_2 = \begin{pmatrix} x_3 & x_4 \\ -x_4 & x_3 \end{pmatrix}, \quad a_3 = \begin{pmatrix} x_5 & x_6 \\ -x_6 & x_5 \end{pmatrix}$$

or

$$a_1 = \begin{pmatrix} y_1 & y_2 & y_3 & y_4 \\ -y_2 & y_1 & -y_4 & y_3 \\ -y_3 & -y_4 & y_1 & y_2 \\ y_4 & -y_3 & y_2 & y_1 \end{pmatrix}, \quad a_2 = \begin{pmatrix} y_5 & y_6 & y_7 & y_8 \\ -y_6 & y_5 & -y_8 & y_7 \\ -y_7 & -y_8 & y_5 & y_6 \\ y_8 & -y_7 & y_6 & y_5 \end{pmatrix},$$

$$a_3 = \begin{pmatrix} y_9 & y_{10} & y_{11} & y_{12} \\ -y_{10} & y_9 & -y_{12} & y_{11} \\ -y_{11} & -y_{12} & y_9 & y_{10} \\ y_{12} & -y_{11} & y_{10} & y_9 \end{pmatrix},$$

or

$$a_1 = \begin{pmatrix} y_1 & y_2 & y_3 & y_4 \\ y_4 & y_1 & y_2 & y_3 \\ y_3 & y_4 & y_1 & y_2 \\ y_2 & y_3 & y_4 & y_1 \end{pmatrix}, \quad a_2 = \begin{pmatrix} y_5 & y_6 & y_7 & y_8 \\ y_8 & y_5 & y_6 & y_7 \\ y_7 & y_8 & y_5 & y_6 \\ y_6 & y_7 & y_8 & y_5 \end{pmatrix}, \quad a_3 = \begin{pmatrix} y_9 & y_{10} & y_{11} & y_{12} \\ y_{12} & y_9 & y_{10} & y_{11} \\ y_{11} & y_{12} & y_9 & y_{10} \\ y_{10} & y_{11} & y_{12} & y_9 \end{pmatrix},$$

or

The figure shows three 4x4 matrices, \$a\_1\$, \$a\_2\$, and \$a\_3\$, each with a grid of elements. In \$a\_1\$, the top row and bottom row are highlighted with orange borders, and the first and third columns are highlighted with red borders. In \$a\_2\$, the top row and bottom row are highlighted with orange borders, and the first and third columns are highlighted with red borders. In \$a\_3\$, the top row and bottom row are highlighted with orange borders, and the first and third columns are highlighted with red borders.

corresponding to binary structure, or

The figure shows three 4x4 matrices, \$a\_1\$, \$a\_2\$, and \$a\_3\$, each with a grid of elements. In \$a\_1\$, the top row and bottom row are highlighted with yellow borders, and the first and third columns are highlighted with red borders. In \$a\_2\$, the top row and bottom row are highlighted with yellow borders, and the first and third columns are highlighted with red borders. In \$a\_3\$, the top row and bottom row are highlighted with yellow borders, and the first and third columns are highlighted with red borders.

corresponding to quaternary structure [4]. This motivates introducing six characteristic triples of a  $3 \times 3$ -matrix (14) applied to the reduction matrices: the *first characteristic triad*

$$(14) \quad (a_{11}, a_{22}, a_{33}), (a_{12}, a_{23}, a_{31}), (a_{13}, a_{21}, a_{32})$$

and the *second characteristic triad*

$$(15) \quad (a_{13}, a_{22}, a_{31}), (a_{12}, a_{21}, a_{33}), (a_{11}, a_{23}, a_{32})$$

(cf. the enclosed scheme (Fig. 2)).

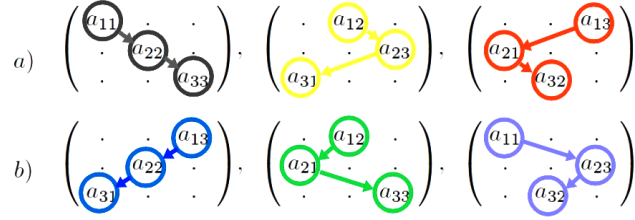


Fig. 1: Scheme for two triads of characteristic triples: a) first b) second characteristic triad.

### 10. Multiplication table for the cubic and nonion algebra generators

We turn our attention now to the cubic and nonion algebras [1–5, 7–10]. Because of (14) we make the following

*Demand 1.* Generators  $T_1, T_2, T_3$  of the cubic algebra form the following second characteristic triad  $T_3(1, 1, 1), T_2(1, 1, 1), T_1(1, 1, 1)$ .

From (15) we deduce the following

**Proposition 1.** *Generators of the cubic algebra read*

$$T_1 = \begin{pmatrix} 1 & 0 & 0 \\ 0 & 1 & 0 \\ 0 & 0 & 1 \end{pmatrix}, \quad T_2 = \begin{pmatrix} 0 & 1 & 0 \\ 0 & 0 & 1 \\ 1 & 0 & 0 \end{pmatrix}, \quad T_3 = \begin{pmatrix} 0 & 0 & 1 \\ 1 & 0 & 0 \\ 0 & 1 & 0 \end{pmatrix}.$$

*Observation 1.* The first characteristic triad corresponding to  $T_1, T_2, T_3$  reads

$$(T_1, T_3, T_2), (T_2, T_1, T_3), (T_3, T_2, T_1).$$

In consequence, we have the following the multiplication table for  $T_1, T_2, T_3$ :

$$\begin{matrix} T_1 & T_2 & T_3 \\ T_2 & T_3 & T_1 \\ T_3 & T_1 & T_2 \end{matrix}.$$

In analogy, because of (14), for generators  $(R_3, Q_2, \bar{Q}_1)$  and  $(R_2, Q_1, \bar{Q}_2)$  we make the following

*Demand 2.* The second characteristic triads for  $(R_3, Q_2, \bar{Q}_1)$  and  $(R_2, Q_1, \bar{Q}_2)$  read

$$\bar{Q}_2(1, 1, \mathbf{j}), Q_1(\mathbf{j}, 1, 1), R_2(1, \mathbf{j}, 1) \quad \text{and} \quad \bar{Q}_1(1, 1, \mathbf{j}^2), Q_2(\mathbf{j}^2, 1, 1), R_3(1, \mathbf{j}^2, 1),$$

respectively, where  $\mathbf{j}^3 = 1$  and  $\mathbf{j} \neq 1$ .

By (14) and Proposition 1 we have

**Proposition 2.** *The generators  $(R_1, Q_3, \bar{Q}_3); (R_3, Q_2, \bar{Q}_1); (R_1, Q_1, \bar{Q}_2)$  read*

$$(16) \quad \begin{aligned} R_1 = T_1 &= \begin{pmatrix} 1 & 0 & 0 \\ 0 & 1 & 0 \\ 0 & 0 & 1 \end{pmatrix}, & Q_3 = T_2 &= \begin{pmatrix} 0 & 1 & 0 \\ 0 & 0 & 1 \\ 1 & 0 & 0 \end{pmatrix}, & \bar{Q}_3 = T_3 &= \begin{pmatrix} 0 & 0 & 1 \\ 1 & 0 & 0 \\ 0 & 1 & 0 \end{pmatrix}, \\ R_3 &= \begin{pmatrix} 1 & 0 & 0 \\ 0 & \mathbf{j}^2 & 0 \\ 0 & 0 & \mathbf{j} \end{pmatrix}, & Q_2 &= \begin{pmatrix} 0 & \mathbf{j}^2 & 0 \\ 0 & 0 & \mathbf{j} \\ 1 & 0 & 0 \end{pmatrix}, & \bar{Q}_1 &= \begin{pmatrix} 0 & 0 & 1 \\ \mathbf{j}^2 & 0 & 0 \\ 0 & \mathbf{j} & 0 \end{pmatrix}, \\ R_2 &= \begin{pmatrix} 1 & 0 & 0 \\ 0 & \mathbf{j} & 0 \\ 0 & 0 & \mathbf{j}^2 \end{pmatrix}, & Q_1 &= \begin{pmatrix} 0 & \mathbf{j} & 0 \\ 0 & 0 & \mathbf{j}^2 \\ 1 & 0 & 0 \end{pmatrix}, & \bar{Q}_2 &= \begin{pmatrix} 0 & 0 & 1 \\ \mathbf{j} & 0 & 0 \\ 0 & \mathbf{j}^2 & 0 \end{pmatrix}, \end{aligned}$$

where  $\mathbf{j}^3 = 1$  and  $\mathbf{j} \neq 1$ .

*Observation 2.* The second characteristic triads for  $(R_3, Q_2, \bar{Q}_1)$  and  $(R_2, Q_1, \bar{Q}_2)$  read

$\bar{Q}_2(1, 1, \mathbf{j})$ ,  $Q_1(\mathbf{j}, 1, 1)$ ,  $R_2(1, \mathbf{j}, 1)$  and  $\bar{Q}_1(1, 1, \mathbf{j}^2)$ ,  $Q_2(\mathbf{j}^2, 1, 1)$ ,  $R_3(1, \mathbf{j}^2, 1)$ , respectively. In consequence, we have the following multiplication tables for  $(R_3, Q_2, \bar{Q}_1)$  and  $(R_2, Q_1, \bar{Q}_2)$ :

$*$	$R_3$	$Q_2$	$\bar{Q}_1$	$*$	$R_2$	$Q_1$	$\bar{Q}_2$
$R_3$	$R_2$	$\mathbf{j}Q_1$	$\bar{Q}_2$	$R_2$	$R_3$	$\mathbf{j}^2Q_2$	$\bar{Q}_1$
$Q_2$	$Q_1$	$\bar{Q}_2$	$\mathbf{j}R_2$	$Q_1$	$Q_2$	$\bar{Q}_1$	$\mathbf{j}^2R_3$
$\bar{Q}_1$	$\mathbf{j}\bar{Q}_2$	$R_2$	$Q_1$	$\bar{Q}_2$	$\mathbf{j}^2\bar{Q}_1$	$R_3$	$Q_2$

Finally, we write down second and first characteristic triads for the triples

$$(17) \quad \begin{aligned} &(R_1 = T_1, Q_3 = T_2, \bar{Q}_3 = T_3) \text{ with } (R_3, Q_2, \bar{Q}_1), \\ &\quad (R_1, Q_3, \bar{Q}_3) \text{ with } (R_2, Q_1, \bar{Q}_2), \\ &\quad (R_3, Q_2, \bar{Q}_1) \text{ with } (R_1, Q_3, \bar{Q}_3), \\ &\quad (R_3, Q_2, \bar{Q}_1) \text{ with } (R_2, Q_1, \bar{Q}_2), \\ &\quad (R_2, Q_1, \bar{Q}_2) \text{ with } (R_1, Q_3, \bar{Q}_3), \\ &\quad (R_2, Q_1, \bar{Q}_2) \text{ with } (R_3, Q_2, \bar{Q}_1). \end{aligned}$$

*Observation 3.* The second and first characteristic triads for (17) read:

$$\begin{aligned} &\bar{Q}_1(1, \mathbf{j}, \mathbf{j}), Q_2(1, 1, \mathbf{j}^2), R_3(1, \mathbf{j}^2, 1); \bar{Q}_2(1, \mathbf{j}^2, \mathbf{j}^2), Q_1(1, 1, \mathbf{j}), R_1(1, \mathbf{j}, 1); \\ &\bar{Q}_1(1, \mathbf{j}^2, 1), Q_2(\mathbf{j}, 1, \mathbf{j}), R_3(1, \mathbf{j}^2, 1); \bar{Q}_3(1, \mathbf{j}, \mathbf{j}^2), Q_3(\mathbf{j}, 1, \mathbf{j}^2), R_1(1, 1, 1); \\ &\bar{Q}_2(1, \mathbf{j}, 1), Q_1(\mathbf{j}^2, 1, \mathbf{j}^2), R_2(1, \mathbf{j}, 1); \bar{Q}_3(1, \mathbf{j}^2, \mathbf{j}), Q_3(\mathbf{j}^2, 1, \mathbf{j}), R_1(1, 1, 1), \end{aligned}$$

respectively. In consequence we have the following multiplication tables:

$*$	$R_3$	$Q_2$	$\bar{Q}_1$	$*$	$R_2$	$Q_1$	$\bar{Q}_2$	$*$	$R_1$	$Q_3$	$\bar{Q}_3$
$R_1$	$R_3$	$Q_2$	$\bar{Q}_1$	$R_1$	$R_2$	$Q_1$	$\bar{Q}_2$	$R_3$	$R_3$	$jQ_2$	$\bar{Q}_1$
$Q_3$	$Q_2$	$j\bar{Q}_1$	$j^2R_3$	$Q_3$	$Q_1$	$j^2\bar{Q}_2$	$jR_2$	$Q_2$	$Q_2$	$j^2\bar{Q}_1$	$j^2R_3$
$\bar{Q}_3$	$j\bar{Q}_1$	$R_3$	$j^2Q_2$	$\bar{Q}_3$	$j^2\bar{Q}_2$	$R_2$	$jQ_1$	$\bar{Q}_1$	$\bar{Q}_1$	$R_3$	$jQ_2$
$*$	$R_2$	$Q_1$	$\bar{Q}_2$	$*$	$R_1$	$Q_3$	$\bar{Q}_3$	$*$	$R_3$	$Q_2$	$\bar{Q}_1$
$R_3$	$R_1$	$jQ_3$	$\bar{Q}_3$	$R_2$	$R_2$	$j^2Q_1$	$\bar{Q}_2$	$R_2$	$R_1$	$j^2Q_3$	$\bar{Q}_3$
$Q_2$	$Q_3$	$j\bar{Q}_3$	$R_1$	$Q_1$	$Q_1$	$j\bar{Q}_2$	$jR_2$	$Q_1$	$Q_3$	$j^2\bar{Q}_3$	$R_1$
$\bar{Q}_1$	$j^2\bar{Q}_3$	$R_1$	$j^2Q_3$	$\bar{Q}_2$	$\bar{Q}_2$	$R_2$	$j^2Q_1$	$\bar{Q}_2$	$j\bar{Q}_3$	$R_1$	$jQ_3$

### 11. Remaining diagonal 3×3-subtables of the multiplication table for the resulting algebra generators

*Observation 4.* In analogy, because of (13), for generators  $(R_4, Q_6, \bar{Q}_6)$ ,  $(R_6, Q_5, \bar{Q}_4)$  and  $(R_5, Q_4, \bar{Q}_4)$  we have the following second characteristic triads

$$\begin{aligned}
 &R_1(1, 1, 1), \bar{Q}_3(1, 1, 1), Q_3(1, 1, 1), \\
 &R_1(j, 1, 1), \bar{Q}_3(1, j, 1), Q_3(j, j, j^2), \\
 &R_1(j^2, 1, 1), \bar{Q}_3(1, j^2, 1), Q_3(j^2, j^2, j),
 \end{aligned}$$

respectively. We have the following multiplication tables:

$*$	$R_4$	$Q_6$	$\bar{Q}_6$	$*$	$R_6$	$Q_5$	$\bar{Q}_4$	$*$	$R_5$	$Q_4$	$\bar{Q}_4$
$R_4$	$R_1$	$\bar{Q}_3$	$Q_3$	$R_6$	$jR_1$	$\bar{Q}_3$	$jQ_3$	$R_5$	$j^2R_1$	$\bar{Q}_3$	$j^2Q_3$
$Q_6$	$Q_3$	$R_1$	$\bar{Q}_3$	$Q_5$	$jQ_3$	$R_1$	$j\bar{Q}_3$	$Q_4$	$j^2Q_3$	$R_1$	$j^2\bar{Q}_3$
$\bar{Q}_6$	$\bar{Q}_3$	$Q_3$	$R_1$	$\bar{Q}_4$	$\bar{Q}_3$	$j^2Q_3$	$R_1$	$\bar{Q}_4$	$\bar{Q}_3$	$jQ_3$	$R_1$

### 12. The resulting algebra generators

The multiplication tables (18) provide a system of nine quadratic equations for the nine unknown generators which lead to the following result

**Theorem.** *The algebra in question is generated by (16) and  $R_4, Q_6, \bar{Q}_6, R_6, Q_5, \bar{Q}_4, R_5, Q_4, \bar{Q}_4$ , where*

$$\begin{aligned}
 R_4 = T_4 &= \begin{pmatrix} 0 & 0 & 1 \\ 0 & 1 & 0 \\ 1 & 0 & 0 \end{pmatrix}, & Q_6 = T_5 &= \begin{pmatrix} 0 & 1 & 0 \\ 1 & 0 & 0 \\ 0 & 0 & 1 \end{pmatrix}, & \bar{Q}_6 = T_6 &= \begin{pmatrix} 1 & 0 & 0 \\ 0 & 0 & 1 \\ 0 & 1 & 0 \end{pmatrix}, \\
 R_6 &= \begin{pmatrix} 0 & 0 & 1 \\ 0 & j^2 & 0 \\ j & 0 & 0 \end{pmatrix}, & Q_5 &= \begin{pmatrix} 0 & j^2 & 0 \\ j & 0 & 0 \\ 0 & 0 & 1 \end{pmatrix}, & \bar{Q}_4 &= \begin{pmatrix} 1 & 0 & 0 \\ 0 & 0 & j^2 \\ 0 & j & 0 \end{pmatrix},
 \end{aligned}$$

$$R_5 = \begin{pmatrix} 0 & 0 & 1 \\ 0 & \mathbf{j} & 0 \\ \mathbf{j}^2 & 0 & 0 \end{pmatrix}, \quad Q_4 = \begin{pmatrix} 0 & \mathbf{j} & 0 \\ \mathbf{j}^2 & 0 & 0 \\ 0 & 0 & 1 \end{pmatrix}, \quad \bar{Q}_5 = \begin{pmatrix} 1 & 0 & 0 \\ 0 & 0 & \mathbf{j} \\ 0 & \mathbf{j}^2 & 0 \end{pmatrix},$$

and where  $\mathbf{j}^3 = 1, \mathbf{j} \neq 1$ .

### 13. $3 \times 3$ -subtables of the multiplication table over the diagonal

In analogy to Observation 4 in the context concerned we have the following

*Observation 5.* For the triples

$$(19) \quad \begin{aligned} & (R_1, Q_3, \bar{Q}_3) \text{ with } (R_4, Q_6, \bar{Q}_6), \quad (R_1, Q_3, \bar{Q}_3) \text{ with } (R_6, Q_5, \bar{Q}_4), \\ & (R_1, Q_3, \bar{Q}_3) \text{ with } (R_5, Q_4, \bar{Q}_5), \quad (R_3, Q_2, \bar{Q}_1) \text{ with } (R_4, Q_6, \bar{Q}_6), \\ & (R_3, Q_2, \bar{Q}_1) \text{ with } (R_6, Q_5, \bar{Q}_4), \quad (R_3, Q_2, \bar{Q}_1) \text{ with } (R_5, Q_4, \bar{Q}_5), \\ & (R_2, Q_1, \bar{Q}_2) \text{ with } (R_4, Q_6, \bar{Q}_6), \quad (R_2, Q_1, \bar{Q}_2) \text{ with } (R_6, Q_5, \bar{Q}_4), \\ & (R_2, Q_1, \bar{Q}_2) \text{ with } (R_5, Q_4, \bar{Q}_5), \quad (R_4, Q_6, \bar{Q}_6) \text{ with } (R_6, Q_5, \bar{Q}_4), \\ & (R_4, Q_6, \bar{Q}_6) \text{ with } (R_5, Q_4, \bar{Q}_5), \quad (R_6, Q_5, \bar{Q}_4) \text{ with } (R_5, Q_4, \bar{Q}_5) \end{aligned}$$

we have the following characteristic triads

$$\begin{aligned} & R_4(1, 1, 1), Q_6(1, 1, 1), \bar{Q}_6(1, 1, 1); \quad R_6(1, \mathbf{j}^2, 1), Q_5(1, 1, \mathbf{j}^2), \bar{Q}_4(1, \mathbf{j}, \mathbf{j}); \\ & R_5(1, \mathbf{j}, 1), Q_4(1, 1, \mathbf{j}), \bar{Q}_5(1, \mathbf{j}^2, \mathbf{j}^2); \quad R_6(1, \mathbf{j}^2, 1), Q_5(\mathbf{j}, 1, \mathbf{j}), \bar{Q}_4(1, \mathbf{j}^2, 1); \\ & R_5(1, \mathbf{j}, 1), Q_4(\mathbf{j}, 1, 1), \bar{Q}_5(1, 1, \mathbf{j}); \quad R_4(1, 1, 1), Q_6(\mathbf{j}, 1, \mathbf{j}^2), \bar{Q}_6(1, \mathbf{j}, \mathbf{j}^2); \\ & R_5(1, \mathbf{j}, 1), Q_4(\mathbf{j}^2, 1, \mathbf{j}^2), \bar{Q}_5(1, \mathbf{j}, 1); \quad R_4(1, 1, 1), Q_6(\mathbf{j}^2, 1, \mathbf{j}), \bar{Q}_6(1, \mathbf{j}^2, \mathbf{j}); \\ & R_6(1, \mathbf{j}^2, 1), Q_5(\mathbf{j}^2, 1, 1), \bar{Q}_4(1, 1, \mathbf{j}^2); \quad R_2(\mathbf{j}, \mathbf{j}, 1), Q_1(1, \mathbf{j}, 1), \bar{Q}_2(1, \mathbf{j}, \mathbf{j}); \\ & R_3(\mathbf{j}^2, \mathbf{j}^2, 1), Q_2(1, \mathbf{j}, 1), \bar{Q}_1(1, \mathbf{j}^2, \mathbf{j}^2); \quad R_2(\mathbf{j}^2, \mathbf{j}, 1), Q_1(1, 1, 1), \bar{Q}_2(\mathbf{j}, \mathbf{j}^2, 1), \end{aligned}$$

respectively, and the corresponding multiplication tables read

$$\begin{array}{c|ccc} * & R_4 & Q_6 & \bar{Q}_6 \\ \hline R_1 & R_4 & Q_6 & \bar{Q}_6 \\ Q_3 & Q_6 & \bar{Q}_6 & R_4 \\ \bar{Q}_3 & \bar{Q}_6 & R_4 & Q_6 \end{array} \quad \begin{array}{c|ccc} * & R_6 & Q_5 & \bar{Q}_4 \\ \hline R_1 & R_6 & Q_5 & \bar{Q}_4 \\ Q_3 & Q_5 & \mathbf{j}\bar{Q}_4 & \mathbf{j}^2R_6 \\ \bar{Q}_3 & \mathbf{j}\bar{Q}_4 & R_6 & \mathbf{j}^2Q_5 \end{array} \quad \begin{array}{c|ccc} * & R_5 & Q_4 & \bar{Q}_5 \\ \hline R_1 & R_5 & Q_4 & \bar{Q}_5 \\ Q_3 & Q_4 & \mathbf{j}^2\bar{Q}_5 & \mathbf{j}R_5 \\ \bar{Q}_3 & \mathbf{j}^2\bar{Q}_5 & R_5 & \mathbf{j}Q_4 \end{array}$$

$*$	$R_4$	$Q_6$	$\overline{Q}_6$	$*$	$R_6$	$Q_5$	$\overline{Q}_4$	$*$	$R_5$	$Q_4$	$\overline{Q}_5$
$R_3$	$R_6$	$\mathbf{j}Q_5$	$\overline{Q}_4$	$R_3$	$R_5$	$\mathbf{j}Q_4$	$\overline{Q}_5$	$R_3$	$R_4$	$\mathbf{j}Q_6$	$\overline{Q}_6$
$Q_2$	$Q_5$	$\mathbf{j}^2\overline{Q}_4$	$\mathbf{j}R_6$	$Q_2$	$Q_4$	$\overline{Q}_5$	$\mathbf{j}R_5$	$Q_2$	$Q_6$	$\mathbf{j}\overline{Q}_6$	$R_4$
$\overline{Q}_1$	$\overline{Q}_4$	$R_6$	$\mathbf{j}Q_5$	$\overline{Q}_1$	$\mathbf{j}\overline{Q}_5$	$R_5$	$Q_4$	$\overline{Q}_1$	$\mathbf{j}^2\overline{Q}_6$	$R_4$	$Q_5$
$*$	$R_4$	$Q_6$	$\overline{Q}_6$	$*$	$R_6$	$Q_5$	$\overline{Q}_4$	$*$	$R_5$	$Q_4$	$\overline{Q}_5$
$R_2$	$R_5$	$\mathbf{j}^2Q_4$	$\overline{Q}_5$	$R_2$	$R_4$	$\mathbf{j}^2Q_6$	$\overline{Q}_6$	$R_2$	$R_6$	$\mathbf{j}^2Q_5$	$\overline{Q}_4$
$Q_1$	$Q_4$	$\mathbf{j}\overline{Q}_5$	$\mathbf{j}R_5$	$Q_1$	$Q_6$	$\mathbf{j}^2\overline{Q}_6$	$R_4$	$Q_1$	$Q_5$	$\overline{Q}_4$	$\mathbf{j}^2R_6$
$\overline{Q}_2$	$\overline{Q}_5$	$R_5$	$\mathbf{j}^2Q_4$	$\overline{Q}_2$	$\mathbf{j}\overline{Q}_6$	$R_4$	$\mathbf{j}Q_6$	$\overline{Q}_2$	$\mathbf{j}^2\overline{Q}_4$	$R_6$	$Q_5$
$*$	$R_6$	$Q_5$	$\overline{Q}_4$	$*$	$R_5$	$Q_4$	$\overline{Q}_5$	$*$	$R_5$	$Q_4$	$\overline{Q}_5$
$R_4$	$\mathbf{j}R_2$	$\overline{Q}_2$	$Q_1$	$R_4$	$\mathbf{j}^2R_3$	$\overline{Q}_1$	$Q_2$	$R_6$	$\mathbf{j}^2R_2$	$\overline{Q}_2$	$\mathbf{j}Q_1$
$Q_6$	$\mathbf{j}Q_1$	$\mathbf{j}R_2$	$\mathbf{j}^2\overline{Q}_2$	$Q_6$	$\mathbf{j}^2Q_2$	$\mathbf{j}^2R_3$	$\mathbf{j}\overline{Q}_1$	$Q_5$	$\mathbf{j}^2Q_1$	$\mathbf{j}R_2$	$\overline{Q}_2$
$\overline{Q}_6$	$\overline{Q}_2$	$\mathbf{j}Q_1$	$R_2$	$\overline{Q}_6$	$\overline{Q}_1$	$\mathbf{j}^2Q_2$	$R_3$	$\overline{Q}_4$	$\overline{Q}_2$	$Q_1$	$R_2$

#### 14. $3 \times 3$ -subtables of the multiplication table below the diagonal

Similarly to previous paragraphs, we have

*Observation 6.* For the triples

$$\begin{aligned}
 (20) \quad & (R_4, Q_6, \overline{Q}_6) \text{ with } (R_1, Q_3, \overline{Q}_3), \quad (R_4, Q_6, \overline{Q}_6) \text{ with } (R_3, Q_2, \overline{Q}_1), \\
 & (R_4, Q_6, \overline{Q}_6) \text{ with } (R_2, Q_1, \overline{Q}_2), \quad (R_6, Q_5, \overline{Q}_4) \text{ with } (R_1, Q_3, \overline{Q}_3), \\
 & (R_6, Q_5, \overline{Q}_4) \text{ with } (R_3, Q_2, \overline{Q}_1), \quad (R_6, Q_5, \overline{Q}_4) \text{ with } (R_2, Q_1, \overline{Q}_2), \\
 & (R_6, Q_5, \overline{Q}_4) \text{ with } (R_4, Q_6, \overline{Q}_6), \quad (R_5, Q_4, \overline{Q}_5) \text{ with } (R_1, Q_3, \overline{Q}_3), \\
 & (R_5, Q_4, \overline{Q}_5) \text{ with } (R_3, Q_2, \overline{Q}_1), \quad (R_5, Q_4, \overline{Q}_5) \text{ with } (R_2, Q_1, \overline{Q}_2), \\
 & (R_5, Q_4, \overline{Q}_5) \text{ with } (R_4, Q_6, \overline{Q}_6), \quad (R_5, Q_4, \overline{Q}_5) \text{ with } (R_6, Q_5, \overline{Q}_4)
 \end{aligned}$$

we have the following second characteristic triads

$$\begin{aligned}
 & R_4(1, 1, 1), Q_6(1, 1, 1), \overline{Q}_6(1, 1, 1); \quad R_5(\mathbf{j}, \mathbf{j}, 1), Q_4(1, \mathbf{j}, \mathbf{j}), \overline{Q}_5(1, \mathbf{j}^2, 1); \\
 & R_6(\mathbf{j}^2, \mathbf{j}^2, 1), Q_5(1, \mathbf{j}^2, \mathbf{j}^2), \overline{Q}_4(1, \mathbf{j}, 1); \quad R_6(1, \mathbf{j}^2, 1), Q_5(\mathbf{j}, 1, \mathbf{j}), \overline{Q}_4(1, \mathbf{j}^2, 1); \\
 & R_4(\mathbf{j}, 1, 1), Q_6(\mathbf{j}, \mathbf{j}, \mathbf{j}^2), \overline{Q}_6(1, \mathbf{j}, 1); \quad R_5(\mathbf{j}^2, \mathbf{j}, 1), Q_4(\mathbf{j}, \mathbf{j}^2, 1), \overline{Q}_5(1, 1, 1); \\
 & R_3(1, \mathbf{j}^2, 1), Q_2(\mathbf{j}, 1, \mathbf{j}), \overline{Q}_1(1, \mathbf{j}^2, 1); \quad R_5(1, \mathbf{j}, 1), Q_4(\mathbf{j}^2, 1, \mathbf{j}^2), \overline{Q}_5(1, \mathbf{j}, 1); \\
 & R_6(\mathbf{j}, \mathbf{j}^2, 1), Q_5(\mathbf{j}^2, \mathbf{j}, 1), \overline{Q}_4(1, 1, 1); \quad R_4(\mathbf{j}^2, 1, 1), Q_6(\mathbf{j}^2, \mathbf{j}^2, \mathbf{j}), \overline{Q}_6(1, \mathbf{j}^2, 1); \\
 & R_2(1, \mathbf{j}, 1), Q_1(\mathbf{j}^2, 1, \mathbf{j}^2), \overline{Q}_2(1, \mathbf{j}, 1); \quad R_3(\mathbf{j}, \mathbf{j}^2, 1), Q_2(\mathbf{j}^2, \mathbf{j}, 1), \overline{Q}_1(1, 1, 1),
 \end{aligned}$$

respectively, and the corresponding multiplication tables read

$*$	$R_1$	$Q_3$	$\bar{Q}_3$		$*$	$R_3$	$Q_2$	$\bar{Q}_1$		$*$	$R_2$	$Q_1$	$\bar{Q}_2$
$R_4$	$R_4$	$\bar{Q}_6$	$Q_6$		$R_4$	$\mathbf{j}R_5$	$\bar{Q}_5$	$Q_4$		$R_4$	$\mathbf{j}^2R_6$	$\bar{Q}_4$	$Q_5$
$Q_6$	$Q_6$	$R_4$	$\bar{Q}_6$		$Q_6$	$\mathbf{j}Q_4$	$\mathbf{j}R_5$	$\mathbf{j}^2\bar{Q}_5$		$Q_6$	$\mathbf{j}^2Q_5$	$\mathbf{j}^2R_6$	$\mathbf{j}\bar{Q}_4$
$\bar{Q}_6$	$\bar{Q}_6$	$Q_6$	$R_4$		$\bar{Q}_6$	$\bar{Q}_5$	$\mathbf{j}Q_4$	$R_5$		$\bar{Q}_6$	$\bar{Q}_4$	$\mathbf{j}^2Q_5$	$R_6$
$*$	$R_1$	$Q_3$	$\bar{Q}_3$		$*$	$R_3$	$Q_2$	$\bar{Q}_1$		$*$	$R_2$	$Q_1$	$\bar{Q}_2$
$R_6$	$R_6$	$\bar{Q}_4$	$\mathbf{j}Q_5$		$R_6$	$\mathbf{j}^2R_4$	$\bar{Q}_6$	$\mathbf{j}Q_6$		$R_6$	$\mathbf{j}^2R_5$	$\bar{Q}_5$	$\mathbf{j}Q_4$
$Q_5$	$Q_5$	$\mathbf{j}^2R_6$	$\mathbf{j}^2\bar{Q}_4$		$Q_5$	$\mathbf{j}Q_6$	$R_4$	$\mathbf{j}\bar{Q}_6$		$Q_5$	$\mathbf{j}^2Q_4$	$\mathbf{j}R_5$	$\bar{Q}_5$
$\bar{Q}_4$	$\bar{Q}_4$	$\mathbf{j}Q_5$	$R_6$		$\bar{Q}_4$	$\bar{Q}_6$	$\mathbf{j}^2Q_6$	$R_4$		$\bar{Q}_4$	$\bar{Q}_5$	$Q_4$	$R_5$
$*$	$R_4$	$Q_6$	$\bar{Q}_6$		$*$	$R_1$	$Q_3$	$\bar{Q}_3$		$*$	$R_3$	$Q_2$	$\bar{Q}_1$
$R_6$	$R_3$	$\bar{Q}_1$	$\mathbf{j}Q_2$		$R_5$	$R_5$	$\bar{Q}_5$	$\mathbf{j}^2Q_4$		$R_5$	$\mathbf{j}R_6$	$\bar{Q}_4$	$\mathbf{j}^2Q_5$
$Q_5$	$Q_2$	$\mathbf{j}^2R_3$	$\mathbf{j}^2\bar{Q}_1$		$Q_4$	$Q_4$	$\mathbf{j}R_5$	$\mathbf{j}\bar{Q}_5$		$Q_4$	$\mathbf{j}Q_5$	$\mathbf{j}^2R_6$	$\bar{Q}_4$
$\bar{Q}_4$	$\bar{Q}_1$	$\mathbf{j}Q_2$	$R_3$		$\bar{Q}_5$	$\bar{Q}_5$	$\mathbf{j}^2Q_4$	$R_5$		$\bar{Q}_5$	$\bar{Q}_4$	$Q_5$	$R_6$
$*$	$R_2$	$Q_1$	$\bar{Q}_2$		$*$	$R_4$	$Q_6$	$\bar{Q}_6$		$*$	$R_6$	$Q_5$	$\bar{Q}_4$
$R_5$	$\mathbf{j}^2R_4$	$\bar{Q}_6$	$\mathbf{j}^2Q_6$		$R_5$	$R_2$	$\bar{Q}_2$	$\mathbf{j}^2Q_1$		$R_5$	$\mathbf{j}R_3$	$\bar{Q}_1$	$\mathbf{j}^2Q_2$
$Q_4$	$\mathbf{j}^2Q_6$	$R_4$	$\mathbf{j}^2\bar{Q}_6$		$Q_4$	$Q_1$	$\mathbf{j}R_2$	$\mathbf{j}\bar{Q}_2$		$Q_4$	$\mathbf{j}Q_2$	$\mathbf{j}^2R_3$	$\bar{Q}_1$
$\bar{Q}_5$	$\bar{Q}_6$	$\mathbf{j}Q_6$	$R_4$		$\bar{Q}_5$	$\bar{Q}_2$	$\mathbf{j}^2Q_1$	$R_2$		$\bar{Q}_5$	$\bar{Q}_1$	$Q_2$	$R_3$

## 15. Conclusions

Although the algebra in question has formally 18 generators a natural question that arises is concerning their linear independence. The algebra might be generated by merely 15 generators because of  $12 \times 12$  complex matrices in (10)–(13) of [4] similarly to the case of nonion algebra and the related  $6 \times 6$  complex matrices in (8), (9) of [4]:

$$12 + (6 - 9) = 15.$$

Another thing that should be checked is the equivalence between relevant structures - firstly the corresponding Cauchy-Riemann equations and secondly, the equivalence between different Galois extensions.

## References

- [1] F. L. Castillo Alvarado, J. Ławrynowicz, Małgorzata Nowak-Kępczyk, *Fractal modelling of alloy thin films. Temperatures characteristic for local phase transitions*, in: Applied Complex and Quaternionic Approximation. Ed. by Ralitzia K. Kovacheva, J. Ławrynowicz, and S. Marchiafava, Ediz. Univ. La Sapienza, Roma 2009, pp. 207–236.

- [2] J. Ławrynowicz, K. Nôno, and O. Suzuki, *Binary and ternary Clifford analysis vs noncommutative Galois extensions II. The correspondence between the binary and ternary field operators*, Bull. Soc. Sci. Lettres Łódź Sér. Rech. Déform. **62**, no. 3 (2012), 109–118.
- [3] J. Ławrynowicz, O. Suzuki, A. Niemczynowicz, and M. Nowak-Kępczyk, *Some algebraical and geometrical aspects of simple orthorhombic Ising-Onsager-like lattices*, to appear.
- [4] M. Nowak-Kępczyk, *An Algebra Governing Reduction of Quaternary Structures to Ternary Structures I, Reductions of Quaternary Structures to Ternary Structures*, Bull. Soc. Sci. Lettres Łódź **51** Sér. Rech. Déform., to appear.
- [5] C. S. Peirce, *On Nonions*, in: Collected Papers of Charles Sanders Peirce, 3rd ed., vol. III, Harvard University Press, Cambridge, Mass. 1967, pp. 411–416.
- [6] I. R. Porteous, *Clifford Algebras and the Classical Groups*, Cambridge studies in advanced mathematics **50**, Cambridge Univ. Press, Cambridge 1995.
- [7] J. J. Sylvester, *A word on nonions*, John Hopkins Univ. Circulars **1** (1882), 241–242; **2** (1883), 46; in: The Collected Mathematical Papers of James Joseph Sylvester, vol. III, Cambridge Univ. Press, Cambridge 1909, pp. 647–650.
- [8] J. J. Sylvester, *On the involution of two matrices of the second order*, Brit. Assoc. Report 1883, 430–432; in: The Collected Mathematical Papers of James Joseph Sylvester, vol. IV, Cambridge Univ. Press, Cambridge 1912, pp. 115–117.
- [9] J. J. Sylvester, *Sur les quantités formant un groupe de nonions analogues aux quaternions de Hamilton*, C. R. Acad. Sci. Paris **97** (1883), 1336–1340; **98** (1884), 273–276, 471–473; in: The Collected Mathematical Papers of James Joseph Sylvester, vol. IV, Cambridge Univ. Press, Cambridge 1912, pp. 154–159.
- [10] J. J. Sylvester, *On quaternions, nonions, sedenions etc.*, Johns Hopkins Univ. Circulars **3** (1984), 7–9; in: The Collected Mathematical Papers of James Joseph Sylvester, vol. IV, Cambridge Univ. Press, Cambridge 1909, pp. 122–132.

The State School of Higher Education in Chełm  
 54 Pocztowa Street, PL-22-100 Chełm  
 Poland  
 e-mail: gosianmk@gmail.com

Presented by Julian Ławrynowicz at the Session of the Mathematical-Physical Commission of the Łódź Society of Sciences and Arts on November 20, 2014

## REDUKCJA STRUKTUR TYPU KWATERNARNEGO DO STRUKTUR TYPU TERNARNEGO II

### ANALIZA TABELI MNOŻENIA GENERATORÓW ODPOWIEDNIEJ ALGEBRY

#### Streszczenie

Analizowana jest tabela mnożenia generatorów algebry rozważanej w Części I tego artykułu. Stosując macierze redukujące z Części I analizowane są tabele mnożenia generatorów algebr kubicznej i nonionowej i stąd wywodzone pozostałe 9 generatorów, a następnie

analizowane ich tabele mnożenia. Zagadnienie liniowej niezależności tak otrzymanych generatorów zostanie poruszone w Części III.

*Słowa kluczowe:* nieprzemienne przedłużenia Galois, algebry skończenie wymiarowe, łączne pierścienie i algebry, pierścienie macierzy

## B U L L E T I N

DE LA SOCIÉTÉ DES SCIENCES ET DES LETTRES DE ŁÓDŹ

2014

Vol. LXIV

Recherches sur les déformations

no. 3

pp. 91–100

*In memory of Professor Claude Surry  
our Dear Friend and Colleague*

*Agnieszka Partyka*

### TEICHMÜLLER DISTANCE IN THE CLASS OF WEAKLY QUASIREGULAR FUNCTIONS

#### Summary

The aim of this paper is to generalize quasiconformal mappings in the complex plane to functions defined in domains in the complex plane and with values in a real unitary space, called weakly quasiregular functions. Then the Teichmüller distance is defined for such functions.

*Keywords and phrases:* quasiconformal mappings, quasiregular functions, Teichmüller distance

#### Introduction

There are many equivalent definitions of quasiconformal mappings in the extended complex plane  $E(\hat{\mathbb{C}}) := (\mathbb{C}, \rho)$ , where  $\hat{\mathbb{C}} := \mathbb{C} \cup \{\infty\}$  and  $\rho$  is the chord metric in  $\hat{\mathbb{C}}$ . We recall the geometric definition which comes from Ahlfors; see. [1, Chap. II, A.], [6, Chap. I, §3]. Let  $\mathbf{Q} = (Q; \gamma_1, \gamma_2)$  be a *quadrilateral*, i.e., a Jordan domain  $Q \subset \hat{\mathbb{C}}$  together with a pair of disjoint closed arcs  $\gamma_1$  and  $\gamma_2$  on the boundary  $\text{fr}(Q)$ ; cf. [1, p. 21], [6, Chap. I, §2]. Write  $\text{Mod}(\mathbf{Q})$  for the *module of quadrilateral*  $\mathbf{Q}$ ; [1, p. 21], [6, Chap. I, §2 and §4]. For any nonempty domain  $\Omega$  in  $E(\hat{\mathbb{C}})$  and  $K \geq 1$  a mapping  $f : \Omega \rightarrow \hat{\mathbb{C}}$  is called *K-quasiconformal* in  $\Omega$  if  $f$  is a sense-preserving homeomorphism from  $\Omega$  onto a domain  $f(\Omega)$  in  $E(\hat{\mathbb{C}})$ , satisfying the inequality

$$\text{Mod}((f(Q); f(\gamma_1), f(\gamma_2))) \leq K \text{Mod}((Q; \gamma_1, \gamma_2))$$

for every quadrilateral  $(Q; \gamma_1, \gamma_2)$  with closure  $\text{cl}(Q) \subset \Omega$ . Write  $\text{QC}(\Omega; K)$  for the class of all *K-quasiconformal* mappings in  $\Omega$  and let  $\text{QC}(\Omega)$  be the class of all quasiconformal mappings in  $\Omega$ , i.e.,

$$\mathrm{QC}(\Omega) := \bigcup_{K \geq 1} \mathrm{QC}(\Omega; K) .$$

A real number

$$(0.1) \quad \mathrm{K}(f) := \inf(\{K \geq 1 : f \in \mathrm{QC}(\Omega; K)\})$$

is said to be the *maximal dillatation* of a mapping  $f \in \mathrm{QC}(\Omega)$ . It is easy to verify that the function

$$(0.2) \quad \mathrm{QC}(\Omega) \times \mathrm{QC}(\Omega) \ni (f_1, f_2) \mapsto \tau(f_1, f_2) := \log \mathrm{K}(f_1 \circ f_2^{-1})$$

is well defined and it satisfies the following properties:

$$(0.3) \quad \begin{aligned} \tau(f_1, f_3) &\leq \tau(f_1, f_2) + \tau(f_2, f_3) , & f_1, f_2, f_3 \in \mathrm{QC}(\Omega) , \\ \tau(f_1, f_2) &= \tau(f_2, f_1) , & f_1, f_2 \in \mathrm{QC}(\Omega) , \\ \tau(f_1, f_1) &= 0 , & f_1 \in \mathrm{QC}(\Omega) , \end{aligned}$$

i.e.  $\tau$  is a pseudo-metric in the class  $\mathrm{QC}(\Omega)$ . We call it the *Teichmüller pseudo-metric* or *Teichmüller distance* in  $\mathrm{QC}(\Omega)$ . Up to the nonessential constant  $1/2$ ; cf. [5, Chap III, §2.1].

The pseudo-metric  $\tau$  can be expressed by a more quantitative form by means of the complex dilatation of a quasiconformal mapping. We recall that by the *complex dilatation of a function*  $f : \Omega \rightarrow \mathbb{C}$  we mean the function  $\mu[f] : \Omega \rightarrow \mathbb{C}$  defined by the formula

$$(0.4) \quad \mu[f](z) := \frac{\bar{\partial}f(z)}{\partial f(z)}$$

provided  $f$  has partial derivatives  $\partial_1 f(z)$  and  $\partial_2 f(z)$  at  $z \in \Omega$  as well as the denominator  $\partial f(z) \neq 0$ , and otherwise  $\mu[f](z) := 0$ . Here and in the sequel  $\partial f$  and  $\bar{\partial}f$  are formal derivatives of  $f$  defined by

$$(0.5) \quad \partial f := \frac{1}{2}(\partial_1 f - i\partial_2 f) \quad , \quad \bar{\partial}f := \frac{1}{2}(\partial_1 f + i\partial_2 f) .$$

Using the formulas (0.5) we can express the Jacobian  $J[f]$  of a function  $f : \Omega \rightarrow \mathbb{C}$  in the following simple form

$$(0.6) \quad J[f](z) = |\partial f(z)|^2 - |\bar{\partial}f(z)|^2 ,$$

if the partial derivatives  $\partial_1 f(z)$  and  $\partial_2 f(z)$  exist at  $z \in \Omega$ . By the analytical characterization of quasiconformal mappings in the complex plane we know that for every  $f \in \mathrm{QC}(\Omega)$  the partial derivatives  $\partial_1 f(z)$  and  $\partial_2 f(z)$  exist for a.e.  $z \in \Omega$  and

$$(0.7) \quad \|\mu[f]\|_{\Omega, \infty} = \frac{\mathrm{K}(f) - 1}{\mathrm{K}(f) + 1} ;$$

cf. e.g. [1, Chap. II, B.] or [6, Chap. IV, §1 and §2]. Here and in the sequel  $\|f\|_{\Omega, \infty}$  stands for the essential supremum norm of a measurable — in a sense of Lebesgue — function  $f : \Omega \rightarrow \mathbb{C}$ , i.e.,

$$(0.8) \quad \|f\|_{\Omega, \infty} := \operatorname{ess\,sup}_{z \in \Omega} |f(z)| .$$

As shown in [7, (2.16)],

$$(0.9) \quad \tau(f_1, f_2) = \log \frac{1 + \kappa(f_1, f_2)}{1 - \kappa(f_1, f_2)}, \quad f_1, f_2 \in \text{QC}(\Omega),$$

where

$$(0.10) \quad \kappa(f_1, f_2) := \left\| \frac{\mu[f_1] - \mu[f_2]}{1 - \overline{\mu[f_2]}\mu[f_1]} \right\|_{\Omega, \infty}, \quad f_1, f_2 \in \text{QC}(\Omega).$$

We intend to extend the Teichmüller distance  $\tau$  to a certain pseudo-metric  $\tau^*$  in the class of all weakly quasiregular functions in a given nonempty domain  $\Omega$  in the complex plane  $E(\mathbb{C})$ , i.e. the standard euclidean complex unitary space supported by  $\mathbb{C}$ . To this end we extend the complex dilatation operator  $\text{QC}(\Omega) \ni f \mapsto \mu[f]$  to a certain operator  $f \mapsto \mu^*[f]$  where  $f$  is a weakly quasiregular function. The last operator is determined by the method of isothermal coordinates.

Weakly quasiregular functions are introduced in Section 1. The extending procedure is described in Section 2.

## 1. Quasiregular functions

Let  $\Omega$  be a nonempty domain in  $E(\mathbb{C})$  and let  $\mathbf{X} = (X; +, \cdot, \langle \cdot | \cdot \rangle)$  be a real unitary space endowed with an inner product  $\langle \cdot | \cdot \rangle$ . It determines the norm  $\| \cdot \|$  in the standard way as follows

$$(1.1) \quad \|x\| := \sqrt{\langle x | x \rangle}, \quad x \in X.$$

We recall that a function  $f : \Omega \rightarrow X$  is differentiable in the Gâteaux sense at a point  $z \in \Omega$  provided the following limit

$$(1.2) \quad d_z f(h) := \lim_{t \rightarrow 0} \frac{1}{t} (f(z + th) - f(z))$$

exists in the space  $\mathbf{X}$  for every  $h \in \mathbb{C}$  and the function  $\mathbb{C} \ni h \mapsto d_z f(h)$  — called the *Gâteaux differential of  $f$  at  $z$*  — is a linear operator from  $E_{\mathbb{R}}(\mathbb{C})$  into  $\mathbf{X}$ , where  $E_{\mathbb{R}}(\mathbb{C})$  denotes the standard euclidean real unitary space supported by  $\mathbb{C}$ . Then the directional derivatives  $d_z f(1)$  and  $d_z f(i)$  exist and

$$(1.3) \quad d_z f(h) = (\text{Re } h)d_z f(1) + (\text{Im } h)d_z f(i), \quad h \in \mathbb{C}.$$

A point  $z \in \Omega$  is said to be a *regular point of a function  $f : \Omega \rightarrow X$*  if  $f$  is differentiable in the Gâteaux sense at  $z$  and  $d_z f(\mathbb{C})$  is a two-dimensional linear set in  $\mathbf{X}$ . Setting  $\text{Reg}(f)$  for the set of all regular points of the function  $f$  we see that the function  $D[f]$  is well defined by the following formula

$$(1.4) \quad \Omega \ni z \mapsto D[f](z) := \begin{cases} \frac{\max(\{\|d_z f(h)\| : h \in \mathbb{T}\})}{\min(\{\|d_z f(h)\| : h \in \mathbb{T}\})} & \text{if } z \in \text{Reg}(f); \\ 1 & \text{if } z \in \Omega \setminus \text{Reg}(f), \end{cases}$$

where  $\mathbb{T}$  is the unit circle, i.e.,  $\mathbb{T} := \{z \in \mathbb{C} : |z| = 1\}$ . By the *maximal dilatation of a function  $f : \Omega \rightarrow X$  at a regular point  $z$  of  $f$*  we mean the value  $D[f](z)$ .

Analyzing the definition of quasiregular mappings in the complex plane (cf. e.g. [3, p. 25] or [6, Chap VI]) we can generalize them as follows.

**Definition 1.1.** *A function  $f$  is said to be a weakly quasiregular  $\mathbf{X}$ -valued function in  $\Omega$  if  $f : \Omega \rightarrow X$ ,  $z \in \text{Reg}(f)$  for almost every (a.e. for short)  $z \in \Omega$  and the following condition holds*

$$(1.5) \quad K^*(f) := \|D[f]\|_{\Omega, \infty} < +\infty .$$

The class of all weakly quasiregular  $\mathbf{X}$ -valued functions in  $\Omega$  will be denoted by  $\text{WQR}(\Omega, \mathbf{X})$ . By analogy to the classes  $\text{QC}(\Omega; K)$ ,  $K \geq 1$ , we can define the following classes

$$(1.6) \quad \text{WQR}(\Omega, \mathbf{X}; K) := \{f \in \text{WQR}(\Omega, \mathbf{X}) : K^*(f) \leq K\} , \quad K \geq 1 .$$

Any  $f \in \text{WQR}(\Omega, \mathbf{X}; K)$  is said to be a *weakly  $K$ -quasiregular  $\mathbf{X}$ -valued function in  $\Omega$* . From the formula (1.6) and the condition (1.5) it follows that

$$(1.7) \quad \text{WQR}(\Omega, \mathbf{X}) = \bigcup_{K \geq 1} \text{WQR}(\Omega, \mathbf{X}; K) .$$

**Lemma 1.2.** *For all  $f : \Omega \rightarrow X$  and  $z \in \text{Reg}(f)$ ,*

$$(1.8) \quad D[f](z) = \left( \frac{E + G + \sqrt{(E - G)^2 + 4F^2}}{E + G - \sqrt{(E - G)^2 + 4F^2}} \right)^{1/2} ,$$

where

$$(1.9) \quad E := \|d_z f(1)\|^2 , \quad F := \langle d_z f(1) | d_z f(i) \rangle \quad \text{and} \quad G := \|d_z f(i)\|^2 .$$

*Proof.* Given  $f : \Omega \rightarrow X$  and  $z \in \text{Reg}(f)$  fix  $h = e^{i\theta} \in \mathbb{T}$ . Then

$$(1.10) \quad d_z f(h) = (\text{Re } h)d_z f(1) + (\text{Im } h)d_z f(i) = \cos(\theta)d_z f(1) + \sin(\theta)d_z f(i) ,$$

whence

$$(1.11) \quad \begin{aligned} \|d_z f(h)\|^2 &= \langle d_z f(h) | d_z f(h) \rangle \\ &= \cos(\theta)^2 E + \sin(\theta)^2 G + \sin(2\theta)F \\ &= (E - G) \cos(\theta)^2 + F \sin(2\theta) + G \\ &= \frac{E - G}{2} \cos(2\theta) + F \sin(2\theta) + \frac{E + G}{2} . \end{aligned}$$

Choosing  $R \geq 0$  and  $\alpha \in \mathbb{R}$  such that

$$(1.12) \quad \frac{E - G}{2} = R \sin(\alpha) \quad \text{and} \quad F = R \cos(\alpha)$$

we conclude from (1.11) that

$$\|d_z f(h)\|^2 = R \sin(\alpha + 2\theta) + \frac{E + G}{2} .$$

Combining this with (1.4) we obtain

$$D[f](z) = \left( \frac{E + G + 2R}{E + G - 2R} \right)^{1/2},$$

which together with (1.12) leads to (1.8).  $\square$

## 2. The Teichmüller type pseudo-metric $\tau^*$

The method of isothermal coordinates can be used in order to introduce a pseudo-metric in the class  $WQR(\Omega, \mathbf{X})$  by means of the Teichmüller pseudo-metric  $\tau$ . Let us recall that a function  $h : \Omega \rightarrow X$  is said to be an *isothermal reparametrization* of a function  $f : \Omega \rightarrow X$  if

$$(2.1) \quad f(z) = h \circ \varphi(z), \quad z \in \Omega,$$

for some sense preserving homeomorphism  $\varphi$  of  $\Omega$  onto itself and the differential  $d_z h$  is independent of a direction for  $z \in \text{Reg}(h)$  in the following sense

$$(2.2) \quad \|d_z h(v)\|_n = \lambda(z)|v|, \quad v \in \mathbb{C}, z \in \text{Reg}(h),$$

where  $\lambda : \Omega \rightarrow \mathbb{R}$  is a certain function with positive values. Let  $C^1(\Omega, \mathbf{X})$  stand for the class of all functions  $f \in \Omega \rightarrow X$  which are differentiable at each point  $z \in \Omega$  and the directional derivatives  $df(1)$  and  $df(i)$  are continuous functions from  $E(\mathbb{C})$  to  $\mathbf{X}$ .

Assume that  $f \in C^1(\Omega, \mathbf{X}) \cap WQR(\Omega, \mathbf{X})$ . We wish to describe all sense preserving diffeomorphic self-mapping  $\varphi$  of  $\Omega$  satisfying (2.1) for some function  $h$  with the property (2.2). Following calculations from [7, Sect. 4] we see that  $\varphi$  satisfies the following condition

$$(2.3) \quad \bar{\partial}\varphi(z) = \tilde{\mu}[f](z) \partial\varphi(z), \quad z \in \text{Reg}(f),$$

where

$$(2.4) \quad \tilde{\mu}[f](z) := \frac{E - G + 2iF}{E + G + 2\sqrt{EG - F^2}}, \quad z \in \text{Reg}(f),$$

with  $E, F$  and  $G$  given by (1.9) and  $\tilde{\mu}[f](z) := 0$  for  $z \in \Omega \setminus \text{Reg}(f)$ . From Lemma 1.2 it follows that for every  $z \in \text{Reg}(f)$ ,

$$(2.5) \quad \begin{aligned} |\tilde{\mu}[f](z)| &= \frac{|E - G + 2iF|}{E + G + 2\sqrt{EG - F^2}} \\ &\leq \frac{|E - G + 2iF|}{E + G} \\ &= \frac{\sqrt{(E - G)^2 + 4F^2}}{E + G} \\ &= \frac{D[f](z)^2 - 1}{D[f](z)^2 + 1}. \end{aligned}$$

Hence and by (1.5),

$$(2.6) \quad \|\tilde{\mu}[f]\|_{\Omega, \infty} \leq \left\| \frac{D[f](z)^2 - 1}{D[f](z)^2 + 1} \right\|_{\Omega, \infty} = \frac{K^*(f)^2 - 1}{K^*(f)^2 + 1} < 1 .$$

Assume now additionally that  $\Omega$  is a simply connected domain in  $E(\mathbb{C})$ . Then by the mapping theorem ([4, p. 39, 45], [6, Chap. V, §1]), we conclude from (2.6) that there exists  $\varphi \in \text{QC}(\Omega)$  satisfying the Beltrami equation

$$(2.7) \quad \bar{\partial}\varphi = \tilde{\mu}[f] \partial\varphi \quad \text{a.e. in } \Omega .$$

Therefore, for every  $f \in C^1(\Omega, \mathbf{X}) \cap \text{WQR}(\Omega, \mathbf{X})$ ,

$$(2.8) \quad \text{QC}_f(\Omega) := \{\varphi \in \text{QC}(\Omega) : \bar{\partial}\varphi = \tilde{\mu}[f] \partial\varphi \text{ a.e. on } \Omega\} \neq \emptyset ,$$

and so the Teichmüller pseudo-metric  $\tau$  in  $\text{QC}(\Omega)$  determines the function

$$(2.9) \quad \mathcal{F} \times \mathcal{F} \mapsto \tilde{\tau}(f_1, f_2) := \sup\{\tau(\varphi_1, \varphi_2) : \varphi_1 \in \text{QC}_{f_1}(\Omega), \varphi_2 \in \text{QC}_{f_2}(\Omega)\} ,$$

where  $\mathcal{F} := C^1(\Omega, \mathbf{X}) \cap \text{WQR}(\Omega, \mathbf{X})$ . Moreover, from [7, Thm. 0.23] it follows that for every  $f \in \mathcal{F}$ ,

$$(2.10) \quad \tau(\varphi_1, \varphi_2) = 0 , \quad \varphi_1, \varphi_2 \in \text{QC}_f(\Omega) ,$$

and consequently,  $\tilde{\tau}$  is a pseudo-metric in  $\mathcal{F}$  expressed by the following analytical formula

$$(2.11) \quad \tilde{\tau}(f_1, f_2) = \log \frac{1 + \tilde{\kappa}(f_1, f_2)}{1 - \tilde{\kappa}(f_1, f_2)} , \quad f_1, f_2 \in \mathcal{F} ,$$

where

$$(2.12) \quad \tilde{\kappa}(f_1, f_2) := \left\| \frac{\tilde{\mu}[f_1] - \tilde{\mu}[f_2]}{1 - \tilde{\mu}[f_2]\tilde{\mu}[f_1]} \right\|_{\Omega, \infty} , \quad f_1, f_2 \in \mathcal{F} ,$$

and  $\tilde{\mu}$  is given by (2.4). We call  $\tilde{\tau}$  the *pseudo-metric in  $\mathcal{F}$  induced from the Teichmüller pseudo-metric  $\tau$  in  $\text{QC}(\Omega)$  by the assignment*

$$(2.13) \quad \mathcal{F} \ni f \mapsto \text{QC}_f(\Omega) .$$

It is worth noting that we do not need to solve the Beltrami equations (2.7), with  $f := f_1$  and  $f := f_2$ , in order to calculate the value  $\tilde{\tau}(f_1, f_2)$  by the formula (2.9). In view of (2.11) and (2.12) it is enough to determine, using the formula (2.4), the functions  $\tilde{\mu}[f_1]$  and  $\tilde{\mu}[f_2]$ . Thus the value  $\tilde{\tau}(f_1, f_2)$  can be expressed explicitly in terms of  $\tilde{\mu}[f_1]$  and  $\tilde{\mu}[f_2]$ , which simplifies considerations dealing with the pseudo-metric  $\tilde{\tau}$ . In particular, we can extend  $\tilde{\tau}$  to the case where  $\Omega$  is an arbitrary domain in  $E(\mathbb{C})$ , not only simply connected, and  $\mathcal{F}$  is replaced by  $\text{WQR}(\Omega, \mathbf{X})$ .

Following the formula (2.4) we define for any  $f \in \text{WQR}(\Omega, \mathbf{X})$ ,

$$(2.14) \quad \mu^*[f](z) := \frac{A_f(z)}{1 + \sqrt{1 - |A_f(z)|^2}} , \quad z \in \Omega ,$$

where for every  $z \in \Omega$ ,

$$(2.15) \quad A_f(z) := \frac{\|d_z f(1)\|^2 - \|d_z f(i)\|^2 + 2i\langle d_z f(1) | d_z f(i) \rangle}{\|d_z f(1)\|^2 + \|d_z f(i)\|^2} ,$$

provided  $f$  is differentiable at  $z$  and the denominator in (2.15) does not vanish, and otherwise  $A_f(z) := 0$ . Note that with the notations (1.9),

$$(2.16) \quad A_f(z) = \frac{E - G + 2iF}{E + G}, \quad z \in \text{Reg}(f).$$

Following calculations from (2.5) and (2.6) we conclude from (2.14) and (2.16) that for every  $f \in \text{WQR}(\Omega, \mathbf{X})$ ,

$$(2.17) \quad |\mu^*[f](z)| \leq |A_f(z)| = \frac{|E - G + 2iF|}{E + G} \leq \frac{D[f](z)^2 - 1}{D[f](z)^2 + 1} < 1, \quad z \in \text{Reg}(f),$$

and consequently,

$$(2.18) \quad \|\mu^*[f]\|_{\Omega, \infty} \leq \frac{K^*(f)^2 - 1}{K^*(f)^2 + 1} < 1 \quad f \in \text{WQR}(\Omega, \mathbf{X}).$$

Therefore we can replace  $\tilde{\mu}$  by  $\mu^*$  in (2.12), which leads to the following formula

$$(2.19) \quad \kappa^*(f_1, f_2) := \left\| \frac{\mu^*[f_1] - \mu^*[f_2]}{1 - \overline{\mu^*[f_2]}\mu^*[f_1]} \right\|_{\Omega, \infty}, \quad f_1, f_2 \in \text{WQR}(\Omega, \mathbf{X})$$

**Lemma 2.1.** *For any nonempty domain  $\Omega$  in  $\mathbb{E}(\mathbb{C})$ ,*

$$(2.20) \quad \kappa^*(f_1, f_2) \leq \frac{K^*(f_1)^2 K^*(f_2)^2 - 1}{K^*(f_1)^2 K^*(f_2)^2 + 1} < 1, \quad f_1, f_2 \in \text{WQR}(\Omega, \mathbf{X}).$$

*Proof.* Write  $\mathbb{D}$  for the unit disk, i.e.,  $\mathbb{D} := \{z \in \mathbb{C} : |z| < 1\}$ . Since

$$|1 - \bar{w}z|^2 - |z - w|^2 = (1 - |z|^2)(1 - |w|^2), \quad w, z \in \mathbb{C},$$

we have

$$\begin{aligned} \frac{|z - w|^2}{|1 - \bar{w}z|^2} &= 1 - \frac{(1 - |z|^2)(1 - |w|^2)}{|1 - \bar{w}z|^2} \\ &\leq 1 - \frac{(1 - |z|^2)(1 - |w|^2)}{(1 + |z||w|)^2} \\ &= \left( \frac{|z| + |w|}{1 + |z||w|} \right)^2, \quad w, z \in \mathbb{D}. \end{aligned}$$

Therefore

$$\frac{|\mu^*[f_1] - \mu^*[f_2]|}{|1 - \overline{\mu^*[f_2]}\mu^*[f_1]|} \leq \frac{\|\mu^*[f_1]\|_{\Omega, \infty} + \|\mu^*[f_2]\|_{\Omega, \infty}}{1 + \|\mu^*[f_1]\|_{\Omega, \infty} \|\mu^*[f_2]\|_{\Omega, \infty}} \quad \text{a.e. in } \Omega.$$

Combining this with (2.18) and (2.19) we obtain (2.20), which is our claim.  $\square$

Replacing now  $\tilde{\kappa}$  by  $\kappa^*$  in (2.11) we can extend  $\tilde{\tau}$  as follows.

**Theorem 2.2.** *For any nonempty domain  $\Omega$  in  $\mathbb{E}(\mathbb{C})$  the function*

$$(2.21) \quad \text{WQR}(\Omega, \mathbf{X}) \times \text{WQR}(\Omega, \mathbf{X}) \ni (f_1, f_2) \mapsto \tau^*(f_1, f_2) := \log \frac{1 + \kappa^*(f_1, f_2)}{1 - \kappa^*(f_1, f_2)}$$

is a pseudo-metric in  $\text{WQR}(\Omega, \mathbf{X})$ .

*Proof.* Given a nonempty domain  $\Omega$  in  $\mathbb{E}(\mathbb{C})$  fix  $f_1, f_2, f_3 \in \text{WQR}(\Omega, \mathbf{X})$ . From (2.17) it follows that

$$|\mu^*[f_k](z)| < 1, \quad z \in \text{Reg}(f_k), \quad k \in \{1, 2, 3\}.$$

Let  $\rho_h$  be the hyperbolic metric (Poincaré metric) in the unit disk  $\mathbb{D}$ ; cf. e.g. [5, Chap I, §1.1] or [2, §1-5] for the definition of  $\rho_h$ . Hence for all  $k, l \in \{1, 2, 3\}$  and for a.e.  $z \in \Omega$ ,

$$\rho_h(\mu^*[f_k](z), \mu^*[f_l](z)) = \frac{1}{2} \log \frac{|1 - \mu^*[f_k](z)\overline{\mu^*[f_l](z)}| + |\mu^*[f_k](z) - \mu^*[f_l](z)|}{|1 - \mu^*[f_k](z)\overline{\mu^*[f_l](z)}| - |\mu^*[f_k](z) - \mu^*[f_l](z)|},$$

which together with the formulas (2.19) and (2.21) leads to

$$(2.22) \quad \text{ess sup}_{z \in \Omega} \rho_h(\mu^*[f_k](z), \mu^*[f_l](z)) = \frac{1}{2} \log \frac{1 + \kappa^*(f_k, f_l)}{1 - \kappa^*(f_k, f_l)} = \frac{1}{2} \tau^*(f_k, f_l).$$

Since  $\rho_h$  is a metric in  $\mathbb{D}$ , it follows that for a.e.  $z \in \Omega$ ,

$$\rho_h(\mu^*[f_1](z), \mu^*[f_3](z)) \leq \rho_h(\mu^*[f_1](z), \mu^*[f_2](z)) + \rho_h(\mu^*[f_2](z), \mu^*[f_3](z)).$$

Combining this with (2.22) we obtain

$$\tau^*(f_1, f_3) \leq \tau^*(f_1, f_2) + \tau^*(f_2, f_3).$$

From the formula (2.19) it follows that

$$\kappa^*(f_1, f_2) = \kappa^*(f_2, f_1) \quad \text{and} \quad \kappa^*(f_1, f_1) = 0,$$

which implies, by (2.21), that

$$\tau^*(f_1, f_2) = \tau^*(f_2, f_1) \quad \text{and} \quad \tau^*(f_1, f_1) = 0.$$

Therefore the conditions (0.3) hold with  $\tau$  and  $\text{QC}(\Omega)$  replaced respectively by  $\tau^*$  and  $\text{WQR}(\Omega, \mathbf{X})$ , which is the desired conclusion.  $\square$

Following [7, Example 0.24] we will show that the pseudo-metrics  $\tau^*$  and  $\tau$  coincide in the class  $\text{QC}(\Omega)$ .

**Theorem 2.3.** *For any nonempty domain  $\Omega$  in  $\mathbb{E}(\mathbb{C})$ ,  $\text{QC}(\Omega) \subset \text{WQR}(\Omega, \mathbb{E}_{\mathbb{R}}(\mathbb{C}))$  and*

$$(2.23) \quad K^*(f) = K(f), \quad f \in \text{QC}(\Omega),$$

as well as

$$(2.24) \quad \tau^*(f_1, f_2) = \tau(f_1, f_2), \quad f_1, f_2 \in \text{QC}(\Omega).$$

*Proof.* Given a domain  $\Omega \neq \emptyset$  in  $\mathbb{E}(\mathbb{C})$  fix  $f \in \text{QC}(\Omega)$ . Then for a.e.  $z \in \Omega$ ,  $z \in \text{Reg}(f)$  and the Jacobian  $J[f](z)$  of  $f$  at  $z$  is positive, which leads, by (0.6), to

$$(2.25) \quad |\partial f(z)|^2 - |\bar{\partial} f(z)|^2 > 0;$$

cf. [6, Chap IV, §1.5]. Using the formulas (1.9) and (0.5) we see that

$$(2.26) \quad \begin{aligned} E &= |\partial f + \bar{\partial} f|^2 = |\partial f|^2 + |\bar{\partial} f|^2 + 2 \operatorname{Re}(\partial f \bar{\partial} f) , \\ F &= -2 \operatorname{Im}(\partial f \bar{\partial} f) , \\ G &= |\partial f - \bar{\partial} f|^2 = |\partial f|^2 + |\bar{\partial} f|^2 - 2 \operatorname{Re}(\partial f \bar{\partial} f) \end{aligned}$$

a.e. in  $\Omega$ . Hence

$$(2.27) \quad \begin{aligned} (E - G)^2 + 4F^2 &= [4 \operatorname{Re}(\partial f \bar{\partial} f)]^2 + 4[-2 \operatorname{Im}(\partial f \bar{\partial} f)]^2 \\ &= 16|\partial f|^2 |\bar{\partial} f|^2 \quad \text{a.e. in } \Omega . \end{aligned}$$

Applying now Lemma 1.2 and (2.25) we have

$$(2.28) \quad \begin{aligned} D[f] &= \left( \frac{E + G + \sqrt{(E - G)^2 + 4F^2}}{E + G - \sqrt{(E - G)^2 + 4F^2}} \right)^{1/2} \\ &= \left( \frac{2|\partial f|^2 + 2|\bar{\partial} f|^2 + 4|\partial f||\bar{\partial} f|}{2|\partial f|^2 + 2|\bar{\partial} f|^2 - 4|\partial f||\bar{\partial} f|} \right)^{1/2} \\ &= \frac{|\partial f| + |\bar{\partial} f|}{|\partial f| - |\bar{\partial} f|} \quad \text{a.e. in } \Omega . \end{aligned}$$

On the other hand side, we can appeal to (0.7) and (1.5), which combined with (0.4) and (2.28) gives

$$(2.29) \quad K^*(f) = \|D[f]\|_{\Omega, \infty} = K(f) ,$$

whence  $f \in \operatorname{WQR}(\Omega, \mathbb{E}_{\mathbb{R}}(\mathbb{C}))$ . Therefore the inclusion  $\operatorname{QC}(\Omega) \subset \operatorname{WQR}(\Omega, \mathbb{E}_{\mathbb{R}}(\mathbb{C}))$  holds, and (2.29) yields the property (2.23). From (2.26) and (2.27) it follows that

$$\begin{aligned} (E + G)^2 - |E - G + 2iF|^2 &= (E + G)^2 - [(E - G)^2 + 4F^2] \\ &= (2|\partial f|^2 + 2|\bar{\partial} f|^2)^2 - 16|\partial f|^2 |\bar{\partial} f|^2 \\ &= 4(|\partial f|^2 - |\bar{\partial} f|^2)^2 \quad \text{a.e. in } \Omega . \end{aligned}$$

Combining this with (2.14), (2.16) and (2.26) we have

$$\begin{aligned} \mu^*[f] &= \frac{E - G + 2iF}{E + G + \sqrt{(E + G)^2 - |E - G + 2iF|^2}} \\ &= \frac{4[\operatorname{Re}(\partial f \bar{\partial} f) - i \operatorname{Im}(\partial f \bar{\partial} f)]}{2|\partial f|^2 + 2|\bar{\partial} f|^2 + \sqrt{4(|\partial f|^2 - |\bar{\partial} f|^2)^2}} \\ &= \frac{2\bar{\partial} f \partial f}{|\partial f|^2 + |\bar{\partial} f|^2 + ||\partial f|^2 - |\bar{\partial} f|^2|} \quad \text{a.e. in } \Omega . \end{aligned}$$

Hence, by (2.25) and by (0.4) we obtain

$$\mu^*[f] = \frac{\bar{\partial} f \partial f}{|\partial f|^2} = \frac{\bar{\partial} f \partial f}{\bar{\partial} \bar{f} \partial f} = \frac{\bar{\partial} f}{\partial f} = \mu[f] \quad \text{a.e. in } \Omega .$$

This means that for every  $f \in \operatorname{QC}(\Omega)$ , the function  $\mu^*[f]$  coincides with the complex dilatation  $\mu[f]$  of  $f$  a.e. in  $\Omega$ . We may now apply the formulas (0.10) and (2.19) to conclude that

$$(2.30) \quad \kappa^*(f_1, f_2) = \kappa(f_1, f_2), \quad f_1, f_2 \in \text{QC}(\Omega).$$

Hence, by (0.9) and by (2.21) we deduce the property (2.24), which completes the proof.  $\square$

## References

- [1] L. V. Ahlfors, *Lectures on Quasiconformal Mappings*, D. Van Nostrand, Princeton, New Jersey-Toronto-New York-London 1966.
- [2] —, *Conformal Invariants: Topics in Geometric Function Theory*, McGraw-Hill, New York 1973.
- [3] K. Astala, T. Iwaniec, and G. Martin, *Elliptic Partial Differential Equations and Quasiconformal Mappings in the Plane*, Princeton Mathematical Series, Princeton University Press, Princeton and Oxford 2009.
- [4] J. Ławrynowicz and J. G. Krzyż, *Quasiconformal Mappings in the Plane: Parametrical Methods*, Lecture Notes in Math. 978, Springer, Berlin 1983.
- [5] O. Lehto, *Univalent Functions and Teichmüller Spaces*, Graduate Texts in Math. 109, Springer, New York 1987.
- [6] O. Lehto and K. I. Virtanen, *Quasiconformal Mappings in the Plane*, 2nd ed., Grundlehren 126, Springer, Berlin 1973.
- [7] A. Partyka, *On metric structures of Teichmüller type*, Bull. Soc. Sci. Lettres Łódź **36** Sér. Rech. Déform. **52** (2002), 35–60.

Institute of Mathematics and Computer Science  
 The John Paul II Catholic University of Lublin  
 Al. Raclawickie 14, P.O. Box 129, PL-20-950 Lublin  
 Poland  
 e-mail: apartyka@kul.lublin.pl

Presented by Julian Ławrynowicz at the Session of the Mathematical-Physical Commission of the Łódź Society of Sciences and Arts on December 18, 2014

## ODLEGŁOŚĆ TEICHMÜLLERA W KLASIE FUNKCJI SŁABO REGULARNYCH

### S t r e s z c z e n i e

Celem pracy jest uogólnienie odwzorowań quasi-konforemnych płaszczyzny zespolonej do funkcji określonych w obszarach płaszczyzny zespolonej i wartościach w przestrzeni unitarnej rzeczywistej, zwanych funkcjami słabo regularnymi. Następnie zdefiniowana jest odległość Teichmüllera dla takich funkcji.

*Słowa kluczowe:* odwzorowania quasi-konforemne, funkcje quasi-regularne, odległość Teichmüllera

## B U L L E T I N

DE LA SOCIÉTÉ DES SCIENCES ET DES LETTRES DE ŁÓDŹ

2014

Vol. LXIV

Recherches sur les déformations

no. 3

pp. 101–114

*In memory of  
Professor Zygmunt Charzyński (1914–2001)*

*Krzysztof Podlaski and Grzegorz Wiatrowski*

**DIFFERENT APPROACHES TO PARTICLE SWARM  
OPTIMIZATION FOR DISCRETE SYSTEMS****Summary**

This paper presents a discussion of different approaches for globally optimizing the objective functions defined in a standard continuous search space when passing to a discrete respective problems. The related techniques are developed in the context of the particle swarm optimization method (PSO). As far as PSO has shown recently a good effectiveness in performing difficult optimization tasks we intend to approve its applicability to discrete systems, i.e. traveling salesman problem (TSP), being well known representative and still most difficult discrete task between all NP-hard problems. To do this we can follow two roads: firstly redefine discrete system in order to use PSO and secondly adjust PSO, using genetic operators, for discrete system.

*Keywords and phrases:* particle swarm optimization, travelling salesman problem, genetic algorithms, global optimal, neighbours distribution, benchmark tasks

**1. Introduction**

Since a long time, the task of minimization of real function with many local, and often also many global minima, is encountered in different scientific as well as technical problems. Usually, this objective/cost function is continuous on the discussed search space, however, the search space of particular problem can have either continuous or discrete structure. Up to now, a number of optimization algorithms has been proposed to deal with the continuous tasks but not everyone of them can be rewritten in a simple way to optimize a discrete case of similar problem. The most known example of such traditional algorithms not working in the latter case is that based on gradient method. Thus, to perform a transition from continuous to discrete problems,

we discuss below a class of another approaches with its origin coming up rather from a family of evolutionary ideas. In that case, a population or swarm of agents penetrates a search space taking into account only minimal number of non-gradient operations and are easy applicable to assumed discrete problems. The related techniques are developed in the context of the particle swarm optimization method (PSO). As far as PSO has shown recently a good effectiveness in performing difficult optimization tasks we intend to approve its applicability to traveling salesman problem (TSP) being well known representative and still most difficult discrete task between all NP-hard problems. To do this we show below the action of several crossover operators leading to the relatively simple but also effective optimization algorithms for TSP.

## 2. Particle Swarm Optimization for continuous space – basic equations

The philosophy behind the original particle swarm optimization (PSO) is to conclude final information from individual own experience and the best individual experience in the whole swarm. The basis for such thinking came from a distributed behavioral model by Craig W. Reynolds in 1987 [1]. This approach to computer animation of flock motion assumed the interaction between the behaviors of individual birds, however, one of the results reported also in this paper was that the aggregate motion strongly depends upon a limited and localized view of the world. The basic Particle Swarm Optimisation algorithm was introduced by R. C. Eberhart and J. Kennedy in 1995 [2] and is based on flocking behaviour of swarm of birds. The algorithm recreates some basic social behaviour of swarm members and on the other hand allows individual reasoning based on member memory and local environment. It should be mentioned here, that this idea became a basis for a more general way of thinking well known as Swarm Intelligence.

In classical approach of PSO type we have swarm of particles (agents) that lives (moves) in  $n$ -dimensional continuous space  $\mathbb{R}^N$ . Each of these particles searches for optimal solution of a given cost function  $f$ . Even though that every member of the swarm is working separately they take into account best results from all swarm members. For every particle in the swarm we can define it's position  $p_i$  in the search space and it's velocity  $v_i$  understood as a change of positions. The leading rule for PSO algorithm is the definition of change of velocity recalculated in every step of the algorithm

$$(1) \quad v'_i = w * v_i + c_1 * (p_{lb} - p_i) + c_2 * (p_{gb} - p_i),$$

where  $v'_i$  is a new velocity of particle  $i$ , while  $v_i$  stands for the actual velocity of this particle  $i$ ,  $p_i$  is a local position of particle  $i$ , while  $p_{lb}$  is historically best position found by this particle and  $p_{gb}$  gives us the best position known from results of all particles in the swarm. The constants  $w$ ,  $c_1$  and  $c_2$  are algorithm parameters and should be established in special way to obtain efficient and stable swarm action in optimization procedure. Coefficient  $w$  represents an inertia of the particle/agent,

while parameters  $c_1$  and  $c_2$  represent strength of influence of historical and swarm best known positions on reasoning.

When we know a new velocity  $v'_i$  of particle  $i$ , we can easily find it's new position  $p'_i$  according to a simple rule

$$(2) \quad p'_i = p_i + v'_i,$$

while the only problem is to verify the value of velocity  $v'_i$  and limit it to a certain maximal value assumed in advance because increased to much leads to long lasting algorithm action when the global minimum is omitted.

This behaviour of particle is basically similar to real behaviour of flocking bird in the swarm. Each of birds before changing it's position often checks where are other members of the swarm (locally or globally). Then, they have to choose individually a new direction of flight in order to find the most promising spot in the search space, what leads to optimization of respective objective function.

### 3. PSO for Simple Discrete Systems

#### 3.1. Function on discrete lattice

The simplest discrete problem can be described as optimization of function over  $N$ -dimensional field of Integer numbers  $f(\mathbb{Z}^N) \rightarrow \mathbb{R}$ . In order to solve this problem we can embeds  $\mathbb{Z}^N$  inside  $\mathbb{R}^N$  and define function  $f'(\mathbb{R}^N) \rightarrow \mathbb{R}$  such that for every  $i \in \mathbb{Z}^N$   $f'(i) = f(i)$ . Now in continuous space  $\mathbb{R}^N$  we optimize function  $f'$  using PSO rounding positions of particles to nearest lattice point at each step of PSO iteration. At the end of this procedure if we should obtain optimal position of  $f$ .

#### 3.2. Binary coding – mapping between continuous and discrete search spaces

The simplest version to achieve binary PSO results has been also proposed by Kennedy, J., Eberhart, R. C. but in 1997 [3]. The above standard real-valued formula for evolution of particle velocity components has been extended applying a sigmoid transformation  $\text{sig}(v_{ij})$  ensuring binary result for particle position such that the probability the  $j$ -th component of particle  $i$ 's position is equal to 1 is given by this sigmoid value from  $[0, 1]$ . However, a number of problems arise from this simple binary PSO version as pointed in many later papers (see e.g. Khaneser et al.). The main is that just mentioned velocity loose its physical meaning and becomes not connected with a change in position but represents rather probability of taking a particular position. We will show later that the problem can be solved using algebraic approach.

#### 3.3. Boolean PSO

On the other hand, we can formulate a Boolean version of PSO (BPSO) where variables are obviously binary while the arithmetic operators “\*”, “+” and “-” in

(1) and (2) become replaced by their logical equivalents, i.e. AND, OR and XOR, respectively. Unfortunately, as it has been shown recently in [4], this algorithm does not scale well to large search space dimensions what makes it less applicable to serious and realistic tasks. However, introducing a specific “pure noise” term to the velocity evolution equation can force the swarm to behave in a better way for large Boolean problems than applying a standard Kennedy, J., Eberhart, R.C. approach [2].

#### 4. TSP as non trivial discrete system

Traveling salesman problem (TSP) is one of the most known discrete NP-hard problem in computer science. The problem can be easily defined as search for optimal (shortest) way of salesman that have to visit all clients in different places. At the beginning one have a set of coordinates of all clients. As a result, we search for shortest route through set of all clients while each of the clients can be visited only once. Researchers, all the time, look for as good as possible optimization algorithms using different techniques, i.e. genetic algorithms, ant colony optimization, simulated annealing, neural networks and many others [5–9]. As for every NP-hard problem the need of some efficient optimization algorithm is still crucial for long time. Also the PSO algorithm is used for this [10,11]. At the beginning, however, we have to observe that usual interpretation of position and velocity is not suitable for this problem. There is not obvious how to define a position in TSP in order to implement mentioned velocity and PSO algorithm without some special modifications. One of the first approaches was introduced by M. Clerc [12] and defines some special algebraic operators of addition in order to introduce special interpretation of position and velocity for TSP. Next, researchers introduced some additional elements/operations to PSO in order to incorporate it with traveling salesman problem.

#### 5. Algebraic approach

PSO algorithm can be easily used for every problem if we can define:

- position  $p_i$  of  $i$ -th particle in the swarm,
- velocity  $v_i$  of  $i$ -th particle in the swarm,
- difference between two arbitrary positions  $p_i - p_k$ ,
- sum of velocity and position  $v + p$ .

As was shown by M. Clerc [12] all these elements can be introduced for TSP in order to use PSO for optimization. At the beginning we have to define all important elements that will be used later.

*Definition 1.* A position of a particle from the swarm in TSP problem is an Hamiltonian cycle in TSP graph.

*Definition 2.* Velocity is defined as an ordered list of transpositions of elements from a Hamilton cycle.

*Example.*  $v = ((1, 2)(3, 4))$  means that we first have to exchange elements 1 and 2 in cycle and later 3 and 4.

*Definition 3.* Let  $v$  be a velocity then opposite of a velocity  $v$  denoted as  $\neg v$  is the same set of transposition as in  $v$  but in reversed order.

*Definition 4.* Let  $p$  be a position of a particle and  $v$  its velocity then new position  $p' = p + v$  is obtained applying all transpositions from velocity on position with appropriate order.

*Example.* If  $p = (1, 2, 3, 4, 5)$  and  $v = ((1, 4)(3, 5))$  then  $p' = p + v = (4, 2, 5, 1, 3)$

*Definition 5.* Let  $p_a$  and  $p_b$  be two positions. The difference  $p_a - p_b$  is an velocity needed to move from position  $p_a$  to  $p_b$ .

*Remark.* It is important that the velocity obtained as subtraction is not uniquely defined, that is why this definition should be used with appropriate algorithm of finding one. There can be many procedures for computing subtraction (i.e. M. Clerc [12]).

Using all presented elements we can now incorporate PSO algorithm for any TSP problem. Moreover in the same way we can adjust many discrete systems for PSO algorithm. Unfortunately presented concepts as velocity and subtraction lost their natural interpretation, and can strongly depend on additional algorithm of subtraction computing.

## 6. PSO with genetic crossover operator

As was presented in previous section it is not easy to define a velocity vector for travelling salesman problem that have some meaningful interpretation. In that case we can try to redefine PSO algorithm itself instead of forcing definition of TSP for standard PSO algorithm. This way we can use PSO in order to solve TSP. First let us analyse if velocity is really needed in order to introduce PSO algorithm. We can define position of a particle as a Hamilton cycle through graph describing TSP problem. When we look at the equations that define PSO algorithm (1,2) it is obvious that velocity is introduced in order to describe change of position between algorithm iterations. This implies that in order to use PSO for TSP we have to define rule for position change. What is important we can omit usage of velocity vector, it is enough to define rules for change of position of a particle between algorithm iterations. Such redefinition of PSO allows us to search for different approaches for this specific problem. From all possible ways of introducing this position change operations the Genetic crossover operator seems to be the best possible choice. If we can introduce a genetic operator which from two Hamilton cycles creates new one we have a good candidate that can be used for solving TSP problem with PSO algorithm.

The modification of PSO in order to use crossover operator has the form:

$$(3) \quad p'_i = p_i \otimes p_{lb} \otimes p_g,$$

where  $\otimes$  is a genetic crossover operator.

The rest of algorithm stays exactly the same. We create a swarm of starting positions, then at each iteration of algorithm we count new position of particles (3), update the best obtained position for each particle and the swarm. As we can see such definition of PSO is very general and independent of actual crossover operator implementation.

### 6.1. Genetic crossover operator for TSP

After introducing Genetic Algorithm (GA) by Holland [13] many crossover operators have been invented and is used in computer science in many areas. Crossover operator is the most important element of Genetic Algorithms (GA). The interpretation of this operator comes from genetic process of creation chromosomes of offspring from chromosomes of its parents. In order to use GA in TSP cases we can define that chromosome is a position of a particle i.e Hamiltonian cycle from TSP graph. There are many already existing genetic crossover operators used in many areas in computer science. The TSP problem has a very specific set of possible chromosomes (Hamilton cycles) and we have to remember the most important property of Hamilton cycle: each element of the cycle occurs only once. Using just simple cut and stitch genetic crossover operation in most of cases we would create new cycles that would not be Hamilton cycle. This implies that in order to use a crossover operator for TSP problem we have to incorporate additional rules to enforce that chromosome of offspring would also be a Hamilton cycle. We can introduce a few of known and used crossover operators for TSP.

#### 6.1.1. Partially Mapped Crossover (PMX)

PMX is one of first crossovers proposed by Goldberg and Lingle in 1985 [14]. In order to create a child cycle from two parent cycles we have to go through four steps:

- Randomly define cutting point and cut both parents chromosomes at the same positions.
- Create proto-child by exchanging selected subcycles.
- Determine the mapping relationship based on the selected subcycles.
- Repair proto-child using the mapping relationship.

*Example.* Through this paper we will use one example of TSP problem with 8 cities on the circle labeled by numbers from 1 to 8. Distance between two consecutive cities is always equal 1. For every case we have selected two parents P1 and P2 in the form:

P1: 1 2 5 6 4 8 3 7  
 P2: 1 4 2 8 6 5 7 3

This cycles can be visualised on graph (Fig. 1).

Suppose the randomly chosen cut points are as follows

P1: 1 2 | 5 6 4 | 8 3 7  
 P2: 1 4 | 2 8 6 | 5 7 3

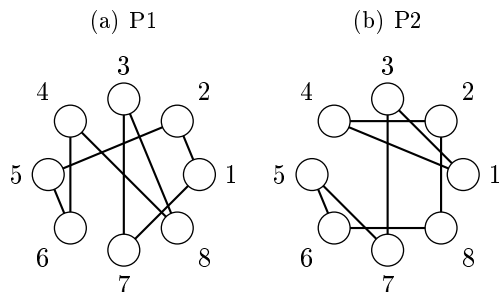


Figure 1: Graphs for Parents P1 and P2

We have to copy appropriate edges into proto-child cycle (see Fig. 2)

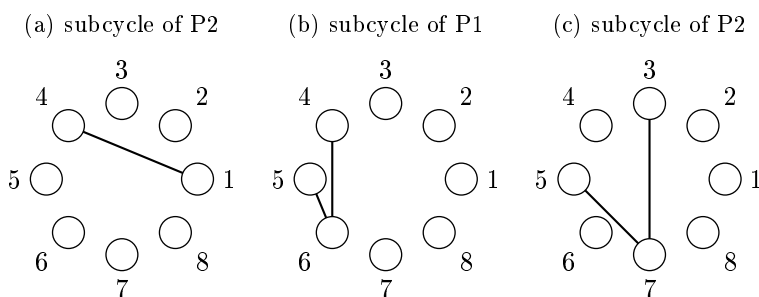


Figure 2: Edges copied from parents into proto-child (PMX)

According to the algorithm we obtained proto-child in the form (see Fig. 3).

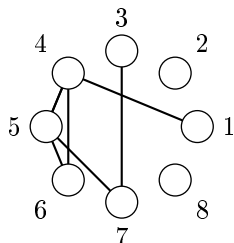


Figure 3: Obtained proto-child (PMX)

PC: 1 4 | 5 6 4 | 5 7 3

Moreover the cutpoints define also mapping  $5 \rightarrow 2$ ,  $6 \rightarrow 8$  and  $4 \rightarrow 6$ .

This child has duplicates 4 and 5. To repair this we use the mapping rule for the sub-cycles inside the cut points as follows. As result we obtain resulting offspring (see Fig. 4):

O12: 1 8 5 6 4 2 7 3

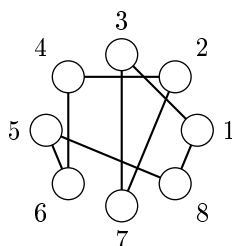


Figure 4: Obtained offspring (PMX)

6.1.2. Variant of Partially Mapped Crossover (VPMX)

Analysing PMX operator we can ask why both parents have cutting points in the same place? There is no reason for that. This implies the next version of our crossover operator, very similar to the first one [15].

*Example.* Using parents as in previous example we have (see Fig. 5, 6):

P1: 1 2 | 5 6 4 | 8 3 7  
 P2: 1 4 2 | 8 6 5 | 7 3

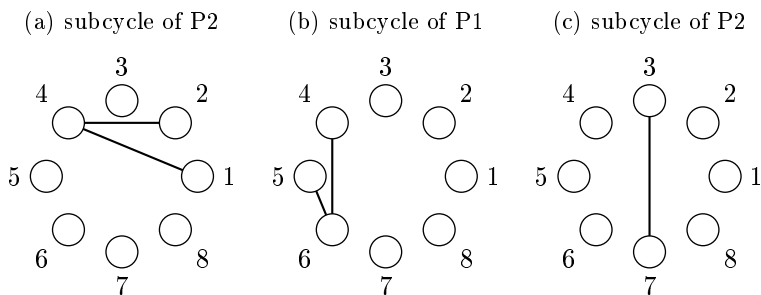


Figure 5: Edges copied from parents into proto-child (VPMX)

As the result we obtained offspring as follows (see Fig. 7):

O12: 1 8 2 5 6 4 7 3

6.1.3. Ordered crossover (OX)

Other type of crossover operator has been designed in order to preserve relative order of cities from the parents [16]. The offspring is produced in simple steps:

- Randomly define two cutting point and cut both parents chromosomes at the same positions.

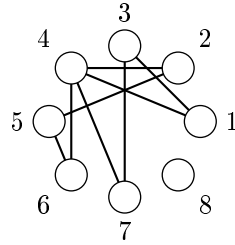


Figure 6: Proto-child VPMX

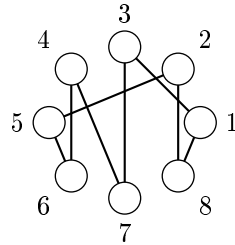


Figure 7: Obtained offspring (VPMX)

- Copy the middle part from one of the parents.
- Copy rest of the elements preserving order and omitting elements already copied into offspring.

*Example.* Using the same parents as previously (offspring on Fig. 8):

P1:	1	2	5	6	4	8	3	7
P2:	1	4	2	8	6	5	7	3
O12:	5	4	2	8	6	3	7	1

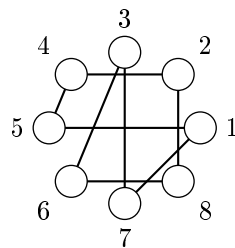


Figure 8: Obtained offspring (OX)

## 6.1.4. Greedy crossover (GX)

This operator is based not only on chromosomes but also on TSP distance matrix [17]. Creation of offspring goes as follows.

- Take (randomly) starting point and copy this to child (suppose its 1).
- Copy shortest edge from all edges in both parents containing this element. In our example these are 1-2 and 1-7 from P1 and 1-4, 1-3 from P2, the shortest from these is edge 1-2.
- Repeat until filling offspring chromosome remembering to omit all already inserted nodes (offspring chromosome is a Hamiltonian cycle).

First few steps of this algorithm are presented on Fig. 9 and resulting cycle on Fig. 10.

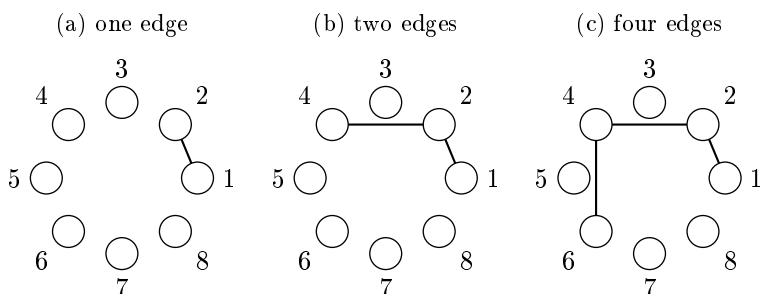


Figure 9: Starting steps of creation of offspring using greedy crossover operator (GX)

It is obvious that this algorithm is more complex than PMX, VPMX and OX and takes longer than the previous three.

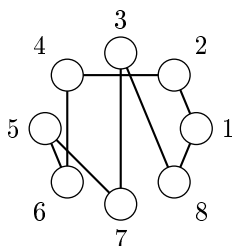


Figure 10: Obtained offspring (GX)

## 6.1.5. Introduction of new genetic crossover operator

In this paper we want to introduce a new crossover operator based on the presented OX. The idea is to preserve the order of elements from parent cycles but use more cutting points than two. We call this new operator Multiple Cut Ordered Crossover (MCOX). The child is created in the following steps:

- Select randomly starting point from first parent.
- Randomize length  $l$  of copied sub-cycles into child cycle.
- Copy  $l$  elements from parent into offspring. However in order to prevent duplicates we have to skip nodes that already have been copied into the child.
- Switch to second parent, and set last inserted position as new starting point.
- Repeat until child cycle has the same length as both parents.

*Example.* Suppose starting point is city 1 and obtained sequence of randomized lengths  $\{2, 3, 2, 1\}$  then at each step we copy into child elements:

Two elements from P1 starting at 1:

P1: 1 2 5 6 4 8 3 7

Three elements from P2 starting from 2:

P2: 1 4 2 8 6 5 7 3

Two elements from P1 starting from 5 (elements 6 and 8 has to be omitted as already copied into child cycle):

P1: 1 2 5 6 4 8 3 7

One element from P1 starting from 3 (it has to be the last missing point 7). As the result we obtain child in the form (see Fig. 11):

O12: 1 2 8 6 5 4 3 7

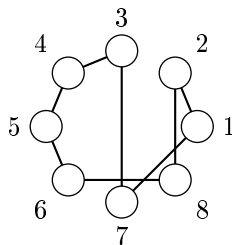


Figure 11: Obtained offspring (MCOX)

## 7. Experimental results

In this paper we present a new crossover operator that can be used in order to solve TSP problem. In order to check usability of this operator we should compare results of optimization using PSO and presented crossover operators for selected TSP problems. We selected four well known TSP problems from set of benchmarks included in TSPLib [18]. For each of benchmark (gr24, fri26, bays29, eli51) we used swarm that contains 50 particles. Each algorithm was run multiple times, for each of the approaches we present best result and average result presented in Table 1. As is shown in presented table the proposed MCOX crossover operator gives good results for all benchmarks.

Crossover	Gr24		Fri26		Bays29		El51	
	avg.	best	avg	best	avg.	best	avg.	best
PMX	2214	1946	1717	1463	3807	3312	1146	1012
VPMX	1293	1272	980	937	2060	2020	464	447
GX	1295	1272	955	937	2060	2020	451	439
CX	2341	2043	1809	1633	2118	2026	1235	1132
OX	1378	1286	1003	937	2057	2032	480	439
MCOX	1311	1272	960	937	2035	2020	433	427

Table 1: Experimental results of PSO using different crossover operators applied to selected TSP cases. In table avg means average result over 25 runs (rounded to nearest integer), best is best result obtained for selected approach in 25 runs.

## 8. Conclusions

Particle Swarm Optimization algorithm was created for optimization problems in continuous space. As is presented in this paper this algorithm can be used also for discrete problems. There are some distinct approaches how to apply PSO. For this paper TSP was selected as representative to discrete problems. Each of presented method can be applied not only to TSP but also other NP hard discrete problems. We introduced new crossover operator that applied for benchmarks gives very promising results. In future works the convergence of MCOX crossover operator will be examined.

## References

- [1] C. W. Reynolds, *Flocks, Herds, and Schools: A distributed behavioral model*, Computer Graphics **21**, no. 4 (1987), 25–34.
- [2] J. Kennedy and R. C. Eberhart, *Particle swarm optimization*, in: Proceedings of the IEEE International Conference on Neural Networks, 1995.
- [3] J. Kennedy and R. C. Eberhart, *A discrete binary version of the particle swarm algorithm*, in: Proceedings of IEEE International Conference on Systems, Man and Cybernetics, IEEE Press, New York 1997, 4101–4108.
- [4] D. Gorse, *Binary particle swarm optimisation with improved scaling behaviour*, in: Proceedings of European Symposium on Artificial Neural Networks, Computational Intelligence and Machine Learning, Bruges, (2013) 239–244.
- [5] G. Gutin and A. Punnen, *The traveling Salesman problem and its variations*, in: Combinatorial Optimization, vol. 12, Kluwer, Dordrecht 2002.
- [6] G. Dantzig, D. Fulkerson, and S. Johnson, *Solution of a large-scale traveling salesman problem*, Operations Research **2** (1954), 393–410.
- [7] D. J. Rosenkrantz, R. E. Stearns, M. Philip, and I. Lewis, *An analysis of several heuristics for the traveling salesman problem*, SIAM Journal on Computing **6**, no. 3 (1977), 563–581.

- [8] D. Fogel, *Applying evolutionary programming to selected traveling salesman problems*, Cybernetics and Systems: An International Journal **24** (1993), 27–36.
- [9] D. Whitley, D. Hains, and A. Howe, *A hybrid genetic algorithm for the traveling salesman problem using generalized partition crossover*, in: Springer-Verlag, eds. R. Schaefer et al., PPSN XI, Part I, LNCS **6238** (2010), 566–575.
- [10] R. Poli, *Analysis of the publications on the applications of particle swarm optimisation*, Journal of Artificial Evolution and Applications *685175* (2008).
- [11] E. F. Goldberg, M. C. Goldberg, G. R. de Souza, *Particle swarm optimization algorithm for the traveling salesman problem*, in: Traveling Salesman Problem, InTech (2008).
- [12] M. Clerc, *Discrete particle swarm optimization, illustrated by the Traveling Salesman Problem*, in: New Optimization Techniques in Engineering, Springer, (2004) 219–239.
- [13] J. H. Holland, *Adaptation in natural and artificial systems*, University of Michigan Press, Ann Arbor, Mich (1975).
- [14] D. E. Goldberg, R. Lingle, *Alleles, loci, and the traveling salesman problem*, in: Proceedings of an International Conference on Genetic Algorithms and Their Applications, Carnegie-Mellon University, (1985), 154–159.
- [15] K. Deep and H. M. Adane, *Variant of partially mapped crossover for the Travelling Salesman problem*, International Journal of Combinatorial Optimization Problems and Informatics **3.1** (2011), 47–69.
- [16] L. Davis, *Applying adaptive algorithms to epistatic domains*, in: Proceeding of the International Joint Conference on Artificial Intelligence, IEEE Computer Society Press, (1985), 162–164.
- [17] J. Grefenstette, R. Gopal, B. Rosmaita, and D. Van Gucht, *Genetic algorithms for the traveling salesman problem*, in: Proceedings of the First International Conference on Genetic Algorithms and their Applications, (1985), 160–168.
- [18] Traveling Salesman Problem Library, <http://comopt.ifi.uni-heidelberg.de/software/TSPLIB95>.

University of Łódź  
 Faculty of Physics and Applied Informatics  
 Pomorska 149/153, PL-90-236 Łódź  
 Poland  
 e-mail: podlaski@uni.lodz.pl  
 wiatr@uni.lodz.pl

Presented by Ilona Zasada at the Session of the Mathematical-Physical Commission of the Łódź Society of Sciences and Arts on November 20, 2014

## OPTYMALIZACJA ROJEM CZĄSTECZEK DLA UKŁADÓW DYSKRETNÝCH

### Streszczenie

W pracy prezentowana jest dyskusja różnych podejść do globalnej optymalizacji funkcji celu, zdefiniowanej standardowo na ciągłej przestrzeni poszukiwań, w przypadku przejścia

do problemów dyskretnych. Opisywane techniki są rozwijane w kontekście metody optymalizacji stadnej/rojem cząsteczek (ang. PSO). Ponieważ metoda PSO wykazała ostatnio dużą efektywność w rozwiązywaniu trudnych zadań optymalizacyjnych, pokazujemy również możliwość jej zastosowań do najbardziej reprezentatywnego wśród dyskretnych NP-trudnych problemów – do zadania komiwojażera (ang. TSP).

*Słowa kluczowe:* optymalizacja globalna, optymalizacja stadna/rojem cząsteczek, genetyczne operatory krzyżowania, problem komiwojażera

## B U L L E T I N

DE LA SOCIÉTÉ DES SCIENCES ET DES LETTRES DE ŁÓDŹ

2014

Vol. LXIV

Recherches sur les déformations

no. 3

pp. 115–125

*In memory of Professor Claude Surry  
our Dear Friend and Colleague*

*Krzysztof Podlaski and Grzegorz Wiatrowski*

**EFFECT OF NEIGHBOURS DISTRIBUTION ON HYBRID GENETIC  
APPROACH TO PARTICLE SWARM OPTIMIZATION  
FOR THE TRAVELING SALESMAN PROBLEM**

**Summary**

To avoid the problem of traditional genetic algorithm (GA) and particle swarm optimization (PSO) trapped into local minimum, we propose new hybrid approach using PSO and GA applied to discrete traveling salesman problem (TSP). Thus, constructed hybrid algorithm with distribution of neighbours in known TSP instances is taken into account. Our experimental results indicate a few advantages of the method used over the standard ones, for example better convergence. The algorithm is effective and does not depend so strongly on initial conditions, as often happens.

*Keywords and phrases:* particle swarm optimization, travelling salesman problem, genetic algorithms, global optimal, neighbours distribution, benchmark tasks

**1. Introduction**

The travelling salesman problem (TSP) is one of the most studied and known NP hard problems. It is easy to describe and on the other hand has great importance in real life (i.e. logistics, computer networks, etc.) [1]. In order to find optimal solution to a TSP with  $n$  cities one needs to check all  $(n - 1)!$  routes, this is very demanding task even for small  $n$ . Even though for many years scientists try to find the best algorithm to search for optimal route (Hamiltonian cycle) through TSP graph, it remains still as one of most challenging problems in Computer Science. There are many approaches to name a few: using dynamic programming [2], linear programming [3], nearest neighbour algorithm [4], insertion algorithms [4] and many more.

There are also approaches with evolutionary algorithms like ant colony optimization, genetic algorithms and particle swarm optimization [5]. Particle swarm optimization (PSO) is a very interesting approach to TSP problem, this algorithm allows to search through huge spaces of all possible solutions in relatively short time.

The main purposes behind this paper can be described as follows:

- to modify the standard PSO approach by using a new recombination method of TSP cycles,
- to apply an experimentally established neighbours distribution to treat the classical TSP problem more efficiently.

Thus, more precisely, we propose a new hybrid genetic operation, leading to new positions of swarm particles, using triple recombination of previous position, local best position and global best position (Hamilton cycles) of particles in the swarm. On the other hand, as the optimal route/cycle in any TSP problem is a combination mostly of the shortest edges between nearest neighbours, so the question arises, what is a distribution (in a mean sense) of neighbour orders along optimal path obtained for well-known TSPLIB examples [6]. Application of the neighbourhood order distribution to cycle recombination mentioned above leads us to much limited number of possibilities and makes the proposed hybrid GA-PSO approach more efficient and stable when compared with the standard approaches with homogeneous search in the total space of all possible permutations.

This paper is organized as follows. First we describe basic implementation of particle swarm optimization for travelling salesman problem with discussion on crossover operator (sec. 2). Section 3 contains analysis of neighbours distribution in TSP cases with known optimal solutions. This is followed by proposed modification of PSO algorithm with use of neighbourhood order distribution (sec. 4). In last two sections we placed experimental results of described methods and conclusions.

## 2. Particle swarm optimization for traveling salesman problem

Particle Swarm Optimization is well established technique proposed by R. C. Eberhart and J. Kennedy in 1995 [7], since then it was used in many areas of computer science [8]. PSO is an optimization algorithm based on observation of flocking bird social behavior. The main goal of PSO is to find, using agent methodology, the point where fitness function has minimal or maximal value. In the usual PSO on continuous space the rule for position change is defined as:

$$(1) \quad \begin{aligned} v_{k,i} &= w * v_{k,i-1} + c_1 * (p_k^{lb} - p_{k,i-1}) + c_2 * (p^{gb} - p_{k,i-1}), \\ p_{k,i} &= p_{k,i-1} + v_{k,i}, \end{aligned}$$

where  $p_{k,i}$  is k-th particle position in i-th iteration of algorithm,  $v_{k,i}$  represents velocity of this particle,  $p_k^{lb}$  is k-th particle local best position and  $p^{gb}$  stands for the

global best position in considered swarm,  $w$ ,  $c_1$ ,  $c_2$  are algorithm parameters (weight coefficients).

In order to use swarm techniques for TSP we have to redefine position and velocity. Position of a particle for TSP problem is one of Hamiltonian cycles in TSP graph. In usual PSO approach velocity is used to describe how particle position changes between iterations. In continuous space like  $\mathbb{R}^n$  velocity is a very intuitive way to describe this changes. When we have discrete space, like in TSP, it is very hard to introduce velocity with as intuitive interpretation as in  $\mathbb{R}^n$ . There exist two ways to define PSO particle position changes for TSP [9]: using some geometric interpretation of space of all possible cycles like in [10], and the approach based on recombination/crossover operation [11]. The latter one is used in this paper. Here, a position of a particle in a swarm is a cycle from space of all possible Hamilton cycles. Each such cycle has well tour length. Tour length measure is used as a fitness function. Thus the goal of PSO is to find a cycle that minimizes this fitness function.

### 2.1. Cycles recombination algorithm

We replace the (1) with:

$$(2) \quad p_{k,i} = \text{Recom}(p_{k,i-1}, p_k^{lb}, p^{gb}),$$

where *Recom* is an operation called cycles recombination (crossover operation) defined below in details.

Inspired by many papers (see, e.g., [12–15]) we introduce a recombination algorithm based on genetic recombination of chromosomes.

The algorithm's input is a sequence  $C$  of cycles  $\{p^{gb}, p_k^{lb}, p_{k,i-1}, p^{\text{rand}}\}$  where:

- $p_{k,i-1}$  –  $k$ -th particle position in previous iteration,
- $p_k^{lb}$  –  $k$ -th particle local best position,
- $p^{gb}$  – global best position in the swarm,
- $p^{\text{rand}}$  – randomly generated cycle (using homogeneous random generator).

Each of these cycles has length  $L$ .

There are many possible candidates that can be used to define Recombination, as was presented in [16] Multiple Cut Ordered Crossover Operator (MCOX) is an interesting candidate.

Based on MCOX we can generate new cycle using algorithm:

- Step 0** initialization: take first cycle from sequence  $C$ , randomly select starting element  $s$  from this cycle;
- Step 1** choose random number  $l$  from 1 to  $L$ ;
- Step 2** copy  $l$  elements of cycle starting from  $s$ ;
- Step 3** set  $s$  as last copied point;
- Step 4** take next cycle from sequence  $C$ ;
- Step 5** go to Step 1 if the new cycle is shorter than  $L$ .

*Example.* Input sequence of cycles:

$$\begin{aligned} p^{gb} &= \{9 \ 8 \ 7 \ 6 \ 5 \ 4 \ 3 \ 2 \ 1\} \\ p_k^{lb} &= \{4 \ 6 \ 2 \ 1 \ 5 \ 8 \ 9 \ 7 \ 3\} \\ p_{k,i-1} &= \{4 \ 2 \ 3 \ 7 \ 6 \ 8 \ 1 \ 9 \ 5\} \\ p^{\text{rand}} &= \{7 \ 5 \ 9 \ 1 \ 6 \ 2 \ 4 \ 3 \ 8\} \end{aligned}$$

Recombination

$$\begin{aligned} p^{gb}, s = 1, l = 3 & \quad \left\{ \begin{array}{|c|c|} \hline 9 & 8 \\ \hline \end{array} 7 \ 6 \ 5 \ 4 \ 3 \ 2 \ \begin{array}{|c|} \hline 1 \\ \hline \end{array} \right\} \rightarrow 1 \ 9 \ 8 \\ p_k^{lb}, s = 8, l = 4 & \quad \left\{ \begin{array}{|c|c|} \hline 4 & 6 \\ \hline \end{array} 2 \ 1 \ 5 \ \begin{array}{|c|c|c|c|} \hline 8 & 9 & 7 & 3 \\ \hline \end{array} \right\} \rightarrow 7 \ 3 \ 4 \ 6 \\ p_{k,i-1}, s = 6, l = 2 & \quad \left\{ \begin{array}{|c|c|} \hline 4 & 2 \\ \hline \end{array} 3 \ 7 \ \begin{array}{|c|c|c|c|} \hline 6 & 8 & 1 & 9 & 5 \\ \hline \end{array} \right\} \rightarrow 5 \ 2 \end{aligned}$$

Resulting cycle:

$$p_{k,i} = \{1 \ 9 \ 8 \ 7 \ 3 \ 4 \ 6 \ 5 \ 2\}$$

Using presented algorithm for TSP problem one can observe that if  $p^{\text{rand}}$  would not be included in sequence  $C$ , the results of PSO algorithm often get stuck a local minimum and never comes near to the global one. Hence, it is important to introduce  $p^{\text{rand}}$  as some “fresh blood” into the system. Moreover in order to prevent the swarm from behaving too randomly global best and local best cycles have to be used more often than  $p_{k,i-1}$  and  $p^{\text{rand}}$ . Taking all this into account we conclude that the best sequence  $C$  used for the recombination algorithm has the form:

$$(3) \quad C = \{p^{gb}, p_k^{lb}, p_{k,i-1}, p^{gb}, p_k^{lb}, p^{\text{rand}}\}.$$

## 2.2. Hybrid GA-PSO algorithm

Now we can describe how to use presented Recombination within PSO algorithm:

**Step 0** Initialization: generate swarm by randomizing all particles positions, define IterMax - maximum number of iterations

**Step 1** for each particle in swarm:

**Step a** create a new cycle for every particle in swarm using Recombination Algorithm;

**Step b** calculate value of fitness function;

**Step c** set actual particle position to position obtained in Step a;

**Step d** update local best  $p_k^{lb}$  if tour length for new cycle is less than for  $p_k^{lb}$ ;

**Step e** update global best  $p^{gb}$  if tour length for new cycle is less than for  $p^{gb}$ ;

**Step 2** Repeat Step 1 until number of iterations reaches IterMax.

**Step 3** Return global best position  $p^{gb}$ .

### 3. Distribution of neighbours in TSP problems

It is well known, that in optimal tour through Hamiltonian cycle of TSP problem, pairs of the nearest neighbours are very probable and often exist. The questions arise how often it happens and how probably it happens and what is a contribution of farther neighbours. Is there any distribution of neighbourhood order? We have taken into account 33 TSP cases with known optimal solutions from Traveling Salesman Problem Library (TSPLIB) [6] and tried to find answers to these questions. Like in TSPLIB we have used all distances rounded to integer values.

#### 3.1. Neighbourhood order distribution

First let us define neighbourhood order  $NO(A, B)$  for two points  $A$  and  $B$  in TSP problem with distance measure  $dist(A, B)$  :

$NO(A, B) = 1$  **iff** there is no point  $X$  such that  $dist(A, X) < dist(A, B)$ . If  $NO(A, B) = 1$  then  $B$  is called a nearest neighbour of  $A$ .

We denote the set of all points  $B$  that  $NO(A, B) = 1$  by  $NO_1(A)$  and we call it the set of neighbours of first order.

$NO(A, B) = 2$  **iff** there is no point  $X \notin NO_1(A)$  such that  $dist(A, X) < dist(A, B)$ .

We denote the set of all points  $B$  that  $NO(A, B) = 2$  by  $NO_2(A)$  and we call it the set of neighbours of second order.

Similarly we can define neighbours of any order.

#### 3.2. Overall neighbourhood order distribution

Taking 33 cases from TSPLIB (with different graph sizes from 16 to 2392 nodes) we create histogram of neighbourhood orders for all cases. We have to remember that distinct cases may have very different number of nodes, in order to treat each case evenly we cannot use classical histogram based on how many elements are in each neighbourhood order. Instead, we use the frequency of neighbourhood order in each case. At the end we obtain global distribution of frequency from 33 TSP cases tested (Fig. 1).

### 4. Modifications of PSO using neighbourhood order distribution

PSO algorithms are often used because they allow to effective search over huge space off all possible solutions. We use particles as agents who thanks to cooperation can easily find optimal solution. One of most important feature of PSO is to test value of fitness in new positions and in the same time find some sequence of positions convergent to optimal one. It is very hard to incorporate these to. After analysis of optimal solutions in some of TSP problems we conclude that using flat random distribution in PSO algorithm often gives back positions very far from optimal one.

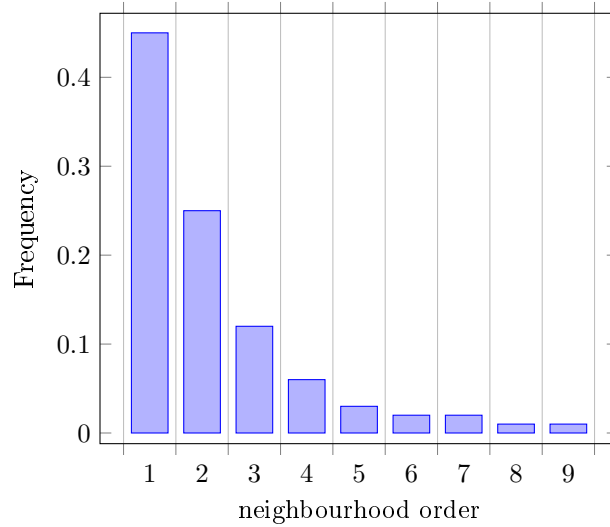


Figure 1: Global distribution of neighbourhood order frequency.

Using different probability distribution can increase a chance to move particle to better position. There are three possible ways one can use neighbourhood order distribution in PSO algorithm:

1. only during initialization (swarm generation),
2. only during each iteration step,
3. both during initialization and during each iteration step.

#### 4.1. Swarm initialization using neighbourhood order distribution

At the beginning of optimization process we have to generate positions for all particles in the swarm randomly, usually we use flat probability distribution  $\rho_{\text{flat}}$ . In our opinion it would be better to use probability distribution  $\rho_{NO}$  based on neighbourhood order distribution (Fig.1).

$$(4) \quad \rho_{NO}(n) = \begin{cases} 45, & \text{for: } n = 1; \\ 25, & \text{for: } n = 2; \\ 12, & \text{for: } n = 3; \\ 6, & \text{for: } n = 4; \\ 12, & \text{for: } n \geq 5 \end{cases}$$

where  $n$  is a neighbourhood order of randomized element. Proposed probability distribution  $\rho_{NO}$  used during cycle random initialization should increase convergence of PSO algorithm. Thus generation of a new Hamiltonian cycle using  $\rho_{NO}$  will have the form:

**Step 0** randomly select first element of cycle  $x_0$  (using  $\rho_{\text{flat}}$ );

- Step 1** randomly choose next element of cycle  $x_i$  (using  $\rho_{\text{flat}}$ );  
**Step 2** find neighbourhood order  $NO(x_{i-1}, x_i)$  for this element;  
**Step 3** randomly generate integer number  $r$ ,  $0 \leq r \leq 100$  (using  $\rho_{\text{flat}}$ );  
**Step 4** if  $r \geq \rho_{NO}(NO(x_{i-1}, x_i))$  repeat from Step 1;  
**Step 5** accept  $x_i$  as next element in cycle;  
**Step 6** generate next elements of the cycle (repeating from Step 1) until we have all possible points in the cycle.

#### 4.2. Modifications of recombination operation using neighbourhood order distribution (PSOwNOD)

We propose a modification of PSO using presented probability distribution (4). In this new PSOwNOD approach we use Recombination Algorithm changed as follows:

- randomized position  $p^{\text{rand}}$  in (3) is generated using non-homogeneous random number generator based on neighbourhood order probability distribution (4).

### 5. Experimental results

In order to estimate efficiency of the proposed PSO implementation we check results for selected benchmarks from TSPLIB (gr24, fri26, bays29, eli51). Each of selected benchmarks is optimized using two versions of algorithms PSO (as described in section 2.2) and PSO with neighbourhood order distribution (PSOwNOD, sec. 4.2) with swarm containing 20 particles and maximum number of iterations set to 2000 (results are presented in Tables 1–4). For most of cases best obtained result was an optimal result (from TSPLIB). The PSO algorithm is mainly based on random operations that means than not every run of algorithm gives back the same result. Tables below show dispersion of obtained results when optimization process was repeated is shown. Margin of error describes efficiency of final result.

The results (Tables 1–4) for optimization processes when neighbourhood order distribution was used (PSOwNOD) are the best. PSO as most of optimization algorithms, strongly depends on starting point, that is the reason why initialization of swarm in most cases has a positive impact on performance of the algorithm. It is worthwhile to observe that for modified algorithm PSOwNOD initialization of the swarm has little or no effect at all on final results. This is a result of strong incorporation of neighbourhood order distribution into recombination algorithm, on each iteration randomness in initialization is moved toward preferred distribution. This implies that PSOwNOD does not depend so strongly on swarm initialization. However not all optimization processes finished with best possible result. On the other hand, they mostly finished with result length no more than 4% longer than an optimal route. Analyzing distribution of results we can stress that PSOwNOD algorithm more often converge to global optimal solution and not so easy trapped with local minimum. It is worth to mention that presented results are better than presented in papers [12, 15] on functions bays29 and eli51 respectively.

	PSO		PSOwNOD	
	random swarm initialization	distribution swarm initialization	random swarm initialization	distribution swarm initialization
optimal route	1272			
best result	1272	1272	1272	1272
results within 2% error	76%	76%	80%	80%
within 2% ÷ 4%	21%	20%	7%	15%
within 4% ÷ 10%	3%	0%	10%	0%
within 10% ÷ 20%	0%	4%	3%	5%

Table 1: PSO results of 100 runs of algorithm for **gr24** with 20 particles, 2000 iterations. For both of algorithms PSO (section 2.2) and PSOwNOD (sect. 4.2) we used both presented ways of swarm initialization (with or without using neighbourhood order distribution). The optimal tour length is best possible solution taken from [6]. Best result means best result obtained in 100 runs of algorithm. PSO algorithms not always finish with optimal solution, that is why distribution of results is presented. Results within 2% error means that difference between final result of algorithm and the optimal solution is not greater than 2%, where 2% ÷ 4% means error lower than 4% and bigger than 2%, etc.

	PSO		PSOwNOD	
	random swarm initialization	distribution swarm initialization	random swarm initialization	distribution swarm initialization
optimal route	937			
best result	937	937	937	937
results within 2% error	80%	88%	100%	84%
within 2% ÷ 4%	7%	12%	0%	12%
within 4% ÷ 10%	6%	0%	0%	0%
within 10% ÷ 20%	7%	0%	0%	0%

Table 2: PSO results of 100 runs of algorithm for **fri26** with 20 particles, 2000 iterations

## 6. Conclusions

New hybrid version of the Particle Swarm Optimization algorithm that uses genetic recombination algorithm is a very effective way to solve TSP tasks. As it is shown, using the neighbourhood distribution we create new recombination/crossover operator that can work even more efficiently. Proposed algorithm was used on known bench-

	PSO		PSOwNOD	
	random swarm initialization	distribution swarm initialization	random swarm initialization	distribution swarm initialization
optimal route	2020			
best result	2020	2020	2020	2020
results within 2% error	48%	68%	92%	80%
within 2% ÷ 4%	25%	29%	8%	15%
within 4% ÷ 10%	27%	3%	0%	5%

Table 3: PSO results of 100 runs of algorithm for **bays29** with 20 particles, 2000 iterations

	PSO		PSOwNOD	
	random swarm initialization	distribution swarm initialization	random swarm initialization	distribution swarm initialization
optimal route	426			
best result	442	435	427	426
results within 2% error	0%	0%	40%	44%
within 2% ÷ 4%	4%	20%	43%	48%
within 4% ÷ 10%	25%	46%	17%	8%
within 10% ÷ 20%	71%	34%	0%	0%

Table 4: PSO results of 100 runs of algorithm for **eli51** with 20 particles, 2000 iterations

marks. For all the presented benchmarks proposed PSOwNOD algorithm gives optimal solution and at least 92% of algorithm runs give result with error less than 4%. This implies better convergence of algorithm to a global optimal solution even for large TSP instances. Moreover this new algorithm does not depend so much on initial conditions (swarm initialization) as it is the case for the usual implementations of PSO.

## References

- [1] G. Gutin and A. Punnen, *The traveling salesman problem and its variations*, vol. 12, Springer, Dordrecht 2002.
- [2] M. Held and R. Karp, *A dynamic programming approach to sequencing problems*, Journal of the Society for Industrial and Applied Mathematics **10** (1962), 196–210.

- [3] G. Dantzig, D. Fulkerson, and S. Johnson, *Solution of a large-scale traveling salesman problem*, *Operations Research* **2** (1954), 393–410.
- [4] D. J. Rosenkrantz, R. E. Stearns, M. Philip, and I. Lewis, *An analysis of several heuristics for the traveling salesman problem*, *SIAM Journal on Computing* **6**, no. 3 (1977), 563–581.
- [5] D. Fogel, *Applying evolutionary programming to selected traveling salesman problems*, *Cybernetics and Systems: An International Journal* **24** (1993), 27–36.
- [6] *Traveling Salesman Problem Library*, <http://comopt.ifi.uni-heidelberg.de/software/TSPLIB95>.
- [7] J. Kennedy and R. C. Eberhart, *Particle swarm optimization*, in: *Proceedings of the IEEE International Conference on Neural Networks*, 1995.
- [8] R. Poli, *Analysis of the publications on the applications of particle swarm optimisation*, *Journal of Artificial Evolution and Applications* (2008), 685175.
- [9] E. F. Goldberg, M. C. Goldberg, and G. R. de Souza, *Particle swarm optimization algorithm for the traveling salesman problem*, in: *Traveling Salesman Problem*, InTech, 2008.
- [10] M. Clerc, *Discrete particle swarm optimization, illustrated by the traveling salesman problem*, in: *Studies in Fuzziness and Soft Computing New optimization techniques in engineering*, Springer, 2004.
- [11] X. Hu, R. C. Eberhart, and Y. Shi, *Swarm intelligence for permutation optimization: A case study of n-queens problem*, in: *Proceedings of the 2003 IEEE Swarm Intelligence Symposium*, 2003.
- [12] H. Fan, *Discrete particle swarm optimisation for TSP based on neighbourhood*, *Journal of Computational Information Systems* **6** (2010).
- [13] K. P. Wang, L. Huang, C. G. Zhou, and W. Pang, *Particle swarm optimization for traveling salesman problem*, in: *Proceedings of the International Conference on Machine Learning and Cybernetics*, 2003.
- [14] Yu. Ling-li and Cai Zi-xing, *Multiple optimization strategies for improving hybrid discrete particle swarm*, *Journal of Central South University (Science and Technology)* **40** (2009).
- [15] X. Wang, A. Huang, and S. Zhou, *ISPO: A new way to solve Traveling Salesman Problem*, *Intelligent Control and Automation* **4** (2013).
- [16] K. Podlaski and G. Wiatrowski, *Different approaches of particle swarm optimization for discrete systems*, this issue, 101–114.

University of Łódź  
Faculty of Physics and Applied Informatics  
Pomorska 149/153, PL-90-236 Łódź  
Poland  
e-mail: podlaski@uni.lodz.pl  
wiatr@uni.lodz.pl

Presented by Ilona Zasada at the Session of the Mathematical-Physical Commission of the Łódź Society of Sciences and Arts on December 18, 2014

## WPLYW ROZKŁADU SĄSIADÓW NA GENETYCZNE HYBRYDOWE PODEJŚCIE DO OPTYMALIZACJI ROJEM CZĄSTECZEK DLA PROBLEMU KOMIWOJAŻERA

### Streszczenie

W celu uniknięcia tradycyjnego problemu zagnieżdżania w minimum lokalnym standardowych algorytmów genetycznych (GA) i optymalizacji stadnej cząstkami (PSO), proponujemy nowe hybrydowe podejście do zastosowań PSO i GA dla dyskretnego zadania komiwojażera (TSP). Konstruujemy hybrydowy algorytm z użyciem rozkładu sąsiadów znalezionym dla znanych przykładowych zadań TSP zebranych w TSP.lib. Numeryczne wyniki doświadczalne pokazują dobrą efektywność oraz kilka innych korzyści tej metody w porównaniu ze standardowym podejściem, np. szybszą zbieżność. Ponadto, taki algorytm jest słabo zależny od warunków początkowych, co w innych przypadkach nie zdarza się często.

*Słowa kluczowe:* optymalizacja globalna, optymalizacja stadna/rojem cząsteczek, genetyczne operatory krzyżowania, problem komiwojażera



## Rapporteurs – Referees

Richard A. Carhart (Chicago)	Henryk Puzkarski (Poznań)
Fray de Landa Castillo Alvarado (México, D.F.)	Jakub Rembieliński (Łódź)
Stancho Dimiev (Sofia)	Carlos Rentería Marcos (México, D.F.)
Pierre Dolbeault (Paris)	Lino F. Reséndis Ocampo (México, D.F.)
Paweł Domański (Poznań)	Stanisław Romanowski (Łódź)
Mohamed Saladin El Nashie (London)	Monica Roşiu (Craiova)
Jerzy Grzybowski (Poznań)	Jerzy Rutkowski (Łódź)
Ryszard Jajte (Łódź)	Ken-Ichi Sakan (Osaka)
Zbigniew Jakubowski (Łódź)	Hideo Shimada (Sapporo)
Tomasz Kapitaniak (Łódź)	Dawid Shoikhet (Karmiel, Israel)
Grzegorz Karwasz (Toruń)	Józef Siciak (Kraków)
Leopold Koczan (Lublin)	Francesco Succi (Roma)
Dominique Lambert (Namur)	Osamu Suzuki (Tokyo)
Andrzej Łuczak (Łódź)	Józef Szudy (Toruń)
Cecylia Malinowska-Adamska (Łódź)	Luis Manuel Tovar Sánchez (México, D.F.)
Stefano Marchiafava (Roma)	Massimo Vaccaro (Salerno)
Andrzej Michalski (Lublin)	Anna Urbaniak-Kucharczyk (Łódź)
Leon Mikołajczyk (Łódź)	Władysław Wilczyński (Łódź)
Yuval Ne'eman (Haifa)	Hassan Zahouani (Font Romeu)
Adam Paszkiewicz (Łódź)	Lawrence Zalcman (Ramat-Gan)
Sergey Plaksa (Kyiv)	Yuri Zeliskiĭ (Kyiv)
Yaroslav G. Prytula (Kyiv)	Natalia Zoriĭ (Kyiv)

CONTENU DU VOLUME LXV, no. 1

1. <b>L. F. Reséndis Ocampo</b> , Holomorphic $Q_p$ -spaces in the unit ball of $\mathbb{C}^n$ .....	ca. 10 pp.
2. <b>J. Grzybowski</b> and <b>R. Urbański</b> , Modeling crystal growth: Polyhedra with faces parallel to planes from a fixed finite set .	ca. 12 pp.
3. <b>K. Polychroniadis</b> and <b>H. M. Polatoglou</b> , Molecular dynamics high performance computing using the graphics processing unit .....	ca. 14 pp.
4. <b>R. Zduńczyk</b> , Simple systems and generalized topologies .....	ca. 8 pp.
5. <b>R. Knapik</b> , Remarks on round metric spaces .....	ca. 13 pp.
6. <b>S. Bednarek</b> , Universal tornado tube .....	ca. 10 pp.
7. <b>M. Nowak-Kępczyk</b> , An algebra governing reduction of quaternary structures to ternary structures III. A study of generators of the resulting algebra .....	ca. 16 pp.
8. <b>G. Oleksik</b> , On the nondegenerate jumps of the Łojasiewicz exponent .....	ca. 8 pp.
9. <b>P. Kuźma</b> , Coupled multistable Rössler systems .....	ca. 9 pp.
10. <b>D. Dudkowski</b> , Lag synchronization in coupled multistable van der Pol-Duffing oscillators .....	ca. 10 pp.